VALUATION OF FINANCIAL DERIVATIVES UNDER THE 4/2 STOCHASTIC VOLATILITY MODEL

A THESIS SUBMITTED TO AUCKLAND UNIVERSITY OF TECHNOLOGY
IN FULFILMENT OF THE REQUIREMENTS FOR THE DEGREE OF
DOCTOR OF PHILOSOPHY

Supervisors

Prof. Jiling Cao

Dr. Wenjun Zhang

Assoc. Prof. Wei Qi Yan

2025

By

Wenqiang Liu

School of Engineering, Computer and Mathematical Sciences

Copyright

Attestation of Authorship

I hereby declare that this submission is my own work and that, to the best of my knowledge and belief, it contains no material previously published or written by another person (except where explicitly defined in the acknowledgements), nor material which to a substantial extent has been accepted for the qualification of any other degree or diploma of a university or other institution of higher learning.

_____

Signature of candidate

Acknowledgements

I sincerely thank everyone who has given me help and support in the process. Especially I am deeply grateful to my supervisors, Prof. Jiling Cao and Dr. Wenjun Zhang for their insightful guidance and continuous support throughout my whole research. Prof. Cao provided continuous guidance and constructive advice throughout my research, and more importantly, inspired me to adopt more effective methods of learning. His rigorous and dedicated attitude deeply influenced me and has had a lasting impact on my academic development. Dr. Wenjun Zhang provided constructive advice at critical stages of this study, which significantly contributed to the progress of my research. Although my thesis does not involve deep learning, I am still very thankful to Assoc. Prof. Wei Qi Yan for agreeing to be my supervisor and for the support provided. In addition, I am also very grateful to Prof. Jeong-Hoon Kim for providing insightful advice that addressed many difficulties encountered during my research.

Moreover, I am truly grateful to Auckland University of Technology for awarding me the Vice-Chancellor's Doctoral Scholarship, which significantly relieved my financial stress and enabled me to concentrate fully on my research.

Finally, I deeply appreciate my family and friends for their support and understanding during my PhD journey. Their encouragement was a crucial source of strength that helped me keep moving forward through times of confusion and difficulty.

Abstract

This research focuses on the valuation of European derivatives and real options under a rescaled double mean-reverting $4/2$ stochastic volatility, which extends the $4/2$ stochastic volatility model originally proposed by Grasselli in 2017 by combining fast and slow mean-reverting terms for asset volatility. Moreover, closed-form approximate pricing formulas are obtained for European derivatives by using an asymptotic analysis approach under the rescaled (double) mean-reverting $4/2$ stochastic volatility model(s). The approximate pricing formulas use the Black–Scholes price as the leading term, combined with correction terms from the asymptotic expansion. The accuracy of closed-form approximate pricing formulas for European derivatives is verified through Monte Carlo simulation and market option data. The results show that the option values obtained from pricing formulas can be well fitted by the simulation results under different maturities and strike price conditions (moneyness), and are also well validated by S&P 500 market data. The advantages of the $4/2$ stochastic volatility model in reflecting option price sensitivity are demonstrated by adjusting parameters and comparing the results with those from the Heston model and the $3/2$ stochastic volatility model.

For real options, closed-form approximate pricing formulas are obtained for the values of real options and investment thresholds by using an asymptotic analysis approach under the double mean-reverting $4/2$ stochastic volatility model. In numerical experiments, sensitivity analysis is performed with respect to the model parameters (the "Heston" and "3/2" factors) and other associated variables. Additionally, the accuracy of

the real option approximate pricing formula is verified by comparisons with simulated values obtained using the Least Squares Monte Carlo method. The results show that all relative errors are below 0.3%, confirming the reliability of the proposed method.

In conclusion, this research provides closed-form approximate pricing formulas for the values of European derivatives, real options and investment thresholds under the rescaled double mean-reverting stochastic volatility model. The accuracy and robustness of these formulas are verified through numerical methods.

Journal Publications

[A] Cao, J., Kim, J-H., Liu, W., and Zhang, W. (2023). Rescaling the double-mean-reverting 4/2 stochastic volatility model for derivative pricing. *Finance Research Letters*, 58, 104374. doi: https://doi.org/10.1016/j.frl.2023.104374

[B] Cao, J., Kim, J-H., Liu, W., and Zhang, W. (2025). Investment opportunity strategy in a double-mean-reverting 4/2 stochastic volatility environment. *The North American Journal of Economics and Finance*, 76, 102358. doi: https://doi.org/10.1016/j.najef.2024.102358

Conference Presentations

[C] Cao, J., Kim, J-H., Liu, W., and Zhang, W. (2023). Rescaling the double-mean-reverting 4/2 stochastic volatility model for derivative pricing. *Oral presentation at the 2023 Derivative Markets Conference*, September 2023, Auckland, New Zealand.

[D] Cao, J., Kim, J-H., Liu, W., and Zhang, W. (2024). Investment opportunity strategy in a double-mean-reverting 4/2 stochastic volatility environment. *Oral presentation at AUT Mathematical Modelling and Analytics Symposium*, December 2024, Auckland, New Zealand

[E] Cao, J., Kim, J-H., Liu, W., and Zhang, W. (2024). Investment opportunity strategy in a double-mean-reverting 4/2 stochastic volatility environment. *Oral presentation at Quantitative Methods in Finance 2024 Conference*, December 2024, Sydney, Australia.

Contents

List of Tables

List of Figures

Chapter 1

Introduction

This chapter presents the background of financial derivative pricing and offers an overview of the fundamental concepts and the evolution of financial derivatives. The literature review section explores a broad range of stochastic volatility models and their applications in the valuation of both European options and real options. Based on this review, the research questions are formulated in Section 1.3. Furthermore, Section 1.4 outlines the main contributions of this thesis and provides an overview of its structure.

1.1 Background

With the increasing complexity and globalization of financial markets, investors have become more focused on strategies to minimize exposure to financial risks. The need for effective risk management tools has grown in parallel with the development of the financial industry. Among sources of risk, the most significant are fluctuations in asset prices and market volatility, which can have substantial impacts on portfolio performance and capital allocation decisions (Martin, 2011; Brockhaus & Long, 2000).

One of the most widely adopted methods for managing these risks is derivatives trading. A derivative is a contract whose value is derived from the performance of one

or more underlying assets, such as stocks, interest rates, commodities, or currencies. These instruments provide investors with mechanisms to hedge against adverse price movements and volatility. The primary types of derivatives include forward contracts, futures, options, and swaps (Broadie & Detemple, 2004).

Forward and futures contracts are commonly used to lock in prices for future transactions, thus offering protection against unfavorable price changes. In contrast, options which grant the holder the right but not the obligation to buy or sell an asset at a predetermined price are especially valuable for hedging against volatility risk (Brockhaus & Long, 2000). Swaps, often used in interest rate or currency risk management, allow parties to exchange cash flows based on different financial instruments or market conditions.

Beyond risk mitigation, derivatives also serve broader roles in speculation, arbitrage, and portfolio diversification, making them essential tools in modern financial engineering. As the demand for more sophisticated risk management strategies grows, so does the need for advanced models that can accurately capture the dynamics of asset prices and volatility. It leads to continued research and innovation in derivative pricing and stochastic modeling.

1.2 Literature Review

This section provides an overview of stochastic volatility models and their applications in financial derivatives trading, with a particular focus on European options and real options. A European option grants the holder the right, but not the obligation, to buy or sell an underlying asset at a predetermined price only at maturity. In contrast, a real option represents the right, but not the obligation, to make strategic investment decisions involving real assets under conditions of uncertainty, such as deferring, confirming, or abandoning a project.

1.2.1 Stochastic Volatility Models

Option pricing depends not only on changes in the underlying asset's value but also on various other factors, such as time to maturity and the risk-free interest rate (Black & Scholes, 1973). In their seminal work, Black & Scholes (1973) introduced the Black-Scholes model, a foundational framework for pricing European options. This model provides a closed-form solution under the assumption of constant volatility, and it has become a cornerstone of modern financial theory.

However, subsequent research has identified significant limitations of the Black-Scholes model, particularly in times of heightened market uncertainty such as financial crises and stock market crashes (Kim et al., 2015; Bates, 2000; Kim et al., 2014). One of the most critical shortcomings is its assumption of constant volatility, which is unrealistic, as shown by empirical studies. Merton (1973) argued that volatility is time-varying, and similar findings have been reported by Brenner & Subrahmanyam (1994) and Jackwerth & Rubinstein (1996), who observed that the implied volatility curve typically exhibits a "smile" or skew that evolves with option maturity. Numerous other studies have also provided evidence against the constant volatility assumption (Fama, 1965; Hull & White, 1987; Johnson & Shanno, 1987; Mandelbrot & Mandelbrot, 1997; Scott, 1987; Wiggins, 1987).

To address this limitation, researchers have developed a variety of stochastic volatility models that allow volatility to follow its own random process (Derman & Miller, 2016; Dupire et al., 1994; Heston, 1993). One of the most influential of these is the Heston model (Heston, 1993), which assumes that volatility evolves according to a Cox-Ingersoll-Ross (CIR) process rather than remaining fixed. The Heston model successfully reproduces several stylized features observed in option markets, such as volatility smiles and skews. Despite its advantages, the Heston model struggles to capture extreme market behavior, particularly when dealing with high volatility-of-volatility

(vol-vol) conditions. It also has difficulty accurately modeling the implied volatility surface for deep out-of-the-money options, as noted by Cox et al. (1985) and Klein (1996). Moreover, other studies also showed that not all features of market volatility can be captured by the Heston model (Duan & Yeh, 2010; Mencia & Sentana, 2013; Papanicolaou & Sircar, 2014).

To improve upon this, the $3/2$ stochastic volatility model was proposed by Heston (1997) and Platen (1997), independently. This model accounts for amplified vol-vol effects and can better reflect market phenomena such as steep volatility skews and upward-sloping implied volatility curves. Empirical studies have validated the $3/2$ model's performance, showing that it aligns well with market data (Bakshi et al., 2006; Jones, 2003; Lewis, 2009). However, due to its non-affine structure, the $3/2$ model presents analytical and computational challenges, making it less tractable in certain applications (Drimus, 2012).

To overcome the individual limitations of the Heston and $3/2$ models, Grasselli (2017) introduced the $4/2$ stochastic volatility model, which combines the dynamics of both frameworks. Specifically, the Heston component tends to flatten the implied volatility slope, while the $3/2$ component allows it to steepen as volatility rises. This hybrid structure enables the $4/2$ model to capture a wider range of volatility behaviors and better match observed market patterns. The $4/2$ model has been proven effective in asset pricing and portfolio management, with its practical utility supported by several studies (Cheng & Escobar-Anel, 2021; Escobar & Gong, 2020; Lin et al., 2017).

1.2.2 Valuation of European Options and Real Options

The Black-Scholes model provides a closed-form solution for pricing European call and put options, enabling investors to efficiently assess the fair value of these derivatives using key variables such as the underlying asset price, time to maturity, risk-free interest

rate, and volatility. A fundamental innovation of the model lies in its assumption that asset prices follow a geometric Brownian motion and its use of a risk-neutral valuation framework (Black & Scholes, 1973). These foundational elements have significantly shaped the development of subsequent option pricing models.

Building upon the Black-Scholes framework, a range of theoretical and numerical methods have been introduced to improve the accuracy of option pricing. Boyle (1977) proposed the Monte Carlo simulation method, which estimates the expected discounted payoff of options by simulating numerous potential paths for the underlying asset. This approach is especially valuable for valuing complex and path-dependent derivatives. Similarly, Cox et al. (1979) introduced the binomial option pricing model, a discrete-time framework that models price evolution via a binomial tree. Under the risk-neutral measure, this model converges to the Black-Scholes solution as the number of time steps increases, making it a robust and theoretically consistent alternative.

In recent years, research on European option pricing has expanded to incorporate more sophisticated dynamics, particularly regarding stochastic volatility. For example, Sabanis (2002) explored the use of stochastic volatility models to hedge market risks that cannot be fully diversified. The study demonstrated that supplementing a portfolio with specific European options can enhance hedging efficiency in incomplete markets compared to using the underlying asset alone.

Chuma & Fadugba (2015) derived a closed-form pricing formula for European options under the Heston model, treating volatility as a stochastic process. Using Fourier inversion techniques, the study showed that this model effectively captures the empirical features of asset returns—namely, fat tails and peaked distributions—through parameter adjustments. Furthermore, Grasselli (2017) introduced the $4/2$ stochastic volatility model, which combines the strengths of the Heston and $3/2$ models. Despite its descriptive power, the complexity of the $4/2$ model's pricing formula limits its practical applicability. These limitations of single-factor stochastic volatility models

have motivated the development of mixed and multi-factor models.

Christoffersen et al. (2009) proposed a two-factor stochastic volatility model in which the volatility factors exhibit distinct stochastic correlations with asset returns, and their relative influence changes over time. Empirical analysis on S&P 500 options—typically European in style—revealed that this model improves in-sample pricing accuracy by 24% and out-of-sample performance by 23% compared to the benchmark Heston model. Extending this idea, Veng et al. (2019) introduced a multi-factor stochastic volatility model based on Heston's framework. This model captures multi-scale volatility dynamics and provides higher pricing accuracy through an approximate analytical formula.

Similarly, Huang & He (2022) proposed a two-factor, non-affine stochastic volatility model for pricing European options. Using Taylor expansion and the Fourier cosine method, they derived an approximate analytical pricing formula. Their numerical results indicate superior performance in both pricing accuracy and volatility fitting relative to existing models.

Other notable multi-factor models include Gatheral (2008), who examined double mean-reverting volatility structures, and Huh et al. (2019), who studied multi-scale, multi-factor models—both of which enhance the modeling of volatility clustering and leverage effects.

In the domain of real options, Myers (1977) was the first to conceptualize investment opportunities as financial options. Building on this insight, Brennan & Schwartz (1982) employed stochastic processes to develop a dynamic valuation framework that emphasized optimal investment timing and managerial flexibility. Subsequently, McDonald & Siegel (1986) used continuous-time stochastic control theory to model investments as American call options, deriving a closed-form expression for the value of waiting and identifying the critical investment threshold.

Dixit & Pindyck (1994) synthesized and extended earlier work, developing a comprehensive real options framework that categorized various real options (e.g., expansion, abandonment) and highlighted the value of waiting. Their analysis established real investment decisions as optimal stopping problems under uncertainty.

Since then, real options research has expanded significantly. For instance, Schwartz (2004) applied the Least Squares Monte Carlo (LSM) method—originally developed by Longstaff & Schwartz (2001)—to evaluate research and development investments. This method uses Monte Carlo simulations and least squares regression to estimate the continuation value, allowing for optimal exercise strategy determination. The study demonstrated that LSM effectively captures uncertainty and improves the valuation of real-world projects.

Borison (2005) critically reviewed existing real options methodologies, particularly those based on Black-Scholes assumptions. He argued that these models often rely on unrealistic premises—such as constant volatility—which can lead to suboptimal investment decisions in practice. In response to this issue, Ting et al. (2013) applied the Heston stochastic volatility model (Heston, 1993) to real options pricing, introducing an approximate closed-form formula to quantify the effects of stochastic volatility on investment thresholds and decision timing.

Expanding this work, Huang et al. (2014) analyzed investment under competition by extending the model to a duopoly setting. Their findings showed that stochastic volatility increases the investment threshold, prolongs the optimal waiting time, and enhances first-mover advantages. These results underscore the role of volatility in investment decision-making, particularly in dynamic market environments.

In addition to the Heston model, other stochastic volatility frameworks have been applied to real options. For example, Li & Wu (2008) utilized a generalized version of the Hull & White (1990) model. Dias & Nunes (2011) and Dias et al. (2024) applied the constant elasticity of variance (CEV) model developed by Cox (1975). Kim et al.

(2014) investigated a stochastic-local volatility framework, while Ewald et al. (2017) and Hillman et al. (2018) explored two-factor and jump-diffusion models, respectively. These studies reflect the ongoing evolution and diversification of real options pricing methodologies to better capture market realities.

In summary, the $4/2$ stochastic volatility model has significant advantages due to its ability to integrate and improve the Heston and $3/2$ models. However, the $4/2$ stochastic volatility model and its multi-factor extensions do not have closed-form solutions, which is a disadvantage. Moreover, under market uncertainty, model calibration is another challenge. In the real option setting, the absence of market-traded data poses an additional difficulty. Since project values and investment opportunities are not directly observable, empirical calibration and validation become challenges. These issues highlight the tension between mathematical rigor and real-world applicability. In subsequent chapters, we will address these challenges through several research questions listed in Section 1.3.

1.3 Research Questions

The main objective of this research is to establish approximate analytical pricing formulas for evaluating the fair value of a European option or a real option and its optimal investment threshold under the 4/2 stochastic volatility model, respectively. Particularly, the study aims to address the following key questions:

Question 1: *What is the fair value of a European derivative under the 4/2 stochastic volatility model?*

Question 2: *What is the fair value of a real option under the 4/2 stochastic volatility model?*

Question 3: *How can we determine the optimal investment threshold for exercising a real option when the underlying follows a 4/2 stochastic volatility model?*

Question 4: *What methods can be used to evaluate the pricing accuracy of the 4/2 stochastic volatility model for European options and real options?*

Question 5: *What methods can be used to conduct sensitivity analysis for assessing the robustness of the 4/2 stochastic volatility model in option pricing?*

1.4 Research Contributions and Thesis Organization

This thesis makes several key contributions. First, it proposes a rescaled double mean-reverting $4/2$ stochastic volatility model, which extends the original $4/2$ model by incorporating both fast and slow mean-reverting terms of asset volatility. This enhancement allows the model to more accurately reflect market-implied volatility characteristics, such as skew and smile. Using asymptotic analysis, an approximate closed-form pricing formula for European derivatives is derived under this extended model. The resulting formula resembles a modified version of the Black-Scholes model and can be efficiently calibrated using market-implied volatility data.

Additionally, the thesis derives approximate formulas for valuing real options and determining investment thresholds within the same modeling framework. The accuracy of these approximations is validated by comparing their results with those obtained from LSM simulations. The comparisons show that the relative pricing errors are below 0.3%, confirming the reliability of the proposed approach.

The rest of the thesis is organized as follows.

Chapter 2 reviews foundational mathematical tools and core concepts in quantitative finance, including probability theory, stochastic calculus, financial derivatives, and risk-neutral pricing. It also introduces numerical methods used throughout the thesis, such as Monte Carlo simulation, LSM, and the Runge-Kutta method.

Chapter 3 introduces the rescaled mean-reverting $4/2$ stochastic volatility model (SVM) and the rescaled double mean-reverting $4/2$ stochastic volatility model, which

are extensions of the original $4/2$ stochastic volatility model. Then, approximate closed-form pricing formulas are provided for European options under the rescaled mean-reverting $4/2$ SVM and the rescaled double mean-reverting $4/2$ SVM, respectively. These formulas address Research Question 1. The accuracy of the European option pricing formula is validated using market data and Monte Carlo simulation results, addressing Research Question 4. Moreover, the chapter includes numerical results analyzing the sensitivity of the European option value with respect to model parameters, addressing Research Question 5.

Chapter 4 presents closed-form pricing formulas to obtain the fair values for real options and investment thresholds under the rescaled double mean-reverting $4/2$ stochastic volatility model, which addresses Research Questions 2 and 3. The accuracy of the real options pricing formula is validated through the least squares Monte Carlo simulation method, addressing Research Question 4. Moreover, it also includes the numerical results on sensitivity analysis of the real option value and investment threshold with respect to model parameters, which addresses Research Question 5.

Chapter 5 concludes the thesis and outlines the research that can be expanded in the future based on the present research.

Chapter 2

Preliminaries

This chapter is devoted to introducing the theoretical and computational background required for later chapters. Section 2.1 introduces fundamental mathematical concepts and tools, such as probability measures, random variables, conditional expectation, stochastic processes, Brownian motion, Itô's Lemma, infinitesimal generators, Poisson equation, and the Feynman-Kac Theorem, etc. Section 2.2 provides some fundamental concepts and models in quantitative finance, including options, risk-neutral pricing and Girsanov's Theorem, the Black-Scholes model and some stochastic volatility models, including the Heston model, the $3/2$ stochastic volatility model and the $4/2$ stochastic volatility model, and an asymptotic method, etc. Section 2.3 describes some numerical methods, including the Monte Carlo simulation, the least squares Monte Carlo simulation, and the Runge-Kutta method. All of these tools described in this chapter will be used throughout the rest of this thesis.

2.1 Mathematical Tools

This section provides an introduction to the essential mathematical concepts and tools required for the subsequent chapters. The core references for this section are (Cont

& Tankov, 2003), (Fouque et al., 2011), (Klebaner, 2005), (Oksendal, 2013), (Pham, 2009), (Ramm, 2001), (Ross, 2014) and (Shreve, 2008).

2.1.1 Probability Measure

The concept of a probability measure is seminal in the formulation and understanding of random variables and stochastic processes. In probability theory, the measure of a given set is often interpreted as a way of the set, essentially providing a mathematical tool for determining the likelihood of certain outcomes (Cont & Tankov, 2003). In this research, probability measures allow us to quantitatively characterize the uncertainty of experimental results and to make decisions based on this uncertainty. Generally, there are three key elements in a probability space: the state space, events and the probability distribution.

State space: A *state space* refers to a set of all possible outcomes, also known as the sample space. In probability theory, it is denoted by Ω. This space provides the basis for defining events and probabilities. Moreover, the power set of Ω, denoted by 2^{Ω}, is the set of all subsets of Ω, including Ω itself and the null or empty set $\varnothing$.

Events: An *event* is a subset of the sample space and represents a specific situation that can occur. An event can be a single outcome or a combination of outcomes.

Probability distribution: A *probability distribution* describes the probability of each event occurring. It is a representation of the probability measure on a specific event, and the probability distribution allows us to know the likelihood of different events occurring.

Before the probability measure is defined, the concept of a σ-algebra is introduced first. For more information, refer to Shreve (2008).

Definition 2.1.1 (σ-algebra)**.** A *σ-algebra $\mathcal{F}$* on a nonempty set Ω is a collection of subsets that satisfies the following conditions:

(1) The empty set $\varnothing$ is in $\mathcal{F}$, i.e., $\varnothing \in \mathcal{F}$.

(2) If a set A belongs to $\mathcal{F}$, then its complement relative to Ω, denoted by $\Omega \setminus A$, also belongs to $\mathcal{F}$.

(3) Any sequence of events $\{A_n\}_{n=1}^{\infty}$ in $\mathcal{F}$ has a countable union $\bigcup_{i=1}^{\infty} A_i$ that also belongs to $\mathcal{F}$.

In this case, the ordered pair $(\Omega, \mathcal{F})$ is referred to as a *measurable space*.

If $\mathcal{F}$ is a σ-algebra on Ω, based on properties (1)-(3) in Definition 2.1.1, for any sequence of events $A_1, A_2, A_3, \ldots$ in $\mathcal{F}$, we have $\bigcap_{i=1}^{\infty} A_i \in \mathcal{F}$. Additionally, we have $\Omega \in \mathcal{F}$, as Ω is the complement of $\varnothing$.

The smallest and the largest σ-algebras on Ω are $\{\varnothing, \Omega\}$ and 2^{Ω}, respectively. Recall that a Borel set of $\mathbb{R}$ is any subset generated from open intervals by applying countable unions, countable intersections, and complements. The collection of all such Borel sets is known to form a σ-algebra. Now, on a measurable space, we proceed to define a probability measure.

Definition 2.1.2 (Probability Measure)**.** Given a measurable space $(\Omega, \mathcal{F})$, a *probability measure* $\mathbb{P}$ on $(\Omega, \mathcal{F})$ is a function $\mathbb{P} : \mathcal{F} \to [0, 1]$ from $\mathcal{F}$ to the unit closed interval $[0, 1]$ that satisfies the following conditions:

(1) The probability measure satisfies $P(\Omega) = 1$,

(2) for any sequence $\{A_i : i \geq 1\}$ of mutually disjoint events (i.e., $A_i \cap A_j = \varnothing$ for all $i \neq j$),

$$P\left(\bigcup_{i=1}^{\infty} A_i\right) = \sum_{i=1}^{\infty} P(A_i).$$

The triple $(\Omega, \mathcal{F}, \mathbb{P})$, where $\mathbb{P}(A)$ represents the probability of event A, is known as a *probability measure space*, or simply a *probability space*.

Based on the properties in Definition 2.1.2, we can deduce that for any event $A \in \Omega$,

$$\mathbb{P}(\Omega \setminus A) = 1 - \mathbb{P}(A).$$

Consequently, we conclude $\mathbb{P}(\varnothing) = 0$. Within a probability space $(\Omega, \mathcal{F}, \mathbb{P})$, if an event A in $\mathcal{F}$ satisfies $\mathbb{P}(A) = 1$, then the event A is said to occur *almost surely*.

Let $\mathbb{P}$ and $\mathbb{Q}$ be two probability measures defined on a measurable space $(\Omega, \mathcal{F})$. We call $\mathbb{P}$ *absolutely continuous with respect to* $\mathbb{Q}$, if whenever $\mathbb{Q}$ assigns zero probability to a measurable set A, $\mathbb{P}$ must also assign zero probability to that set, i.e.,

$$\mathbb{Q}(A) = 0 \Longrightarrow \mathbb{P}(A) = 0.$$

For simplicity, if a probability measure $\mathbb{Q}$ assigns zero probability to an event, then the measure $\mathbb{P}$ should likewise assign zero probability to that event. Two probability measures, $\mathbb{P}$ and $\mathbb{Q}$, defined on a measurable space $(\Omega, \mathcal{F})$, are said to be *equivalent* if they are absolutely continuous with respect to each other. This relationship can be expressed as follows:

$$\mathbb{P} \sim \mathbb{Q} \iff \text{for every } A \in \mathcal{F},\ \mathbb{P}(A) = 0 \text{ if and only if } \mathbb{Q}(A) = 0.$$

This equivalence implies that $\mathbb{P}$ and $\mathbb{Q}$ assign zero probability to identical measurable sets, i.e., sharing the same collection of impossible events.

2.1.2 Random Variables

Roughly speaking, random variable denotes a function that assigns a numerical value to each possible outcome of the random experiment.

Definition 2.1.3 (Random Variable)**.** A *random variable* on a probability space $(\Omega, \mathcal{F}, \mathbb{P})$

is a real-valued function $X : \Omega \to \mathbb{R}$ which satisfies the property that for any Borel subset $B \subseteq \mathbb{R}$, the preimage set

$$\{X \in B\} = \{\omega \in \Omega : X(\omega) \in B\}$$

belongs to the σ-algebra $\mathcal{F}$. (Shreve, 2008).

Consider a probability space $(\Omega, \mathcal{F}, \mathbb{P})$ and a random variable X defined on it. The σ-algebra generated by X, symbolized as $\sigma(X)$, consists of all events in Ω for which membership is determined by the values of X lying in Borel subsets B of $\mathbb{R}$, specifically:

$$\{\omega \in \Omega : X(\omega) \in B\}.$$

This σ-algebra is always a subset of $\mathcal{F}$. When a sub-σ-algebra $\mathcal{G}$ of $\mathcal{F}$ contains $\sigma(X)$, the random variable X is said to be measurable with respect to $\mathcal{G}$. In essence, this means that the information encapsulated by $\mathcal{G}$ suffices to fully characterize X.

Consider a random variable X defined on a probability space $(\Omega, \mathcal{F}, \mathbb{P})$. Following (Shreve, 2008), its distribution measure, denoted by μ_X, is a probability measure that assigns to each Borel set B of $\mathbb{R}$ the value $\mu_X(B) = \mathbb{P}\{X \in B\}$.

The behavior of a random variable X can be described through its cumulative distribution function (CDF), denoted by $F_X(x)$, which is defined as

$$F_X(x) = \mathbb{P}\{X \leq x\} = \mu_X(-\infty, x], \quad x \in \mathbb{R}.$$

Provided that the CDF F is available, the measure of the interval $(x, y]$ for any $x, y \in \mathbb{R}$ with $x < y$ can be expressed as

$$\mu_X(x, y] = F_X(y) - F_X(x).$$

Moreover, the connection between the CDF and the probability density function (PDF) for X is given by

$$\mu_X[a,b] = \mathbb{P}\{a \le X \le b\} = F_X(b) - F_X(a) = \int_a^b f_X(x)dx,$$

where $-\infty < a \le b < \infty$, and f_X represents the PDF of X. In the case of a discrete random variable, the integral is substituted by a summation.

The following result on random variables is from (Shreve, 2008) [1]

Theorem 2.1.1. *Suppose that X is a random variable defined on the probability space $(\Omega, \mathcal{F}, \mathbb{P})$. The following properties are true:*

(a) If X takes only finitely many values $y_0, y_1, \ldots, y_n$, then its expectation can be expressed as

$$\int_\Omega X(\omega)dP(\omega) = \sum_{k=0}^{n} y_k P(X = y_k).$$

(b) (Integrability) The variable X is said to be integrable if and only if

$$\int_\Omega |X(\omega)|d\mathbb{P}(\omega) < \infty.$$

Let Y be another random variable on the same probability space.

(c) (Comparison) Provided that $X \le Y$ almost surely (that is, $\mathbb{P}\{X \le Y\} = 1$), and both X and Y are integrable, then

$$\int_\Omega X(\omega)d\mathbb{P}(\omega) \le \int_\Omega Y(\omega)d\mathbb{P}(\omega).$$

In particular, if $X = Y$ almost surely and one of the integrals is finite, then both

[1] Note: the value range for a random variable can also be allowed to be from $+\infty$ to $-\infty$ in some situations.

exist and

$$\int_\Omega X(\omega)d\mathbb{P}(\omega) = \int_\Omega Y(\omega)d\mathbb{P}(\omega).$$

(d) (Linearity) When α and β are real numbers and X and Y are integrable, or when α and β are non-negative real numbers and X and Y are also non-negative, then

$$\int_\Omega (\alpha X(\omega) + \beta Y(\omega))dP(\omega) = \alpha \int_\Omega X(\omega)dP(\omega) + \beta \int_\Omega Y(\omega)dP(\omega).$$

As mentioned at the beginning of this section, the value of a random variable is uncertain due to the random nature of events. Nevertheless, it is still possible to calculate the mean of a random variable to obtain its expected value.

Definition 2.1.4 (Expectation)**.** Consider a random variable X defined on a probability space $(\Omega, \mathcal{F}, \mathbb{P})$. The *expectation* or *expected value* of X is given by

$$\mathbb{E}^{\mathbb{P}}[X] = \int_\Omega X(\omega)d\mathbb{P}(\omega).$$

This definition holds provided that X is integrable or almost surely non-negative. For convenience, the expectation is often denoted simply by $\mathbb{E}[X]$ when there is no ambiguity regarding the underlying probability measure.

The expectation represents the weighted average of X over the entire sample space Ω, with weights determined by the probability measure $\mathbb{P}$. In short, it reflects the average outcome of X accounting for all possible results.

It is important to note that the existence of $\mathbb{E}^{\mathbb{P}}[X]$ implies that at least one of the expectations of the positive part X^+ or the negative part X^- is finite, where these parts are defined as

$$X^+(\omega) = \max\{X(\omega), 0\} \quad \text{and} \quad X^-(\omega) = \max\{-X(\omega), 0\},$$

for any $\omega \in \Omega$.

Next, a significant result concerning the equivalence of probability measures will be presented.

Theorem 2.1.2 (Radon-Nikodým Theorem)**.** *Consider two equivalent probability measures $\mathbb{P}$ and $\mathbb{Q}$ defined on a measurable space $(\Omega, \mathcal{F})$. There exists a random variable Z on the probability space $(\Omega, \mathcal{F}, \mathbb{P})$ which is almost surely positive and satisfies*

$$\mathbb{E}^{\mathbb{P}}[Z] = 1,$$

such that for every A in $\mathcal{F}$,

$$\mathbb{Q}(A) = \int_A Z(\omega)\, d\mathbb{P}(\omega).$$

The variable Z in this theorem is known as the *Radon-Nikodým derivative* of $\mathbb{Q}$ with respect to $\mathbb{P}$, commonly denoted by

$$Z = \frac{d\mathbb{Q}}{d\mathbb{P}}.$$

We will demonstrate later that both the existence of an equivalent measure $\mathbb{Q}$ and the Radon-Nikodým derivative of $\mathbb{Q}$ relative to $\mathbb{P}$ are fundamental in the framework of risk-neutral pricing in financial mathematics.

2.1.3 Conditional Expectation

When a random experiment takes place and produces an outcome ω, we might obtain some information, though it may not be sufficient to precisely determine the value of ω. Still, this partial information can limit the likelihood of ω happening.

In some extreme situations, the information contained in $\mathcal{F}$ might not provide

any useful clues for assessing a random variable X. In such cases, we say that X is independent of the information contained in $\mathcal{F}$.

Definition 2.1.5 (Independence)**.** Consider a probability space $(\Omega, \mathcal{F}, \mathbb{P})$ with two sub-σ-algebras $\mathcal{G}$ and $\mathcal{H}$ of $\mathcal{F}$. These σ-algebras are called *independent* if for every A in $\mathcal{G}$ and B in $\mathcal{H}$,

$$P(A \cap B) = P(A) \times P(B).$$

Random variables X and Y on $(\Omega, \mathcal{F}, \mathbb{P})$ are independent if their generated σ-algebras $\sigma(X)$ and $\sigma(Y)$ are independent. Moreover, if $\sigma(X)$ is independent of a sub-σ-algebra $\mathcal{G}$, then X is said to be independent of the information contained in $\mathcal{G}$.

Theorem 2.1.3 (Shreve (2008))**.** *Suppose that U and V are independent random variables. Then the following statements are equivalent:*

1. *The joint cumulative distribution function equals to the product of:*

$$F_{U,V}(x, y) \quad = \quad F_U(x) \cdot F_V(y) \quad \textit{for all } x \in \mathbb{R}, y \in \mathbb{R}. \tag{2.1}$$

2. *The joint distribution can be expressed as the product of measures:*

$$P_{U,V}(S \times T) = P_U(S) \cdot P_V(T) \quad \textit{for all } S \subseteq \mathbb{R},\ T \subseteq \mathbb{R}. \tag{2.2}$$

3. *The joint moment-generating function equals to the product of:*

$$\mathbb{E}[e^{sU+tV}] \quad = \quad \mathbb{E}[e^{sU}] \cdot \mathbb{E}[e^{tV}], \tag{2.3}$$

for all $s \in \mathbb{R}, t \in \mathbb{R}$ for which the expectations are finite.

4. The joint density is expressed as the product of:

$$f_{U,V}(u,v) \quad = \quad f_U(u) \cdot f_V(v) \quad \textit{for almost every } u \in \mathbb{R}, v \in \mathbb{R}. \tag{2.4}$$

5. The factors of exception:

$$\mathbb{E}[UV] \quad = \quad \mathbb{E}[U] \cdot \mathbb{E}[V], \quad \textit{if} \quad \mathbb{E}[|UV|] < \infty. \tag{2.5}$$

In some situations, the value of a random variable X may be approximated using the information available in $\mathcal{G}$, though this approximation is not exact. This is referred to as the conditional expectation of X. Accordingly, the conditional expectation of X given $\mathcal{G}$ can be defined, as detailed in (Shreve, 2008, p.68).

Definition 2.1.6 (Conditional expectation)**.** Let X be a random variable on a probability space $(\Omega, \mathcal{F}, \mathbb{P})$, either non-negative or integrable. The *conditional expectation* of X given $\mathcal{G}$, denoted by $\mathbb{E}[X|\mathcal{G}]$, is defined as any random variable that meets the following criteria:

(1) $\mathbb{E}[X|\mathcal{G}]$ is measurable with respect to $\mathcal{G}$;

(2) For every set A in $\mathcal{G}$,

$$\int_A \mathbb{E}[X|\mathcal{G}](\omega) d\mathbb{P}(\omega) = \int_A X(\omega) d\mathbb{P}(\omega).$$

Suppose X and Y are integrable random variables on $(\Omega, \mathcal{F}, \mathbb{P})$ and $\mathcal{G}$ is a sub-σ-algebra of $\mathcal{F}$. The conditional expectation satisfies the following fundamental properties (Shreve, 2008, p.68):

1. (Linearity) Given constants c_1 and c_2, it holds that

$$\mathbb{E}[c_1X + c_2Y|\mathcal{G}] = c_1\mathbb{E}[X|\mathcal{G}] + c_2\mathbb{E}[Y|\mathcal{G}].$$

2. (Pulling out known factors) Suppose XY is integrable and X is measurable with respect to $\mathcal{G}$, then

$$\mathbb{E}[XY|\mathcal{G}] = X\mathbb{E}[Y|\mathcal{G}].$$

3. (Tower property) If $\mathcal{H}$ is a sub-σ-algebra of $\mathcal{G}$, then

$$\mathbb{E}[\mathbb{E}[X|\mathcal{G}]|\mathcal{H}] = \mathbb{E}[X|\mathcal{H}].$$

4. (Independence) When X is independent of $\mathcal{G}$, it follows that

$$\mathbb{E}[X|\mathcal{G}] = \mathbb{E}[X].$$

2.1.4 Brownian Motion and Itô's Lemma

This subsection introduces some fundamental concepts and tools in stochastic calculus, including Brownian motion, geometric Brownian motion and Itô's Lemma.

Definition 2.1.7. A *stochastic process* defined on a probability space $(\Omega, \mathscr{F}, \mathbb{P})$ consists of a collection of random variables $\{X_t : t \in T\}$ indexed by $t \in T$, where T is a subset of the real numbers. The set T is known as the *time horizon* of the process, while the collection of values taken by X_t forms the *state space* of the process.

The index t for these variables may be either continuous or discrete (Cont & Tankov, 2003). When $T = \mathbb{N}$, the collection $\{X_t : t \in T\}$ is called a *discrete-time* stochastic process (i.e., a sequence of random variables). When T is an interval in $\mathbb{R}$, typically

$[0, +\infty)$, the process $\{X_t : t \in T\}$ is referred to as a *continuous-time* stochastic process. For each $\omega \in \Omega$, the mapping $t \mapsto X_t(\omega)$ is known as a *sample path* of the process. If the state space consists of integers or natural numbers, the process is termed a *discrete* or *integer-valued stochastic process*. If the state space is the real line, it is called a *real-valued stochastic process* or a *process with a continuous state space*. If the state space is an n-dimensional Euclidean space, the stochastic process is called an *n-dimensional vector process* or an *n-vector process*.

We consider a sequence of σ-algebras $\mathcal{F}_0, \mathcal{F}_1, \ldots, \mathcal{F}_m, \ldots, \mathcal{F}_n, \ldots$ defined on a non-empty sample space Ω, indexed by time and satisfying the nesting property $\mathcal{F}_m \subseteq \mathcal{F}_n$ whenever $m < n$. As time moves forward from 0 to n, information accumulates, which means $\mathcal{F}_n$ holds more information than the previous σ-algebras in the sequence, especially $\mathcal{F}_i$ for $i = 0, 1, 2, \ldots, n-1$. This increasing sequence of σ-algebras is referred to as a *filtration*. Next, the continuous-time formulation of filtrations will be discussed.

Definition 2.1.8 (Filtration)**.** Let Ω be a non-empty sample space. For each $t \geq 0$, assume there exists a σ-algebra $\mathcal{F}_t$ on Ω such that $\mathcal{F}_s \subseteq \mathcal{F}_t$ whenever $0 \leq s \leq t$. Then, the collection $\{\mathcal{F}_t : t \geq 0\}$ is called a *filtration*. A probability space $(\Omega, \mathcal{F}, \mathbb{P})$ equipped with such a filtration, where $\mathcal{F}_t \subseteq \mathcal{F}$ for each $t \geq 0$, is referred to as a *filtered probability space*, denoted by $(\Omega, \mathcal{F}, \{\mathcal{F}_t\}_{t\geq 0}, \mathbb{P})$.

A stochastic process $\{X_t : t \geq 0\}$ on a filtered probability space $(\Omega, \mathcal{F}, \{\mathcal{F}_t\}_{t\geq 0}, \mathbb{P})$ is called *adapted* if for every $t \geq 0$, the random variable X_t is measurable with respect to $\mathcal{F}_t$.

Definition 2.1.9 (Martingale)**.** On a filtered probability space $(\Omega, \mathcal{F}, \{\mathcal{F}_t\}_{t\geq 0}, \mathbb{P})$, an adapted stochastic process $\{X_t : t \geq 0\}$ is called a *martingale* if the expected absolute value $\mathbb{E}[|X_t|]$ is finite for every $t \geq 0$, and if for all $0 \leq s < t$, the conditional expectation

of X_t given $\mathcal{F}_s$ equals to X_s, i.e.,

$$\mathbb{E}\left[X_t \mid \mathcal{F}_s\right] = X_s.$$

Definition 2.1.10 (Brownian motion)**.** A stochastic process $\{W_t : t \geq 0\}$ on a probability space $(\Omega, \mathcal{F}, \mathbb{P})$ is called *Brownian motion* or *Wiener process* with drift μ and volatility σ ($\sigma > 0$) if it satisfies the following conditions:

(1) The initial value is zero, $W_0 = 0$;

(2) (Independent increments) For any sequence $0 < t_1 < \cdots < t_n$, the random variables W_{t_0}, $W_{t_1} - W_{t_0}$, $W_{t_2} - W_{t_1}$, ..., $W_{t_n} - W_{t_{n-1}}$ are independent; and

(3) (Normal increments) the increment $W_t - W_s$ is normally distributed with mean μ and variance $\sigma^2(t-s)$ for all $0 \leq s < t$.

This Brownian motion $\{W_t : t \geq 0\}$ is referred to as *standard* if $\mu = 0$ and $\sigma = 1$.

For each $\omega \in \Omega$, the sample path $t \mapsto X_t(\omega)$ of Brownian motion$\{W_t : t \geq 0\}$ is a continuous and nowhere differentiable function of t.

Definition 2.1.11 (Filtration for Brownian motion)**.** Let $(\Omega, \mathcal{F}, \{\mathcal{F}_t\}_{t\geq 0}, \mathbb{P})$ be a filtered probability space on which a Brownian motion $\{W_t : t \geq 0\}$ is defined. If

(1) (Adaptivity) each random variable W_t is measurable with respect to $\mathcal{F}_t$ for all $t \geq 0$; and

(2) (Independence of future increments) for any $0 \leq s < t$, the increment $W_t - W_s$ is independent of the σ-algebra $\mathcal{F}_s$;

then $\{\mathcal{F}_t : t \geq 0\}$ is called the *filtration associated with* the process $\{W_t : t \geq 0\}$.

Consider a Brownian motion $\{W_t : t \geq 0\}$ defined on a probability space $(\Omega, \mathcal{F}, \mathbb{P})$. Let $\mathcal{F}_t$ denote the σ-algebra that is generated by the set of random variables $\{X_s :$

$0 \leq s \leq t\}$. It can be verified that $\{\mathcal{F}_t : t \geq 0\}$ is a filtration for the Brownian motion $\{W_t : t \geq 0\}$. This filtration is commonly referred to as the *filtration generated by the Brownian motion* $\{W_t : t \geq 0\}$. Moreover, with respect to any such filtration, the Brownian motion qualifies as a martingale.

Now, we are ready to introduce two versions of Itô's Lemma.

Theorem 2.1.4 (Itô's Lemma for Brownian Motion)**.** *Let $f(t, x)$ be a twice continuously differentiable function. Let $\{W_t : t \geq 0\}$ be a standard Brownian motion defined on a probability space $(\Omega, \mathcal{F}, \mathbb{P})$. Then*

$$df(t, W_t) = \frac{\partial f}{\partial t}(t, W_t)\, dt + \frac{\partial f}{\partial x}(t, W_t)\, dW_t + \frac{1}{2}\frac{\partial^2 f}{\partial x^2}(t, W_t)\, dt. \tag{2.6}$$

Next, we provide an extension of Theorem 2.1.4 to Itô processes. First, let us recall the definition of an Itô process. A stochastic process $\{X_t : t \geq 0\}$ on a filtered probability space $(\Omega, \mathcal{F}, \{\mathcal{F}_t\}_{t\geq 0}, \mathbb{P})$ is called an *Itô process* if it satisfies

$$dX_t = \mu_t dt + \sigma_t dW_t$$

where $\{\mu_t : t \geq 0\}$ and $\{\sigma_t : t \geq 0\}$ are $\mathcal{F}_t$-adapted processes such that

$$\int_0^T |\mu_t| dt < \infty \quad \text{and} \quad \int_0^T \sigma_t^2 dt < \infty,$$

and $\{W_t : t \geq 0\}$ is a standard Brownian motion on $(\Omega, \mathcal{F}, \{\mathcal{F}_t\}_{t\geq 0}, \mathbb{P})$ associated with the filtration $\{\mathcal{F}_t : t \geq 0\}$, refer to (Klebaner, 2005) or (Shreve, 2008).

Theorem 2.1.5 (Itô Lemma for Itô processes)**.** *Let $\{X_t : t \geq 0\}$ be an Itô process defined on a filtered probability space $(\Omega, \mathcal{F}, \{\mathcal{F}_t\}_{t\geq 0}, \mathbb{P})$ such that*

$$dX_t = \mu_t dt + \sigma_t dW_t,$$

and let $f(t,x)$ be a twice continuously differentiable function. Then,

$$df(t,X_t) = \frac{\partial f}{\partial t}(t,W_t)\,dt + \frac{\partial f}{\partial x}(t,W_t)\,\mu_t dt + \frac{\partial f}{\partial x}(t,W_t)\,\sigma_t dW_t + \frac{1}{2}\frac{\partial^2 f}{\partial x^2}(t,W_t)\,\sigma_t^2 dt. \tag{2.7}$$

In addition to Brownian motion, financial modeling also requires the concept of geometric Brownian motion. Essentially, a geometric Brownian motion (GBM), also called exponential Brownian motion, is a continuous-time stochastic process where the logarithm of the variable evolves according to a Brownian motion (Ross, 2014).

Next, we present a rigorous definition of geometric Brownian motion.

Definition 2.1.12 (Geometric Brownian Motion)**.** A stochastic process $\{X_t : t \geq 0\}$ on a probability space $(\Omega, \mathscr{F}, \mathbb{P})$ is called a *geometric Brownian motion* if it satisfies the following stochastic differential equation (SDE):

$$dX_t = \mu X_t\,dt + \sigma X_t\,dW_t, \tag{2.8}$$

where μ and σ are constants, and $\{W_t : t \geq 0\}$ is a standard Brownian motion. Here, μ is called the *drift* and σ is called the *volatility* of $\{X_t : t \geq 0\}$.

Applying Theorem 2.1.5 to function $f(x) = \ln x$, we can solve Equation (2.8) to obtain

$$X_t \;=\; X_0 \exp\left(\left(\mu - \frac{\sigma^2}{2}\right)t + \sigma W_t\right). \tag{2.9}$$

Equation (2.9) implies that for any time $t \geq 0$, X_t is a random variable with a lognormal distribution. Moreover, the expectation and variance of X_t are given by

$$\mathbb{E}[X_t] = X_0 e^{\mu t} \quad \text{and} \quad \text{Var}[X_t] = X_0^2 e^{2\mu t}\left(e^{\sigma^2 t} - 1\right). \tag{2.10}$$

2.1.5 Infinitesimal Generators and Invariant Distributions

In this subsection, invariant distributions and infinitesimal generators for stochastic processes are introduced. Let $\{X_t : t \geq 0\}$ be a stochastic process on a filtered probability space $(\Omega, \mathcal{F}, \{\mathcal{F}_t\}_{t\geq 0}, \mathbb{P})$.

Definition 2.1.13. (Oksendal, 2013) The *infinitesimal generator* $\mathcal{L}$ of $\{X_t : t \geq 0\}$ is defined by

$$\mathcal{L}f(x) = \lim_{t\to 0} \frac{\mathbb{E}[f(X_t)|X_0 = x] - f(x)}{t}$$

for any function $f(\cdot)$.

Now, we assume that $\{X_t : t \geq 0\}$ is a time-homogeneous Itô process, i.e.,

$$dX_t = r(X_t)dt + \sigma(X_t)dW_t,$$

and the function $f(\cdot)$ is twice continuously differentiable. By Theorem 2.1.5, we get the following equation

$$df(X_t) = \left[r(X_t)\frac{\partial f(X_t)}{\partial x} + \frac{1}{2}\sigma^2(X_t)\frac{\partial^2 f(X_t)}{\partial x^2}\right]dt + \sigma(X_t, t)\frac{\partial f(X_t)}{\partial x}dW_t.$$

Then

$$M_t = f(X_t) - \int_0^t \left[r(X_s)\frac{\partial f(X_s)}{\partial x} + \frac{1}{2}\sigma^2(X_s)\frac{\partial^2 f(X_s)}{\partial x^2}\right]ds \tag{2.11}$$

defines a martingale. Evaluating the expectations on both sides of Equation (2.11) and

reorganizing the resulting terms give

$$\mathbb{E}[f(X_t)|X_0 = x] - f(x) = \mathbb{E}\left[\int_0^t \left[r(X_s)\frac{\partial f(X_s)}{\partial x} + \frac{1}{2}\sigma^2(X_s)\frac{\partial^2 f(X_s)}{\partial x^2}\right] ds \middle| X_0 = x\right]. \tag{2.12}$$

According to Definition 2.1.13, if we divide Equation (2.12) by t and take the limits as $t \to 0$, we obtain

$$\begin{aligned}
\mathcal{L}f(x) &= \mathbb{E}\left[\lim_{t\to 0}\frac{1}{t}\int_0^t \left[r(X_s)\frac{\partial f(X_s)}{\partial x} + \frac{1}{2}\sigma^2(X_s)\frac{\partial^2 f(X_s)}{\partial x^2}\right] ds \middle| X_0 = x\right], \\
&= \mathbb{E}\left[\lim_{t\to 0}\left[r(X_t)\frac{\partial f(X_t)}{\partial x} + \frac{1}{2}\sigma^2(X_t)\frac{\partial^2 f(X_t)}{\partial x^2}\right] \middle| X_0 = x\right], \\
&= r(x)\frac{\partial f}{\partial x} + \frac{1}{2}\sigma^2(x)\frac{\partial^2 f}{\partial x^2}.
\end{aligned} \tag{2.13}$$

Thus, Equation (2.13) gives the infinitesimal generator of the process $\{X_t : t \geq 0\}$. Note that $\{X_t : t \geq 0\}$ only depends on the running time (not on a specific time), since it is time-homogeneous.

Given a distribution of X_0, if X_t has the same distribution for all $t > 0$, then this distribution is called an *invariant distribution* for $\{X_t : t \geq 0\}$. To determine an invariant distribution of $\{X_t : t \geq 0\}$, we try to find the distribution of X_0 such that

$$\frac{d}{dt}\mathbb{E}[f(X_t)] = \frac{d}{dt}\mathbb{E}[\mathbb{E}[f(X_t)|X_0]] = 0, \tag{2.14}$$

where $f(\cdot)$ is an arbitrary function. Moreover, based on Definition 2.1.13, Equation

(2.14) can be rewritten as

$$\begin{aligned}\frac{d}{dt}\mathbb{E}[f(X_t)] &= \lim_{\Delta t\to 0}\frac{\mathbb{E}[f(X_{t+\Delta t})]-\mathbb{E}[f(X_t)]}{\Delta t}\\ &= \mathbb{E}\left[\lim_{\Delta t\to 0}\frac{\mathbb{E}[f(X_{t+\Delta t}|X_t)]-f(X_t)}{\Delta t}\right]\\ &= \mathbb{E}\left[\lim_{\Delta t\to 0}\frac{\mathbb{E}[f(X_{\Delta t}|X_0)]-f(X_0)}{\Delta t}\right]\\ &= \mathbb{E}[\mathcal{L}f(X_0)] = 0. \end{aligned} \tag{2.15}$$

Hence, an invariant distribution for $\{X_t : t \geq 0\}$ must satisfy $\mathbb{E}[\mathcal{L}f(X_0)] = 0$ for an arbitrary function $f(\cdot)$. Next, as an example, we discuss the Cox-Ingersoll-Ross (CIR) process $\{V_t : t \geq 0\}$, which satisfies the following stochastic differential equation:

$$dV_t = a(\theta - V_t)\,dt + \sigma\sqrt{V_t}\,dW_t, \tag{2.16}$$

where $\{W_t : t \geq 0\}$ is a standard Brownian motion, and a, θ and σ are positive parameters. The parameter θ is the long-term mean value of $\{V_t : t \geq 0\}$, a is the value of reverting speed to θ, and σ is volatility. By Equation (2.13), the infinitesimal generator of $\{V_t : t \geq 0\}$ can be obtained as follows

$$\mathcal{L} = a(\theta - v)\frac{\partial}{\partial v} + \frac{1}{2}\sigma^2 v\frac{\partial^2}{\partial v^2}. \tag{2.17}$$

Now, we find an invariant distribution for the CIR process $\{V_t : t \geq 0\}$. According to Definition 2.1.13 and Equation (2.15), an invariant distribution for the CIR process in (2.16) must satisfy the equation $\mathbb{E}[\mathcal{L}f(V_0)] = 0$ for an arbitrary function $f(\cdot)$. If the probability density function of this distribution is defined by Φ_{CIR}, then

$$\mathbb{E}[\mathcal{L}f(V_0)] = \int_0^\infty \Phi_{\mathrm{CIR}}(v)\mathcal{L}f(v)dv = 0, \tag{2.18}$$

where Φ_{CIR} also should satisfy the following conditions

$$\Phi_{\mathrm{CIR}}(0) = 0, \tag{2.19}$$

$$\Phi_{\mathrm{CIR}}(v) \to 0, \qquad \text{as } v \to \infty, \tag{2.20}$$

$$v\Phi_{\mathrm{CIR}}(v) \to 0, \qquad \text{as } v \to \infty, \tag{2.21}$$

$$v\Phi'_{\mathrm{CIR}}(v) \to 0, \qquad \text{as } v \to \infty, \tag{2.22}$$

and the function $f(\cdot)$ and its derivative are bounded. Moreover, using integration by parts, we can rewrite Equation (2.18) as

$$\int_0^\infty f(v)\mathcal{L}^*\Phi_{\mathrm{CIR}}(v)dv = 0, \tag{2.23}$$

where $\mathcal{L}^*$ is the adjoint operator of $\mathcal{L}$ and is defined by

$$\mathcal{L}^* = -a\frac{\partial}{\partial v}((\theta - v)\cdot) + \frac{1}{2}\sigma^2\frac{\partial^2}{\partial v^2}(v\cdot). \tag{2.24}$$

To guarantee that Equation (2.23) holds for an arbitrary smooth function $f(\cdot)$, we must have

$$\mathcal{L}^*\Phi_{\mathrm{CIR}}(v) = 0. \tag{2.25}$$

Then the unique solution to Equation (2.25) with the constraint $\int_0^\infty \Phi_{\mathrm{CIR}}(v)dv = 1$ is the Gamma distribution with the following form

$$\Phi_{\mathrm{CIR}}(v) = \frac{\left(\frac{2a}{\sigma^2}\right)^{\frac{2a\theta}{\sigma^2}}}{\Gamma\left(\frac{2a\theta}{\sigma^2}\right)} e^{-\frac{2av}{\sigma^2}} v^{\frac{2a\theta}{\sigma^2}-1}, \tag{2.26}$$

where Γ is the gamma function, refer to (Fouque et al., 2011, Chapter 3) for details. Thus, we have obtained the invariant distribution Φ_{CIR} of the CIR process. It is important to

note that Φ_{CIR} only meets additional conditions (2.19)–(2.22) when $2a\theta > \sigma^2$.

In the subsequent chapters, we will use $\langle f \rangle$ to denote the expectation of a function $f(\cdot)$ with respect to the invariant distribution Φ_{CIR} of the CIR process $\{V_t : t \geq 0\}$ defined in Equation (2.16), that is,

$$\langle f(v) \rangle \quad = \int_0^\infty f(v)\Phi_{\mathrm{CIR}}(v)dv.$$

The following lemma, which is related to the growth condition on the solutions to the equation $\mathcal{L}p(x,v) = 0$, is useful in Chapters 3 and 4.

Lemma 2.1.1. *Let $\mathcal{L}$ be the infinitesimal generator of the CIR process. Assume that the equation $\mathcal{L}p(x,v) = 0$ admits only solutions that do not grow as fast as*

$$\frac{\partial p(x,v)}{\partial v} \quad \sim \quad v^{-\frac{2a}{\sigma^2}\theta}\, e^{\frac{2a}{\sigma^2}v}$$

when $v \to \infty$. Then the solution p does not depend on the variable v.

Proof. The equation $\mathcal{L}p(x,v) = 0$ can be re-written as

$$\frac{\partial^2 p(x,v)}{\partial v^2} \Big/ \frac{\partial p(x,v)}{\partial v} = \frac{2a}{\sigma^2} - \frac{2a\theta}{\sigma^2 v}.$$

Integrating both sides of the above equation yields

$$\ln\left(\frac{\partial p(x,v)}{\partial v}\right) = \frac{2a}{\sigma^2}v - \frac{2a\theta}{\sigma^2}\ln v + c(x),$$

which implies

$$\frac{\partial p(x,v)}{\partial v} = e^{c(x)}\, v^{-\frac{2a}{\sigma^2}\theta}\, e^{\frac{2a}{\sigma^2}v},$$

and thus the result follows. □

2.1.6 Poisson Equation

The CIR process defined in Equation (2.16) has the mean reverting property, which is closely related to the concept of ergodicity. Generally, a stochastic process is called *ergodic* if it admits a unique invariant distribution, and the long-time time average of any measurable bounded function of the process converges almost surely to the statistical average of the same function with respect to the invariant distribution (Fouque et al., 2011). It is known that the CIR process is a Markov, ergodic, time-homogeneous and reversible process. Here, *reversibility* means that its infinitesimal generator $\mathcal{L}$ is self-adjoint on the space $L^2(\Phi_{\mathrm{CIR}})$, that is,

$$\langle f\mathcal{L}g\rangle = \langle g\mathcal{L}f\rangle \tag{2.27}$$

for all test functions f, g in $L^2(\Phi_{\mathrm{CIR}})$. The partial differential equation of the following form

$$\mathcal{L}\phi(v) + f(v) = 0, \tag{2.28}$$

is called a *Poisson equation* associated with the CIR process given in (2.16).

Lemma 2.1.2. *For a given function f in $L^2(\Phi_{\mathrm{CIR}})$ space, the Poisson equation* (2.28) *has a solution ϕ if and only if the function f satisfies the following condition*

$$\langle f\rangle = 0, \tag{2.29}$$

which is called the solvability or centring condition.

Proof. This is a version of the Fredholm alternative theorem. For more details, refer to (Ramm, 2001) or Section 3.2 in (Fouque et al., 2011). □

2.1.7 Feynman-Kac Theorem

Feynman-Kac Theorem is a widely used tool for solving derivative pricing problems in financial mathematics. It establishes a connection between partial differential equations (PDEs) and stochastic differential equations (SDEs) that can obtain the PDE solution by using probabilistic methods. In this subsection, we introduce Feynman-Kac Theorem in one-dimensional and multidimensional cases. More details on Feynman-Kac Theorem can be found in (Shreve, 2008) and other references.

Theorem 2.1.6. (Shreve, 2008) *Considering a one-dimensional stochastic process* $\{X_t : t \geq 0\}$ *on a probability space* $(\Omega, \mathcal{F}, \mathbb{Q})$*, which satisfies the following stochastic differential equation:*

$$dX_t = a(X_t, t)dt + b(X_t, t)dW_t, \tag{2.30}$$

where $\{W_t : t \geq 0\}$ *is a standard one-dimensional Brownian motion. Let* $h(\cdot)$ *be a Borel-measurable function and* $r > 0$ *be constant. Fix* $T > 0$ *and let* $0 \leq t \leq T$ *be given. Define the function* $P(x, t)$ *by letting*

$$P(x, t) := \mathbb{E}^{\mathbb{Q}}\left[e^{-r(T-t)}h(X_T)\middle|X_t = x\right]. \tag{2.31}$$

Then $P(x, t)$ *satisfies the following partial differential equation:*

$$\frac{\partial P}{\partial t} + a(x, t)\frac{\partial p}{\partial x} + \frac{1}{2}b(x, t)^2\frac{\partial^2 p}{\partial x^2} - rp(x, t) = 0, \tag{2.32}$$

with the terminal condition $P(x, T) = h(x)$ *for all* $x \in \mathbb{R}$*.*

In Chapters 3 and 4 of this thesis, we shall use a two-dimensional Feynman-Kac Theorem. So, we need to extend Theorem 2.1.6 to the multi-dimensional case. A multi-dimensional Feynman-Kac Theorem can be found in many references, e.g., (Fouque et

al., 2011), (Oksendal, 2013) and (Pham, 2009).

Theorem 2.1.7 ((Fouque et al., 2011)). *Consider an n-dimensional stochastic process $\{X_t : t \geq 0\}$ on a probability space $(\Omega, \mathcal{F}, \mathbb{Q})$, where $X_t = (X_t^1, \dots X_t^n)^\top$, which satisfies the following system of stochastic differential equations:*

$$dX_t^i = a_i(X_t, t)dt + b_{ij}(X_t, t)dW_t^i, \quad i = 1, \dots, n, \tag{2.33}$$

where $\{W_t^i : t \geq 0\}$, $i = 1, \dots, n$, are n uncorrelated standard Brownian motions. We assume that the functions $a_i(x,t)$ and $b_{ij}(x,t)$ are smooth and at most linearly growing at infinity, so that this system has a unique solution adapted to the filtration $\{\mathcal{F}_t : t \geq 0\}$ generated by the Brownian motions W_t^i, $i = 1, \dots, n$. Let $h(\cdot)$ be a Borel-measurable function and $r > 0$ be constant. Fix $T > 0$ and let $0 \leq t \leq T$ be given. Define the function $P(x,t)$ by letting

$$P(x,t) := \mathbb{E}^{\mathbb{Q}}\left[e^{-r(T-t)}h(X_T)\middle|X_t = x\right]. \tag{2.34}$$

Then the $P(x,t)$ satisfies the following partial differential equation:

$$\frac{\partial P}{\partial t} + \sum_{i=1}^{n} a_i(x,t)\frac{\partial P}{\partial x_i} + \frac{1}{2}\sum_{i,j=1}^{n}\left[b(x,t)\,b(x,t)^\top\right]_{ij}\frac{\partial^2 P}{\partial x_i \partial x_j} - r\,P(x,t) = 0 \tag{2.35}$$

with the terminal condition $P(x,T) = h(x)$ for all $x \in \mathbb{R}^n$.

2.2 Fundamentals of Quantitative Finance

In this section, we introduce some key concepts, theories and models in quantitative finance, including financial derivatives, risk-neutral pricing, and some mathematical models such as the Black-Scholes model, stochastic volatility models and multi-factor stochastic volatility models. This section also explores the asymptotic analysis method

used for pricing European-style derivatives, providing a theoretical basis for the subsequent numerical implementation. The core references for this section are (Black, 1975), (Broadie & Detemple, 2004), (Carr & Sun, 2007), (Christoffersen et al., 2009), (Cox et al., 1985), (Cox et al., 2014), (Fouque et al., 2000), (Fouque et al., 2011), (Grasselli, 2017), (Kariya & Liu, 2003) and (Merton, 1973).

2.2.1 Financial Derivatives

A financial derivative is a financial contract whose value is based on its underlying asset (such as stocks). The value of a derivative is derived from the price fluctuations of its underlying asset, rather than its own intrinsic value. Derivatives are mainly used for the following purposes: hedging, speculating, and arbitrage. In this thesis, we mainly consider options and real options.

An *option* is a type of agreement that gives the right, but not the obligation, to buy or sell an underlying asset at a predetermined price (called the *strike* or *exercise price*) before or on a specified future date (called the *maturity* or *expiry date*) in the future. A *call* option gives the buyer the right to buy, and a *put* option gives the buyer the right to sell. Generally, the basic components of options are underlying asset, strike price, expiration date and premium. Moreover, the buyer of the option pays a premium to the seller for this right (Broadie & Detemple, 2004). In simple words, an option contract is a contract about the right to buy or sell a specific commodity at a strike price before or at a maturity time in the future. Options can be categorized in different ways. For example, options can be divided into European options and American options based on whether the option can be exercised before maturity. *American* options can be exercised at any time before maturity; but *European* options can only be exercised at maturity time (Kariya & Liu, 2003). In this thesis, we mainly concern about European options. Options are a flexible and multi-functional financial tool that can help investors

effectively manage risks and returns and fulfill diverse investment needs; for example, options can be used to control risks and help investors reduce the volatility of investment portfolios (Cox et al., 2014; Kariya & Liu, 2003).

The valuation of a (European) option does not depend on the expected movement of the underlying asset (stock) at a specified stock price. In the case of stock, the value of an option (call option) on stock expected to go up has the same value as the option value (put option) on stock expected to decrease (Black, 1975). Let $\{X_t : 0 \leq t \leq T\}$ denote the underlying asset price, and then the payoff of a European call with the strike price K at the maturity time T is given by $\max\{X_T - K, 0\}$. When the market price of the underlying asset at the maturity is higher than the strike price (i.e., $X_T \geq K$), the call option will be exercised with return $X_T - K$. Similarly, the payoff of a European put with the strike price K at the maturity time T is given by $\max\{K - X_T, 0\}$. When the market price of the underlying asset at the maturity is lower than the strike price (i.e,. $X_T \leq K$), the put option will be exercised with return $K - X_T$. Otherwise, the option will not be executed, and the return is 0.

In 1977, Myers first proposed the concept of a real option that gives investors the right to buy or sell the underlying asset at an agreed price when the contract expires, rather than an obligation. The underlying assets of real options are real (non-financial) assets rather than financial assets (stock or futures). In simple words, the exercise result of real options is to deliver the underlying asset itself, not cash (Myers, 1977). Moreover, there is no suitable data available for references, as information related to real options is typically private and usually concerns internal investment opportunities. Real options are commonly used to guide investment decisions under uncertainty, especially in irreversible projects, by helping determine when to proceed with actions such as investing, expanding, or abandoning (Dixit & Pindyck, 1994).

In addition to constructing the theoretical framework of real options, Dixit and Pindyck in (Dixit & Pindyck, 1994) also described closed-form pricing formulas under

specific random assumptions. Let X_t denote the value of an investment project at time t. Assume that X_t satisfies the following stochastic differential equation:

$$dX_t = \alpha X_t\, dt + \sigma X_t\, dW_t^x, \tag{2.36}$$

where σ is the volatility of the project value, α is expected growth rate of the project. Then, the value of real option V, as a function of x (assume that $X_t = x$), is given by the following formula:

$$V(x) = \begin{cases} (x^* - K)\left(\dfrac{x}{x^*}\right)^{\mu}, & \text{if } x < x^*, \\ x - K, & \text{if } x \geq x^*, \end{cases} \tag{2.37}$$

where K is a sunk cost paid at an optimal point, x^* is the investment threshold value (free boundary value), μ is a positive value that determines the curvature of the value function, and the economically relevant solution requires $\mu > 1$ to ensure a finite option value and convexity of the value function. It satisfies the characteristic equation

$$\frac{1}{2}\sigma^2\mu(\mu - 1) + \alpha\mu - r = 0.$$

where r is the discount rate that is also can be understood as the "lowest rate of return", refer to (Dixit & Pindyck, 1994, Chapter 5).

2.2.2 Risk-Neutral Pricing

Let us define a probability space $(\Omega, \mathcal{F}, \mathbb{P})$ for the modeled asset prices. The probability measure $\mathbb{P}$ is referred to as the *real-world* measure (or called the *physical* measure) that can be used to explain the real expected rate of return of assets and the risk preferences of investors. When we use financial mathematics to value derivatives, our objective is

not merely to describe the evolution of asset prices, but more importantly, to construct a pricing framework that satisfies the no-arbitrage principle. However, it will not guarantee the consistency and satisfaction of the no-arbitrage principle if we price derivatives directly based on the real-world measure $\mathbb{P}$. The price evolution does not conform to the assumption of an arbitrage-free market, because the asset price under the real-world measure $\mathbb{P}$ reflects the risk premium of investors, which is not a risk-free interest rate. Thus, a risk-neutral measure, denoted by $\mathbb{Q}$, that satisfies the conditions of no arbitrage is constructed, which is derived from the inference of asset price evolution under real-world measurements. Under the risk-neutral measure, the discounted price process of any asset is a martingale, and the expected rate of asset return is a risk-free interest rate. The change of measure from the real-world measure $\mathbb{P}$ to the risk-neutral measure $\mathbb{Q}$ can be achieved via Girsanov's theorem.

Theorem 2.2.1. (Shreve, 2008, One-dimensional Girsanov Theorem) *Let* $\{W_t : 0 \le t \le T\}$ *be a one-dimensional standard Brownian motion defined on a probability space* $(\Omega, \mathcal{F}, \mathbb{P})$ *along with its filtration* $\{\mathcal{F}_t : 0 \le t \le T\}$. *Furthermore, an adapted process* $\{\Theta_t : 0 \le t \le T\}$ *is given. We define*

$$\begin{aligned} Z_t &= \exp\left(-\int_0^t \Theta_s dW_s - \frac{1}{2}\int_0^t \Theta_s^2 ds\right), \\ \widetilde{W}_t &= W_t + \int_0^t \Theta_s ds, \end{aligned} \tag{2.38}$$

and assume that the following condition

$$\mathbb{E}\left[\int_0^T \Theta_t^2 Z_t^2 dt\right] < \infty \tag{2.39}$$

is satisfied. Then $\mathbb{E}[Z_T] = 1$, *and under the probability measure* $\mathbb{Q}$, *defined by*

$$\mathbb{Q}(A) = \int_A Z(\omega) d\mathbb{P}(\omega) \quad \textit{for all } A \in \mathcal{F}, \tag{2.40}$$

the process $\{\widetilde{W}_t : 0 \le t \le T\}$ *is a one-dimension standard Brownian motion.*

Note that in Theorem 2.2.1, the probability measures $\mathbb{P}$ and $\mathbb{Q}$ are equivalent. Next, we demonstrate how Theorem 2.2.1 can be applied to risk-neutral pricing. Let $\{X_t : 0 \le t \le T\}$ be an asset price process on a real-world probability space $(\Omega, \mathcal{F}, \mathbb{P})$ and let $\{\mathcal{F}_t : 0 \le t \le T\}$ be a filtration for this process. Assume that $\{X_t : 0 \le t \le T\}$ satisfies the following stochastic differential equation:

$$dX_t = \alpha_t X_t\, dt + \sigma_t X_t\, dW_t, \quad 0 \le t \le T, \tag{2.41}$$

where the mean rate of return α_t and the volatility σ_t are allowed to be adapted processes, and $\{W_t : 0 \le t \le T\}$ is a standard Brownian motion under $\mathbb{P}$. The stock price logically is a generalized geometric Brownian motion and thus

$$X_t = X_0 \exp\left(\int_0^t \sigma_s dW_s + \int_0^t \left(\alpha_s - \frac{1}{2}\sigma_s^2\right) ds\right). \tag{2.42}$$

Moreover, if we have an adapted risk-free interest rate process $\{R_t : 0 \le t \le T\}$, and then we can define the discount process $\{D_t : 0 \le t \le T\}$ as follows:

$$D_t = \exp\left(-\int_0^t R_s ds\right). \tag{2.43}$$

Then, we have

$$dD(t) = -R_t D(t)\, dt. \tag{2.44}$$

Hence, the discounted asset price process is given by:

$$D_t X_t = X_0 \exp\left(\int_0^t \sigma_s dW_s + \int_0^t \left(\alpha_s - R_s - \frac{1}{2}\sigma_s^2\right) ds\right), \tag{2.45}$$

and the differential form of Equation (2.45) is given by

$$\begin{aligned} d(D_t X_t) &= (\alpha_t - R_t) D_t X_t dt + \sigma_t D_t X_t dW_t \\ &= \sigma_t D_t X_t \left[\frac{\alpha_t - R_t}{\sigma_t} dt + dW_t \right]. \end{aligned} \tag{2.46}$$

Let $\Theta_t = \frac{\alpha_t - R_t}{\sigma_t}$. Based on Theorem 2.2.1, we can define the standard Brownian motion $\{\widetilde{W}_t : 0 \le t \le T\}$ under the probability measure $\mathbb{Q}$ by

$$W_t := \widetilde{W}_t - \int_0^t \Theta_s ds. \tag{2.47}$$

Consequently, the discounted asset price under the measure $\mathbb{Q}$ can be expressed as:

$$D_t X_t = X_0 + \int_0^t \sigma_s D_s X_s d\widetilde{W}_s, \tag{2.48}$$

and $\int_0^t \sigma_s D_s X_s d\widetilde{W}_s$ is a martingale under $\mathbb{Q}$. Finally, by substituting W_t in Equation (2.47) into Equation (2.41), under the probability measure $\mathbb{Q}$, the asset price dynamics becomes:

$$dX_t = R_t X_t dt + \sigma_t X_t d\widetilde{W}_t. \tag{2.49}$$

As we can see, in Equation (2.49), the drift term is driven by the risk-free rate process $\{R_t : 0 \le t \le T\}$ under $\mathbb{Q}$.

2.2.3 Black–Scholes-Merton Model

In 1973, Black and Scholes proposed a mathematical model for pricing European options in (Black & Scholes, 1973). In the same year, Merton also consider the same problem in (Merton, 1973). Nowadays, this model is called the *Black-Scholes-Merton*

model. Under this model, the price system of a risky asset $\{X_t : 0 \le t \le T\}$ satisfies the following stochastic differential equation:

$$dX_t = \mu X_t dt + \sigma X_t dW_t, \quad 0 \le t \le T, \tag{2.50}$$

where μ and $\sigma > 0$ are constants, and $\{W_t : 0 \le t \le T\}$ is a standard Brownian motion. Here, μ is called the *drift* and σ is called *volatility*.

The Black-Scholes-Merton has several assumptions: All pricing should be conducted under the assumption of a no-arbitrage market; the asset pays no dividends or other distributions; the short-term interest rate and volatility are constant; the option should be a European option; and there are zero transaction costs when buying or selling the asset or the option. Short selling can be done without any penalties. Also, it is allowed to borrow any part of a security's price at the short-term interest rate to buy or hold it. Under these assumption, we first apply Theorem 2.2.1 to transform Equation (2.50) into the following SDE under the risk-neutral measure $\mathbb{Q}$:

$$dX_t = rX_t dt + \sigma X_t \, d\widetilde{W}_t, \quad 0 \le t \le T, \tag{2.51}$$

where r is the short-term risk-free interest rate and $\{\widetilde{W}_t : 0 \le t \le T\}$ is a standard Brownian motion under $\mathbb{Q}$. Applying Theorem 2.1.5, we can solve Equation (2.51) analytically to obtain

$$X_t = X_0 \exp\left(\left(r - \frac{1}{2}\sigma^2\right)t + \sigma\widetilde{W}_t\right). \tag{2.52}$$

Under the Black-Scholes-Merton model and its assumptions, the price C_t of a European call option with strike price K and maturity time T, at any time $0 \le t < T$, is

given by

$$C_t = e^{-r(T-t)}\mathbb{E}^{\mathbb{Q}}\left[\max\{X_T - K, 0\}\right]. \tag{2.53}$$

Black and Scholes derived the following formula for C_t in (Black & Scholes, 1973):

$$C_t = X_t N(d_1) - K e^{-r(T-t)} N(d_2), \tag{2.54}$$

where $N(\cdot)$ denotes the cumulative distribution function of the standard normal distribution, and d_1 and d_2 are given by

$$d_1 = \frac{\log(X_t/K) + \left(r + \frac{1}{2}\sigma^2\right)(T-t)}{\sigma\sqrt{T-t}}, \tag{2.55}$$

$$d_2 = d_1 - \sigma\sqrt{T-t}, \tag{2.56}$$

Equation (2.54) is called the *Black-Scholes pricing formula*. The price of a European put option with strike price K and maturity time T, at time $0 \leq t < T$, is given by

$$P_t = e^{-r(T-t)}\mathbb{E}^{\mathbb{Q}}\left[\max\{K - X_T, 0\}\right]. \tag{2.57}$$

Similarly, we can also derive the following pricing formula for P_t:

$$P_t = K e^{-r(T-t)} N(-d_2) - X_t N(-d_1). \tag{2.58}$$

Moreover, by using Theorem 2.1.6, we can derive the following PDE for C_t (or P_t):

$$\frac{\partial C}{\partial t} + \frac{1}{2}\sigma^2 S^2 \frac{\partial^2 C}{\partial S^2} + rS\frac{\partial C}{\partial S} - rC = 0. \tag{2.59}$$

Equation (2.59) is referred to as the *Black-Scholes PDE* in the literature.

2.2.4 Cox-Ingersoll-Ross Model

In 1985, Cox, Ingersoll and Ross introduced the Cox-Ingersoll-Ross model (for short, CIR model) to study the term structure of interest rates (Cox et al., 1985). The CIR model is a mean-reverting process that describes the tendency of some financial variables (such as interests rates and volatility) to revert to a long-term mean with a high probability, whether these financial variables are above or below the mean value. In this thesis, we will use the CIR model for modeling the instantaneous variance of return of a risky asset at time $t \geq 0$, denoted by V_t, due to the mean-reverting feature of volatility of risky assets.

We will continue to use Equation (2.16) to express the CIR process, as shown below:

$$dV_t = a(\theta - V_t)dt + \sigma\sqrt{V_t}dW_t,$$

where $\theta > 0$ is the long-term mean value of this variance process, $a > 0$ is the reverting speed of variance returns to the θ, $\sigma > 0$ is the volatility of the variance V_t and $\{W_t : t \geq 0\}$ is a standard Brownian motion on a probability space $(\Omega, \mathcal{F}, \mathbb{P})$. It can be shown that the above equation has a unique t-continuous solution V_t so that V_t is adapted to the σ-algebra generated by V_0 and all W_s, $s \leq t$ and

$$\mathbb{E}\left[\int_0^T |V_t|^2 dt\right] < \infty.$$

for any $T > 0$. Furthermore, it can be shown that if the following condition is satisfied

$$2a\theta \geq \sigma^2 \tag{2.60}$$

and $V_0 > 0$, then $V_t > 0$ for all $t > 0$. On the other hand, if this condition does not hold, then the process V_t almost surely hits zero in a finite time. Equation (2.60) is

called *Feller's condition* (Feller, 1951). The CIR process is ergodic and has an invariant distribution with probability density function given in Equation (2.26). It can be shown that the mean and variance of V_t are given by

$$\mathbb{E}[V_t] = \theta + e^{-at}(V_0 - \theta) \tag{2.61}$$

and

$$\mathbb{V}ar[V_t] = \frac{\sigma^2}{a} V_0 \left(e^{-at} - e^{-2at}\right) + \frac{\theta\sigma^2}{2a}\left(1 - 2e^{-at} + e^{-2at}\right), \tag{2.62}$$

respectively. Hence, the mean and variance of the invariant distribution are θ and $\frac{\theta\sigma^2}{2a}$, respectively.

2.2.5 Stochastic Volatility Models

In this subsection, we introduce different stochastic volatility models, including the Heston model, the 3/2 stochastic volatility model, the 4/2 stochastic volatility model, and multi-factor stochastic volatility models.

Heston Model

As mentioned in Subsection 2.2.3, in the Black-Scholes model, the volatility is assumed to be a constant. However, a lot of empirical evidence show that the volatility of an underlying price is not constant (Merton, 1973). To overcome this issue, many stochastic volatility models have been proposed and the Heston model, introduced by Heston in (Heston, 1993), is regarded as one of the most successful advancement by addressing a key limitation of the Black-Scholes model, as mentioned in Subsection 1.1. In the Heston model, the volatility follows a CIR process that is able to capture the volatility smile phenomenon in the real market. The Heston model can be expressed by

the following system of stochastic differential equations (SDEs):

$$\begin{aligned} dX_t &= rX_t dt + \sqrt{V_t} X_t dW_t^x, \\ dV(t) &= \kappa(\theta - V(t))dt + \sigma\sqrt{V(t)} dW_t^v, \end{aligned} \tag{2.63}$$

where X_t is the underlying price at time t, V_t is the variance of underlying asset price return at time t, r is the risk-free interest rate, $\{W_t^x : t \geq 0\}$ and $\{W_t^v : t \geq 0\}$ are correlated standard Brownian motion with correlation coefficient $-1 \leq \rho \leq 1$, i.e., $dW_t^x dW_t^v = \rho dt$, θ is a long-term mean-variance value of the underlying asset, κ is reverting speed for V_t to θ, and σ is called the *volatility of volatility*. Furthermore, V_t should satisfy Equation (2.60) to ensure the variance is a non-negative value. Although the Heston model can effectively capture the features of the volatility smile, it is unable to capture all features of market volatility. Specifically, its performance is less effective in highly volatile markets and under extreme market conditions.

3/2 Stochastic Volatility Models

As mentioned in Subsection 2.2.5, not all stochastic volatility models (such as the Heston model) are able to effectively capture the features of volatility under extreme market conditions or in some highly volatile market. To address these issues, Heston (1997) and Platen (1997) proposed the following 3/2 stochastic volatility model:

$$\begin{aligned} dX_t &= rX_t dt + \frac{b}{\sqrt{Z_t}} X_t dW_t^x \\ dZ_t &= \kappa(\theta - Z_t)dt + \sigma\sqrt{Z_t} dW_t^z, \end{aligned} \tag{2.64}$$

where r is risk free interest rate, b is a real number, κ is reverting speed, θ is the long term mean of variance V_t, σ is volatility of volatility, $\{W_t^x : t \geq 0\}$ and $\{W_t^z : t \geq 0\}$ are standard Brownian motions which satisfy $dW_t^x, dW_t^z = \rho\, dt$, with $-1 \leq \rho \leq 1$. From

Equation (2.64), it is unclear why this model is called the 3/2 stochastic volatility model. Let $V_t = \frac{1}{Z_t}$. Applying Theorem 2.1.5, we can convert Equation (2.64) to the following system of SDEs:

$$\begin{aligned} dX_t &= r\,X_t dt + b\sqrt{V_t}\,X_t dW_t^x, \\ dV_t &= \tilde{\kappa}V_t(\tilde{\theta} - V_t)dt + \tilde{\sigma}V_t^{3/2}dW_t^v, \end{aligned} \tag{2.65}$$

where $\tilde{\kappa}$, $\tilde{\theta}$ and $\tilde{\sigma}$ are given by

$$\tilde{\kappa} = \kappa\theta - \sigma^2, \qquad \tilde{\theta} = \frac{\kappa}{\kappa\theta - \sigma^2}, \quad \text{and} \quad \tilde{\sigma} = -\sigma. \tag{2.66}$$

Compared to the Heston model, the 3/2 stochastic volatility model augments the random volatility of variance to make the model effective in simulating the sharp volatility that is always observed in the market. Moreover, the simulation of the payoff results shows fatter tails, which are consistent with empirical observations. This fatter-tail property enhances the ability of the $3/2$ stochastic volatility model to measure and price risk in extreme situations because volatility tends to cluster and spike sharply during financial crises or extreme events. However, the non-affine diffusion term $V_t^{3/2}$ makes the calculation complexity of numerical approximation, which means higher computational costs. This non-affine feature also means that the 3/2 stochastic volatility model is not applicable in all scenarios (for example, high-frequency trading and other fast computing scenarios).

4/2 Stochastic Volatility Model

In 2017, Grasselli introduced a pricing model, which is called the *4/2 stochastic volatility model* (Grasselli, 2017). This model is designed to unify the Heston model and the 3/2 stochastic volatility model. Let X_t be the price of a financial asset and V_t be the

instantaneous variance of X_t at time t, respectively. Then the $4/2$ stochastic volatility model is given by the following system of stochastic differential equations:

$$\begin{aligned} dX_t &= rX_t dt + \left(a\sqrt{V_t} + \frac{b}{\sqrt{V_t}}\right) X_t dW_t^x, \\ dV_t &= \kappa(\theta - V_t)\, dt + \sigma\sqrt{V_t}\, dW_t^v, \end{aligned} \tag{2.67}$$

where κ, θ, σ are positive values with the same financial meanings as in those the CIR process, $a,\ b$ are real numbers, $\{W_t^x : t \geq 0\}$ and $\{W_t^v : t \geq 0\}$ are correlated standard Brownian motions on a probability space $(\Omega, \mathcal{F}, \mathbb{Q})$ such that $dW_t^x dW_t^v = \rho\, dt$ with $-1 \leq \rho \leq 1$. Moreover, we assume that the Feller condition $2\kappa\theta \geq \sigma^2$ is satisfied.

In the $4/2$ stochastic volatility model, the CIR (Heston model factor) and flipped CIR ($3/2$ stochastic volatility model factor) factors capture the smile and skew feature of the implied volatility surface. Moreover, the Heston model factor will predict a flattening of the implied volatility slope, while the 3/2 stochastic volatility model will predict a steepening of the slope as instantaneous volatility increases. In addition, when a and b are positive, the volatility process is uniformly bounded away from zero, with a lower bound greater than $2ab$. This is a feature that cannot be replicated in the Heston or 3/2 stochastic volatility models. The 4/2 stochastic volatility model can capture the volatility features that the Heston model and the 3/2 stochastic volatility model cannot describe alone. Theoretically, the 4/2 stochastic volatility model has all the advantages of the Heston model and the 3/2 stochastic volatility model.

Grasselli (2017) also proposed a closed-form solution to European derivative pricing under the $4/2$ stochastic volatility model. However, the complexity of this closed-form pricing formula limits its practical applicability in real-world markets. More details about this closed-form expression for the characteristic function of the log-asset price can be found in Grasselli (2017).

Multi-factor Stochastic Volatility Models

There is only one volatility factor to be considered to describe the reverting speed in the traditional single-factor stochastic volatility model (such as the Heston model). It is challenging to capture all the features of the dynamic volatility. Moreover, the correlation between asset returns and volatility is always considered constant (always denoted by ρ), which limits its ability to reflect the market situation, such as the effect of leverage to change over time. Thus, Christoffersen et al. (2009) introduced multi-factor stochastic volatility to overcome the problems that exist in the single-factor stochastic volatility model (Christoffersen et al., 2009).

Under the multi-factor stochastic volatility model, the underlying price dynamics follows the following system of stochastic partial differential equations:

$$\begin{aligned} dX_t &= r\,X_t\,dt \;+\; \sqrt{V_1}\,X_t\,dW_t^{x_1} \;+\; \sqrt{V_2}\,X_t\,dW_t^{x_2}, \\ dV_1 &= \kappa_1\big(\theta_1 - V_1\big)\,dt \;+\; \sigma_1\sqrt{V_1}\,dW_t^{v_1}, \\ dV_2 &= \kappa_2\big(\theta_2 - V_2\big)\,dt \;+\; \sigma_2\sqrt{V_2}\,dW_t^{v_2}, \end{aligned} \tag{2.68}$$

where X_t denotes the underlying price at time $t > 0$, V_1 and V_2 are independent volatility components of the asset return at time $t > 0$, and $r > 0$, $\kappa_i > 0$, $\theta_i > 0$ and $\sigma_i > 0$ $(i = 1, 2)$ are constants. Here, the variance of underlying return is the sum of two variance factors

$$\mathbb{V}\mathrm{ar}\left[\frac{dX_t}{X_t}\right]\Big/ dt \;= V_1 + V_2 := V.$$

In simple words, the variance is the sum of two uncorrelated factors that may individually influence the underlying asset returns based on different events. Among four Brownian motions $\{W_t^{x_1} : t \geq 0\}$, $\{W_t^{x_2} : t \geq 0\}$, $\{W_t^{v_1} : t \geq 0\}$ and $\{W_t^{v_2} : t \geq 0\}$ in Equation (2.68), we assume that $dW_t^{x_1} dW_t^{v_1} = \rho_1 dt$ and $dW_t^{x_2} dW_t^{v_2} = \rho_2 dt$, where $-1 \leq \rho_1, \rho_2 \leq 1$, but each of the pairs $W_t^{v_1}$ and $W_t^{v_2}$, $W_t^{x_1}$ and $W_t^{x_2}$, $W_t^{x_1}$ and $W_t^{v_2}$, $W_t^{x_2}$ and $W_t^{x_1}$ are

uncorrelated, respectively.

Compared to single-factor stochastic volatility models, this multi-factor stochastic volatility model makes up for the shortcomings that a single factor is often difficult to cover all information. This multi-factor stochastic volatility model is able to more accurately describe the changes in volatility smile because it decomposes the volatility into distinct components, such as short-term and long-term volatility. Moreover, the description of this multi-factor volatility model is more in line with the situation in the actual market, where multiple factors always work together.

2.2.6 Asymptotics for Pricing European Derivatives

In this subsection, we introduce an asymptotic method for pricing European derivatives, based on singular perturbation analysis. The details can be found in Chapter 5 of (Fouque et al., 2000). For this purpose, we assume that under the risk neutral probability measure $\mathbb{Q}$, the price dynamics of the underlying asset $\{X_t : t \geq 0\}$ follows the following system of SDEs:

$$\begin{aligned} dX_t &= rX_t\,dt + f(V_t)X_t\,dW_t^x, \\ dV_t &= \frac{1}{\epsilon}(\theta - V_t)\,dt + \frac{\xi}{\sqrt{\epsilon}}\sqrt{V_t}\,dW_t^v, \end{aligned} \tag{2.69}$$

where r is the risk-free interest rate, ϵ, θ and ξ are positive real numbers, $\{W_t^x : t \geq 0\}$ and $\{W_t^v : t \geq 0\}$ represent two correlated standard Brownian motions defined on a filtered probability space $(\Omega, \mathcal{F}, \{\mathcal{F}\}_{t\geq 0}, \mathbb{Q})$ with a corelation coefficient parameter $\rho \in [-1, 1]$. Here, please note that the process $\{V_t : t \geq 0\}$ is the CIR process given in (2.16) with $a = \frac{1}{\epsilon}$ and $\sigma = \frac{\xi}{\sqrt{\epsilon}}$.

We consider a European derivative given by its nonnegative payoff function $h(\cdot)$ and its maturity time T. Then, the price at time $t < T$ of this derivative, denoted by

$P^\epsilon(t,x,v)$, is given by

$$P^\epsilon(t,x,v) = \mathbb{E}^{\mathbb{Q}}\left[e^{-r(T-t)}h(X_T)|\, X_t = x, V_t = v\right].$$

By Theorem 2.1.7, P^ϵ satisfies the following partial differential equation:

$$\begin{aligned}\frac{\partial P^\epsilon}{\partial t} + \frac{1}{2}f(v)^2x^2\frac{\partial^2 P^\epsilon}{\partial x^2} + \frac{\rho\xi\sqrt{v}}{\sqrt{\epsilon}}xf(v)\frac{\partial^2 P^\epsilon}{\partial x\partial v} + \frac{\xi^2 v}{2\epsilon}\frac{\partial^2 P^\epsilon}{\partial v^2} \\ + \frac{1}{\epsilon}(\theta - v)\frac{\partial P^\epsilon}{\partial v} + r\left(x\frac{\partial P^\epsilon}{\partial x} - P^\epsilon\right) = 0 \end{aligned} \tag{2.70}$$

with the terminal condition $P^\epsilon(T,x,v) = h(x)$. Equation (2.70) can be re-written as

$$\begin{aligned}\mathcal{L}^\epsilon P^\epsilon(t,x,v) = 0, \quad 0 \le t < T, \\ P^\epsilon(T,x,v) = h(x),\end{aligned} \tag{2.71}$$

where the PDE operator $\mathcal{L}^\epsilon$ is decomposed as

$$\mathcal{L}^\epsilon = \tfrac{1}{\epsilon}\mathcal{L}_0 + \tfrac{1}{\sqrt{\epsilon}}\mathcal{L}_1 + \mathcal{L}_2 \tag{2.72}$$

with $\mathcal{L}_0$, $\mathcal{L}_1$ and $\mathcal{L}_2$ defined by

$$\begin{aligned}\mathcal{L}_0 &= (\theta - v)\partial_v + \frac{1}{2}\xi^2 v\partial_{vv}, \\ \mathcal{L}_1 &= \rho\xi\sqrt{v}xf(v)\partial_{xv}, \\ \mathcal{L}_2 &= \partial_t + \frac{1}{2}f(v)^2x^2\partial_{xx} + r\left(x\partial_x - \cdot\right).\end{aligned}$$

Furthermore, since Equation (2.71) is a singular perturbation problem, we are interested in an asymptotic solution P^ϵ of the form

$$P^\epsilon(t,x,v) = \sum_{i=0}^{\infty}(\sqrt{\epsilon})^i\, P_i(t,x,v),$$

where $P_0, P_1, \ldots$ are functions of t, x, v to be determined such that $P_0(T, x, v) = h(x)$. In most cases, we are primarily interested in the first two terms $P_0 + \sqrt{\epsilon}P_1$. The terminal condition for the second term is $P_1(T, x, v) = 0$.

Substituting the expansion form of P^ϵ into Equation (2.71) leads to

$$\frac{1}{\epsilon}\mathcal{L}_0 P_0 + \frac{1}{\sqrt{\epsilon}}\left(\mathcal{L}_0 P_1 + \mathcal{L}_1 P_0\right) + \left(\mathcal{L}_0 P_2 + \mathcal{L}_1 P_1 + \mathcal{L}_2 P_0\right) + \sqrt{\epsilon}\left(\mathcal{L}_0 P_3 + \mathcal{L}_1 P_2 + \mathcal{L}_2 P_1\right) + \cdots = 0. \tag{2.73}$$

Equating terms of order $1/\epsilon$, we mus have

$$\mathcal{L}_0 P_0 = 0. \tag{2.74}$$

Note that $\frac{1}{\epsilon}\mathcal{L}_0$ is the infinitesimal generator of the CIR process. Hence, under the condition of Lemma 2.1.1, P_0 does not depend on the variable v. Similarly, in order to eliminate the term in $1/\sqrt{\epsilon}$, we must have

$$\mathcal{L}_0 P_1 + \mathcal{L}_1 P_0 = 0. \tag{2.75}$$

Since P_0 is independent of v, we have $\mathcal{L}_1 P_0 = 0$. Again, under the condition of Lemma 2.1.1, from Equation (2.75), P_1 does not depend on the variable v. Having eliminated the terms of order $1/\epsilon$ and $1/\sqrt{\epsilon}$, we can continue to eliminate the terms of order 1, $\sqrt{\epsilon}$, ϵ, and so on successively, since we are interested in asymptotic approximations that are more and more accurate as the parameter ϵ goes to zero. The order-1 terms give

$$\mathcal{L}_0 P_2 + \mathcal{L}_1 P_1 + \mathcal{L}_2 P_0 = 0.$$

Since P_1 is independent of v, $\mathcal{L}_1 P_1 = 0$. So, this equation reduces to

$$\mathcal{L}_0 P_2 + \mathcal{L}_2 P_0 = 0. \tag{2.76}$$

Note that Equation (2.76) is a Poisson equation. Thus, by Lemma 2.1.2, we have $\langle \mathcal{L}_2 P_0 \rangle = 0$. Since P_0 does not depend on v, we obtain $\langle \mathcal{L}_2 \rangle P_0 = 0$. From the definition of $\mathcal{L}_2$, we deduce that $\langle \mathcal{L}_2 \rangle = \mathcal{L}_{\mathrm{BS}}(\overline{\sigma})$, where $\overline{\sigma}$ is given by $\overline{\sigma} = \sqrt{\langle f^2 \rangle}$. Therefore, the zero-order term P_0 is the solution to the Black-Scholes equation

$$\mathcal{L}_{\mathrm{BS}}(\overline{\sigma}) P_0 = 0 \tag{2.77}$$

with the terminal condition $P_0(T, x) = h(x)$. Once we obtain P_0, we can use Equation (2.76) to solve P_2. Having chosen P_0 such that the first three terms in Equation (2.73) are zero, the next-order term in $\sqrt{\epsilon}$ must be zero. In this way, we can determine the terms P_1, which is called *the first correction term*. Here, we do not discuss the details in general. However, we will solve the terms P_1 and P_2 for particular models in the subsequent chapters.

When we consider multiscale stochastic volatility models for pricing European derivatives, the previous singular perturbation analysis can be extended to multiscale perturbation analysis, including both regular and singular perturbation analysis. Chapter 4 of (Fouque et al., 2011) presents details on multiscale perturbation analysis. In Chapters 3 and 4 of this thesis, we will employ both singular and multiscale perturbation analysis in our models for pricing European derivatives.

2.3 Numerical Methods

This section introduces some numerical methods, including Monte Carlo simulation, the least squares Monte Carlo (LSM) approach, and the 4th-order Runge–Kutta method for solving ordinary differential equations. The core references for this section are (Hildebrand, 1987), (Longstaff & Schwartz, 2001), (Chen & Hong, 2007) and (Jäckel, 2002).

2.3.1 Monte Carlo Simulation

In financial mathematics, a few common scenarios of applications (such as complex derivatives and real options pricing) involve highly complex problems with multivariate, path-dependent, extreme events, or non-linear characteristics. The Monte Carlo simulation is a suitable choice for dealing with derivative pricing problems with uncertainty and complexity in the real market. Moreover, the essence of Monte Carlo simulation is that it can approximate the real results by simulating all possible future states with many random samples. This is the reason why Monte Carlo simulation is considered as a good tool to analyze and evaluate these complex financial pricing problems. More detailed characteristics of Monte Carlo simulations and their typical applications can be found in (Chen & Hong, 2007) and (Jäckel, 2002).

Monte Carlo simulation is an algorithm that normally generates a lot of paths to obtain the expected value of a random variable (simply by taking the average). The algorithms used in this thesis typically include four steps: defining initial parameters, generating sample paths, evaluating the payoff along each path, and calculating the expected value of payoff (Chen & Hong, 2007).

In this thesis, the Euler-Maruyama scheme is used to generate sample paths for stochastic variables. The Euler-Maruyama method extends the classical Euler method by integrating the randomness of Brownian motion, allowing it to handle the stochastic

differential equations. Let $\{X_t : 0 \le t \le T\}$ be a stochastic process which satisfies the following stochastic differential equation:

$$dX_t = \mu(X_t)\,dt + \sigma(X_t)\,dW_t, \quad \text{with} \quad X_0 = x,$$

where $\mu(X_t)$ is the drift term of this process, $\sigma(X_t)$ is the diffusion term of the process, $\{W_t : t \ge 0\}$ is a standard Brownian motion, and $X_0 = x$ is the initial condition. The Euler-Maruyama method simulates the path of a random process by changing the continuous time to discrete time. It can transform the stochastic differential equation into a form that can be numerically approximated by step-by-step iteration. In each step, the Euler-Maruyama method combines drift with Brownian motion to simulate and update the path of the process. More precisely, the interval $[0, T]$ is divided into N equal length sub-intervals, and each step is given by $\Delta t = \frac{T}{N}$. Then a discrete time grid can be obtained, as shown below:

$$0 = t_0 < t_1 < \cdots < t_{N-1} < t_N = T.$$

Under the Euler–Maruyama scheme, the value of the stochastic process X_t at time t_j is approximated by X_{t_j}, defined recursively as follows:

$$X_{t_j} = X_{t_{j-1}} + \mu(X_{t_{j-1}})\Delta t + \sigma(X_{t_{j-1}})\Delta W_{t_j}, \quad X_0 = X,$$

where $\Delta W_j = W_{t_j} - W_{t_{j-1}}$ is a normal distribution with mean 0 and variance Δt.

2.3.2 Least Squares Monte Carlo (LSM) Approach

Section 2.3.1 describes the traditional Monte Carlo simulation that can be used to obtain the expected value by simulating a huge number of sample paths for the given stochastic

process under a terminal condition. However, not all scenarios are suitable for the traditional Monte Carlo simulation. For example, as mentioned in Section 2.2.1, real options allow flexible exercise of the right at any time before maturity. Thus, real option pricing exhibits dynamic programming characteristics, as the decision-making process is staged so that choices are made at each stage and the choice of each stage will affect the future outcomes and payoffs. To deal with this type of problems, Longstaff & Schwartz (2001) proposed a regression-based algorithm called the *least squares Monte Carlo* (LSM) approach. This approach simulates lots of paths of a stochastic process (such as asset price or real project value) through Monte Carlo simulation. Moreover, it approximates the expectation of the "continue to hold" option through the least squares regression at each possible decision time. Then, the approximation of the optimal stopping strategy is achieved by comparing the simulated continuation value with the immediate exercise payoff to determine whether the option should be exercised at that point of time.

The valuation of a real option is used as an example to illustrate the key steps of the least squares Monte Carlo (LSM) approach (Longstaff & Schwartz, 2001). Let a stochastic process $\{X_t : 0 \le t \le T\}$ on a probability space $(\Omega, \mathcal{F}, \mathbb{Q})$ represent a project value. Monte Carlo simulation is used to generate N paths of the stochastic process X_t under the risk-neutral measure $\mathbb{Q}$ with the risk-free interest rate r:

$$X_{t_0}^{(i)}, X_{t_1}^{(i)}, \ldots, X_{t_M}^{(i)}, \quad i = 1, \ldots, N,$$

where $t_0 = 0 < t_1 < \cdots < t_M = T$. After simulating multiple paths of this stochastic process, we initialize the payoff at maturity time (or the project deadline) T, where the payoff is defined by

$$V_T = h(X_T) = \max(X_T - I, 0),$$

with I denoting the investment cost.

To determine the optimal exercise time, the LSM algorithm proceeds backward in time from maturity to the present time for each time step t_m, considering only those paths where the project value exceeds the investment cost. For these paths, a least squares regression is used to estimate the continuation value which is the expected payoff from holding the option. The regression uses the discounted future payoff as the dependent variable and the current project value as the independent variable in the following formula:

$$\mathbb{E}^{\mathbb{Q}}\left[e^{-r\Delta t}V_{t_{m+1}}^{(i)} \mid X_{t_m}^{(i)}\right] \approx \sum_{j=0}^{J} \beta_j \phi_j(X_{t_m}^{(i)}),$$

where $\phi_j(X_t)$, $j = 0, \cdots, J$, are basis functions (e.g., polynomials) of the current project value, Δt is the time step size and β_j, $j = 0, \cdots, J$, are the regression coefficients.

Next, the estimated continuation value is compared with the immediate exercise value. If the immediate exercise value is larger or equal to the estimated continuation value, $h(X_{t_m}) \geq \mathbb{E}^{\mathbb{Q}}\left[e^{-r\Delta t}V_{t_{m+1}}^{(i)} \mid X_{t_m}^{(i)}\right]$, then exercising the option is optimal at time t_m; otherwise, it is optimal to continue holding the option.

For each simulated path, the optimal exercise time $\tau^{(i)}$ is recorded. The estimated value of the real option is then obtained by averaging the discounted payoffs at optimal exercises time across all simulated paths.

$$\text{Real Option Value} \approx \frac{1}{N}\sum_{i=1}^{N} e^{-r\tau^{(i)}} h(X_{\tau^{(i)}}^{(i)}).$$

2.3.3 Runge-Kutta Methods

Runge-Kutta methods are commonly used numerical approaches for solving ordinary differential equations (ODEs) of the form:

$$\frac{dP}{dt} = f(t, P), \quad P(t_0) = P_0. \tag{2.78}$$

The most widely used member of this family is the classical fourth-order Runge-Kutta method (RK4), which approximates the solution with fourth-order accuracy. Given an initial value problem as described in Equation (2.78), and a step size $h > 0$, the RK4 method proceeds as follows:

$$\begin{aligned} P_{n+1} &= P_n + \frac{h}{6}(k_0 + 2k_1 + 2k_2 + k_3) + O(h^4), \\ t_{n+1} &= t_n + h, \end{aligned}$$

for $n = 0, 1, 2, \ldots$, where the intermediate values are computed as:

$$\begin{aligned} k_0 &= f(t_n, P_n), \\ k_1 &= f\left(t_n + \frac{1}{2}h, P_n + \frac{1}{2}hk_0\right), \\ k_2 &= f\left(t_n + \frac{1}{2}h, P_n + \frac{1}{2}hk_1\right), \\ k_3 &= f(t_n + h, P_n + hk_2). \end{aligned}$$

For more details, refer to Hildebrand (1987).

The RK4 method can also be extended to solve systems of ODEs. Consider the

following system:

$$\begin{aligned}\frac{dP}{dt} &= f(t,P,Q), \quad P(t_0) = P_0,\\ \frac{dQ}{dt} &= g(t,P,Q), \quad Q(t_0) = Q_0.\end{aligned}$$

In this case, the RK4 method provides the following approximations:

$$\begin{aligned}P_{n+1} &= P_n + \frac{h}{6}\left(k_0 + 2k_1 + 2k_2 + k_3\right) + O(h^4),\\ Q_{n+1} &= Q_n + \frac{h}{6}\left(m_0 + 2m_1 + 2m_2 + m_3\right) + O(h^4),\end{aligned}$$

where the intermediate quantities are defined as:

$$\begin{aligned}k_0 &= f(t_n, P_n, Q_n),\\ k_1 &= f\left(t_n + \frac{1}{2}h, P_n + \frac{1}{2}hk_0, Q_n + \frac{1}{2}hm_0\right),\\ k_2 &= f\left(t_n + \frac{1}{2}h, P_n + \frac{1}{2}hk_1, Q_n + \frac{1}{2}hm_1\right),\\ k_3 &= f(t_n + h, P_n + hk_2, Q_n + hm_2),\end{aligned}$$

and

$$\begin{aligned}m_0 &= g(t_n, P_n, Q_n),\\ m_1 &= g\left(t_n + \frac{1}{2}h, P_n + \frac{1}{2}hk_0, Q_n + \frac{1}{2}hm_0\right),\\ m_2 &= g\left(t_n + \frac{1}{2}h, P_n + \frac{1}{2}hk_1, Q_n + \frac{1}{2}hm_1\right),\\ m_3 &= g(t_n + h, P_n + hk_2, Q_n + hm_2).\end{aligned}$$

Again, we refer the reader to Hildebrand (1987) for further explanation and derivation.

Chapter 3

Pricing European Derivatives Under the Rescaled 4/2 Stochastic Volatility Model

3.1 Introduction

In this chapter, we consider the problem of pricing European derivatives under rescaled 4/2 stochastic volatility models. In Section 3.2, we introduce a rescaled mean-reverting 4/2 volatility model given in terms of a small positive parameter. In Section 3.3, we consider the problem of pricing European derivatives under the model set up in Section 3.2 and obtain a closed-form approximate pricing formula for European derivatives. In Section 3.4, we extend the rescaled mean-reverting 4/2 volatility model in Section 3.2 to a double-mean-reverting 4/2 stochastic volatility model, and present a closed-form approximate pricing formula for European derivatives. In Section 3.5, we do some numerical experiments about accuracy of our analytic formula obtained from the rescaled mean-reverting 4/2 volatility model, model calibration via market data and sensitivity analysis to volatility parameters. Finally, we give some concluding remarks in Section

3.6. The contents of this chapter are based on (Cao et al., 2023a) and (Cao et al., 2023b).

3.2 Rescaled Mean-reverting 4/2 Stochastic Volatility Model

In this section, we present a rescaled mean-reverting 4/2 stochastic volatility model. Let $\{X_t : t \geq 0\}$ be the price process of an asset. Under the risk-neutral probability measure $\mathbb{Q}$, we consider the following rescaled mean-reverting 4/2 stochastic volatility model:

$$\begin{aligned} dX_t &= rX_t\,dt + \left(a\sqrt{V_t} + \frac{b}{\sqrt{V_t}}\right) X_t\,dW_t^x, \\ dV_t &= \frac{1}{\epsilon}(\theta - V_t)\,dt + \frac{\xi}{\sqrt{\epsilon}}\sqrt{V_t}\,dW_t^v, \end{aligned} \tag{3.1}$$

where r is the risk-free interest rate, ϵ, θ and ξ are positive real numbers, a and b are real numbers, $\{W_t^x : t \geq 0\}$ and $\{W_t^v : t \geq 0\}$ represent two correlated standard Brownian motions defined on a filtered probability space $(\Omega, \mathcal{F}, \{\mathcal{F}_t\}_{t\geq 0}, \mathbb{Q})$ whose correlation coefficient parameter is $\rho \in [-1, 1]$. The Feller condition $2\theta \geq \xi^2$ is assumed to ensure that V_t is bounded below by zero.

If we take $a \neq 0$ and $b = 0$, (3.1) reduces to the Heston model. If we take $a = 0$ and $b \neq 0$, then (3.1) becomes the 3/2 model. In (3.1), ϵ governs the rate of mean-reversion and is assumed to be a small parameter satisfying $0 < \epsilon \ll 1$ and so the process $\{V_t : t \geq 0\}$ is fast mean-reverting. By substituting $a = \frac{1}{\epsilon}$, $b = \theta$, $\sigma = \frac{\xi}{\sqrt{\epsilon}}$, and $y = v$ into (2.26), we obtain the probability density function of the invariant distribution of $\{V_t : t \geq\}$ as

$$\Phi_{\text{CIR}}(v) = \frac{(2/\xi^2)^{\frac{2\theta}{\xi^2}}}{\Gamma(2\theta/\xi^2)} v^{\frac{2\theta}{\xi^2}-1} e^{-\frac{2v}{\xi^2}}.$$

We note that if ϵ goes to zero, then the variance approaches to the mean level θ, and thus (3.1) reduces to the Black-Scholes model with constant volatility $a\sqrt{\theta} + b/\sqrt{\theta}$.

In (3.1), the volatility of the asset is given by

$$\sigma_t := a\sqrt{V_t} + \frac{b}{\sqrt{V_t}}.$$

By Itô's formula, we have

$$\begin{aligned} d\sigma_t &= \frac{1}{\epsilon}\left[\frac{1}{2}(\theta - V_t)\left(\frac{a}{\sqrt{V_t}} - \frac{b}{V_t^{3/2}}\right) + \frac{1}{8}\xi^2\left(\frac{3b}{V_t^{3/2}} - \frac{a}{\sqrt{V_t}}\right)\right]dt \\ &\quad + \frac{1}{2\sqrt{\epsilon}}\xi\left(a - \frac{b}{V_t}\right)dW_t^v. \end{aligned} \tag{3.2}$$

If we define the quantity $\tilde{\rho}$ by

$$\begin{aligned} \tilde{\rho} &:= \operatorname{sign}(\sigma_t)\operatorname{sign}\left(a - \frac{b}{V_t}\right)\rho \\ &= \operatorname{sign}\left(a + \frac{b}{V_t}\right)\operatorname{sign}\left((a - \frac{b}{V_t})\rho\right), \end{aligned} \tag{3.3}$$

then ρ is not only one that controls the sign of $\tilde{\rho}$ and in fact the sign changes over time whenever the random process V_t crosses $\left|\frac{b}{a}\right|$. This indicates that leverage effect would not always hold. That is, the correlation between the asst return and its volatility change is not always negative. Sometimes, higher volatility risk can yield higher return on asset. Even in the Heston model case, the sign of $\tilde{\rho}$ is exactly the same as the sign of ρ. This random movement of leverage effect is also one of important reasons why the constant elasticity of variance (CEV) model of Cox in (Cox, 1975), one of the well-known local volatility models, needs to be extended, in order to capture the changing leverage effect. We refer the reader to, the stochastic-local volatility (SAB) model of Hagan et al. in (Hagan et al., 2002), the stochastic-local volatility (SVCEV) model of Choi et al. in (Choi et al., 2013) and the stochastic elasticity of variance (SEV) model of Kim et al. in (Kim et al., 2015) for further details on this matter.

3.3 Pricing European Derivatives under the Rescaled Mean-reverting 4/2 Stochastic Volatility Model

In this section, we consider the problem of pricing European derivatives under our model (3.1). Using the asymptotic approach in Section 2.2.6, we obtain a closed-form approximation formula for values of European derivatives.

We consider a European derivative given by its nonnegative payoff function $h(\cdot)$ and its maturity time T. Then, the price at time $0 < t < T$ of this derivative, denoted by $P^\epsilon(t,x,v)$, is given by

$$P^\epsilon(t,x,v) \;:=\; \mathbb{E}^{\mathbb{Q}}\left[e^{-r(T-t)}h(X_T) \mid X_t = x, V_t = v\right]. \tag{3.4}$$

Note that model (3.1) is a special case of (2.69) with

$$f(V_t) = a\sqrt{V_t} + \frac{b}{\sqrt{V_t}}.$$

Thus, by substituting

$$f(v) = a\sqrt{v} + \frac{b}{\sqrt{v}}$$

into Equation (2.70), we obtain that $P^\epsilon(t,x,v)$ satisfies the following PDE:

$$\mathcal{L}^\epsilon P^\epsilon(t,x,v) \;=\; 0, \quad 0 < t < T, \tag{3.5}$$

$$P^\epsilon(T,x,v) \;=\; h(x), \tag{3.6}$$

We decompose the operator $\mathcal{L}^\epsilon$ as follows:

$$\mathcal{L}^\epsilon = \frac{1}{\epsilon}\mathcal{L}_0 + \frac{1}{\sqrt{\epsilon}}\mathcal{L}_1 + \mathcal{L}_2,$$

where

$$\begin{aligned}\mathcal{L}_0 &:= \frac{1}{2}\xi^2 v\partial_{vv} + (\theta - v)\partial_v,\\ \mathcal{L}_1 &:= \rho\xi(av+b)\mathcal{D}_1\partial_v,\\ \mathcal{L}_2 &:= \partial_t + \frac{1}{2}\left(a\sqrt{v} + \frac{b}{\sqrt{v}}\right)^2\mathcal{D}_2 + r\left(\mathcal{D}_1 - I\right).\end{aligned} \tag{3.7}$$

Here, I is the identity operator, $\mathcal{D}_1$ and $\mathcal{D}_2$ are differential operators defined by $\mathcal{D}_1 = x\partial_x$ and $\mathcal{D}_2 = x^2\partial_{xx}$, respectively. As mentioned in Section 2.2.6, we are interested in an asymptotic solution P^ϵ of the form

$$P^\epsilon(t,x,v) = \sum_{i=0}^{\infty}(\sqrt{\epsilon})^i P_i(t,x,v).$$

Let $\bar{\sigma}_{4/2}$ denote the average of the volatility term $\sigma_{4/2}$ with respect to the invariant distribution Φ_{CIR}, i.e.,

$$\bar{\sigma}_{4/2} = \left\langle\left(a\sqrt{\cdot} + \frac{b}{\sqrt{\cdot}}\right)^2\right\rangle^{\frac{1}{2}},$$

and let $\mathcal{L}_{\text{BS}}(\bar{\sigma}_{4/2})$ denote the Black-Scholes pricing operator with constant volatility $\bar{\sigma}_{4/2}$, i.e.,

$$\mathcal{L}_{\text{BS}}(\bar{\sigma}_{4/2}) = \partial_t + \frac{1}{2}\bar{\sigma}_{4/2}^2\mathcal{D}_2 + r\left(\mathcal{D}_1 - I\right). \tag{3.8}$$

Then, following the asymptotic analysis in Section 2.2.6, the zero-order term P_0 is the solution of the following Black-Scholes equation

$$\mathcal{L}_{\text{BS}}(\bar{\sigma}_{4/2})P_0(t,x) = 0 \tag{3.9}$$

with the terminal condition $P_0(T,x) = h(x)$.

Now, let $\phi_{ab}(v)$ be a function defined by

$$\mathcal{L}_0\phi_{ab} = \left(a\sqrt{v} + \frac{b}{\sqrt{v}}\right)^2 - \left\langle\left(a\sqrt{\cdot} + \frac{b}{\sqrt{\cdot}}\right)^2\right\rangle. \tag{3.10}$$

We determine the terms P_1 and P_2 in the following proposition.

Proposition 3.3.1. *If $\phi_{ab}(v)$ is the solution to (3.10) and satisfies $\langle\phi_{ab}(\cdot)\rangle = 0$ and $\psi_{ab}(v)$ is the solution to*

$$\mathcal{L}_0\psi_{ab} = av\phi'_{ab}(v) + b\phi'_{ab}(v) - \left(a\langle\cdot\phi'_{ab}(\cdot)\rangle + b\langle\phi'_{ab}(\cdot)\rangle\right), \tag{3.11}$$

then the term P_1 satisfies the following PDE:

$$\begin{aligned}\mathcal{L}_{\mathrm{BS}}(\bar{\sigma}_{4/2})P_1(t,x) &= F\mathcal{D}_1\mathcal{D}_2P_0,\\ F &:= \frac{1}{2}\rho\xi\left(a\langle\cdot\,\phi'_{ab}(\cdot)\rangle + b\langle\phi'_{ab}(\cdot)\rangle\right).\end{aligned} \tag{3.12}$$

Furthermore, the term $P_2(t,s,v)$ is given by

$$P_2(t,s,v) = -\frac{1}{2}\phi_{ab}(v)\mathcal{D}_2P_0 + c(t,s),$$

where $c(t,s)$ is the solution to

$$\begin{aligned}\mathcal{L}_{\mathrm{BS}}(\bar{\sigma}_{4/2})c(t,s) &= \left(B_1\left(\mathcal{D}_1\right)^2\mathcal{D}_2 + B_2\left(\mathcal{D}_2\right)^2\right.\\ &\quad\left.-F^2(T-t)\left(\mathcal{D}_1\right)^2\left(\mathcal{D}_2\right)^2\right)P_0, \quad t<T,\\ c(T,s) &= 0,\end{aligned} \tag{3.13}$$

where B_1 and B_2 are, respectively, given by

$$\begin{aligned} B_1 &= -\frac{1}{2}(\rho\xi)^2\left(a\langle\cdot\,\psi'_{ab}(\cdot)\rangle + b\langle\psi'_{ab}(\cdot)\rangle\right), \\ B_2 &= \frac{1}{4}\left\langle\phi_{ab}(\cdot)\left(\left(a\sqrt{\cdot}+\frac{b}{\sqrt{\cdot}}\right)^2 - \left\langle\left(a\sqrt{\cdot}+\frac{b}{\sqrt{\cdot}}\right)^2\right\rangle\right)\right\rangle. \end{aligned} \tag{3.14}$$

Proof. Plugging

$$P^\epsilon(t,x,v) = \sum_{i=0}^{\infty}\left(\sqrt{\epsilon}\right)^i P_i(t,x,v)$$

into $\mathcal{L}^\epsilon P^\epsilon(t,x,v) = 0$, we obtain the PDE systems

$$\mathcal{L}_0 P_k + \mathcal{L}_1 P_{k-1} + \mathcal{L}_2 P_{k-2} = 0, \quad k = 0,1,2,..., \tag{3.15}$$

where $P_{-1} = 0$ and $P_{-2} = 0$ are defined. For the derivation of the second order term P_2, from

$$\mathcal{L}_0 P_2 + \mathcal{L}_2 P_0 = 0,$$

we observe that

$$\mathcal{L}_0 P_2 = -\mathcal{L}_2 P_0 = -\left(\mathcal{L}_2 - \langle\mathcal{L}_2\rangle\right) P_0 = -\frac{1}{2}\mathcal{L}_0(\phi_{ab}\mathcal{D}_2 P_0)$$

holds. Then P_2 is given in the form of

$$P_2(t,x,v) = -\frac{1}{2}\phi_{ab}(v)\mathcal{D}_2 P_0 + c(t,x)$$

for some function $c(t,x)$ independent of v. Puting $k = 3$ in (3.15) yields

$$\mathcal{L}_0 P_3 + \mathcal{L}_1 P_2 + \mathcal{L}_2 P_1 = 0.$$

This is a Poisson equation for P_3 with respect to $\mathcal{L}_0$. So, by Lemma 2.1.6, we have

$$\langle \mathcal{L}_1 P_2 + \mathcal{L}_2 P_1 \rangle = 0.$$

By plugging P_2 in this equation, we obtain

$$\mathcal{L}_{\text{BS}}(\bar{\sigma}_{4/2}) = \langle \mathcal{L}_2 \rangle P_1 = -\langle \mathcal{L}_1 P_2 \rangle = F \mathcal{D}_1 \mathcal{D}_2 P_0$$

with F given in Equation (3.12). It remains to find a PDE problem that $c(t, s)$ satisfies. We expect that the desired result comes from the PDE of $k = 4$, i.e.,

$$\mathcal{L}_0 P_4 + \mathcal{L}_1 P_3 + \mathcal{L}_2 P_2 = 0,$$

which is a Poisson equation. By Lemma 2.1.6, we have

$$\langle \mathcal{L}_1 P_3 + \mathcal{L}_2 P_2 \rangle = 0.$$

Now, we consider the two terms $\mathcal{L}_2 P_2$ and $\mathcal{L}_1 P_3$. For the term $\mathcal{L}_2 P_2$, we have

$$\begin{aligned} \langle \mathcal{L}_2 P_2 \rangle &= \left\langle \mathcal{L}_2 \left(-\frac{1}{2} \phi_{ab} \mathcal{D}_2 P_0 + c \right) \right\rangle \\ &= -\frac{1}{2} \langle \phi_{ab} \mathcal{D}_2 \mathcal{L}_2 P_0 \rangle + \langle \mathcal{L}_2 \rangle c \\ &= -\frac{1}{2} \mathcal{D}_2 \langle \phi_{ab} (\mathcal{L}_2 - \langle \mathcal{L}_2 \rangle) P_0 \rangle + \langle \mathcal{L}_2 \rangle c \\ &= -B_2 \mathcal{D}_2^2 P_0 + \langle \mathcal{L}_2 \rangle c. \end{aligned} \tag{3.16}$$

To consider the term $\mathcal{L}_1 P_3$, we first use

$$\mathcal{L}_0 P_3 + \mathcal{L}_1 P_2 + \mathcal{L}_2 P_1 = 0$$

and Lemma 2.1.6 to derive that

$$\begin{aligned}
\mathcal{L}_0 P_3 &= -(\mathcal{L}_1 P_2 - \langle \mathcal{L}_1 P_2 \rangle) - (\mathcal{L}_2 - \langle \mathcal{L}_2 \rangle) P_1 \\
&= \frac{1}{2}\rho_{sv}\xi(av+b)\phi'_{ab}\mathcal{D}_1\mathcal{D}_2 P_0 - \frac{1}{2}\rho_{sv}\xi\langle (a\cdot + b)\phi'_{ab}(\cdot)\rangle \mathcal{D}_1\mathcal{D}_2 P_0 \\
&\quad -\frac{1}{2}(\mathcal{L}_0\phi_{ab})\mathcal{D}_2 P_1 \\
&= \frac{1}{2}\rho_{sv}\xi\mathcal{L}_0(\psi_{ab}\mathcal{D}_1\mathcal{D}_2 P_0) - \frac{1}{2}\mathcal{L}_0(\phi_{ab}\mathcal{D}_2 P_1),
\end{aligned}$$

which leads to

$$P_3(t,x,v) = \frac{1}{2}\rho\xi\psi_{ab}\mathcal{D}_1\mathcal{D}_2 P_0 - \frac{1}{2}\phi_{ab}\mathcal{D}_2 P_1 + c_1(t,x)$$

for some function $c_1(t,)$ independent of v. Hence, $\langle \mathcal{L}_1 P_3 \rangle$ becomes

$$\langle \mathcal{L}_1 P_3 \rangle = -B_1\mathcal{D}_1^2\mathcal{D}_2 P_0 - F\mathcal{D}_1\mathcal{D}_2 P_1. \tag{3.17}$$

Finally, by inserting (3.16) and (3.17) into $\langle \mathcal{L}_1 P_3 + \mathcal{L}_2 P_2 \rangle = 0$, we obtain

$$\langle \mathcal{L}_2 \rangle c = \left(B_1\mathcal{D}_1^2\mathcal{D}_2 + B_2\mathcal{D}_2^2\right) P_0 + F\mathcal{D}_1\mathcal{D}_2 P_1.$$

So, from

$$P_1 = -(T-t)F\mathcal{D}_1\mathcal{D}_2 P_0,$$

the function c satisfies the PDE in (3.13). The singular perturbation problem creates a terminal layer near expiration. The appropriate terminal condition for the second order term P_2 is $\langle P_1(T,x,\cdot)\rangle = 0$ as discussed by Fouque et al. in (Fouque et al., 2016). Using the assumption $\langle \phi(\cdot)\rangle = 0$, we obtain the terminal condition $c(T,x) = 0$. □

Solving Equations (3.9) and (3.12), we obtain an approximate derivative price

formula given by

$$\tilde{P}^{\epsilon}(t,x) \coloneqq P_0(t,x) + \sqrt{\epsilon}P_1(t,x).$$

We can use this formula to calculate $\tilde{P}^{\epsilon}(t,x)$ by starting the calculation of the Black-Scholes derivative price P_0 and some of call option Greeks. In fact, $\tilde{P}^{\epsilon}$ is a linear combination of the Black-Scholes price P_0 and two Greeks, Gamma $\frac{\partial^2 P_0}{\partial s^2}$ and Speed $\frac{\partial^3 P_0}{\partial s^3}$ as shown below in Proposition 3.3.2. Gamma is a measure of the convexity of a derivative's price which is important for a trader who seeks to set up an effective delta-hedge for a portfolio over a wider range of underlying price movements. Speed is an important Greek to monitor when a trader delta-hedges a portfolio.

Proposition 3.3.2. *Under the risk-neutral dynamics (3.1) of the underlying asset price, the derivative price defined by (3.4) is approximated by*

$$\tilde{P}^{\epsilon}(t,x) \coloneqq P_0(t,x) + \sqrt{\epsilon}P_1(t,x),$$

which is

$$\tilde{P}^{\epsilon}(t,x) \;=\; P_{\text{BS}}(\bar{\sigma}_{4/2})(t,x) - (T-t)F^{\epsilon}\mathcal{D}_1\mathcal{D}_2 P_{\text{BS}}(\bar{\sigma}_{4/2})(t,x), \tag{3.18}$$

where

$$F^{\epsilon} \;\coloneqq\; \frac{1}{2}\sqrt{\epsilon}\,\rho\xi\left(a\langle\cdot\,\phi'_{ab}(\cdot)\rangle + b\langle\phi'_{ab}(\cdot)\rangle\right)$$

and $P_{\text{BS}}(\bar{\sigma}_{4/2})(t,x)$ is the solution to the first equation for $P_0(t,x)$ in (3.9) with the terminal condition $P_0(T,x) = h(x)$.

Proof. The solution of the first PDE in (3.9) with the final condition $P_0(T,x) = h(x)$ is exactly the Black-Scholes derivative price with volatility $\bar{\sigma}_{4/2}$. For the correction term

$P_1(t,x)$, using the fact that the operators ∂_t, I, $\mathcal{D}_1$ and $\mathcal{D}_2$ commute, we find

$$\begin{aligned}
\langle \mathcal{L}_2 \rangle \left(-(T-t)F\mathcal{D}_1\mathcal{D}_2P_0\right) &= \left(\partial_t + \frac{1}{2}\bar{\sigma}_{4/2}^2\mathcal{D}_2 + r\left(\mathcal{D}_1 - I\right)\right)\left((t-T)F\mathcal{D}_1\mathcal{D}_2P_0\right) \\
&= F\mathcal{D}_1\mathcal{D}_2P_0 + (t-T)F\mathcal{D}_1\mathcal{D}_2\partial_t P_0 \\
&\quad +(t-T)F\mathcal{D}_1\mathcal{D}_2\left(\frac{1}{2}\bar{\sigma}_{4/2}^2\mathcal{D}_2 + r\left(\mathcal{D}_1 - I\right)\right)P_0 \\
&= F\mathcal{D}_1\mathcal{D}_2P_0 + (t-T)F\mathcal{D}_1\mathcal{D}_2 \cdot 0 \quad (\text{as } \mathcal{L}_{\text{BS}}(\bar{\sigma}_{4/2})P_0 = 0) \\
&= F\mathcal{D}_1\mathcal{D}_2P_0.
\end{aligned}$$

So, $-(T-t)F\mathcal{D}_1\mathcal{D}_2P_0$ solves the second equation for $P_1(t,x)$ in (3.12) and satisfies the terminal condition $P_1(T,x,z) = 0$. □

All the original model parameters are not required to price European derivatives. In fact, from Proposition 3.3.2, one can notice that the number of necessary parameters for the derivative price is reduced considerably from 6 to 2 as follows:

$$a,\, b,\, \epsilon,\, \theta,\, \xi,\, \rho \quad \Longrightarrow \quad \bar{\sigma}_{4/2},\, F^{\epsilon}.$$

The parameters $\bar{\sigma}_{4/2}$ and F^{ϵ} are required to be estimated for pricing the derivatives. In order to estimate these parameters, one can utilize calibration from near-the-money European call option implied volatilities. So, we need an implied volatility formula to follow a procedure to fit the skew from the European option prices.

We define the implied volatility $I^{\epsilon}(t,x,v)$ of a call option as a solution to the equation

$$P_{\text{BS}}(t,x;I^{\epsilon}) = \tilde{P}^{\epsilon}(t,x),$$

where $P_{\text{BS}}(t,x;\sigma)$ stands for the Black-Scholes formula for call options with constant

volatility σ, and we seek I^ϵ in the form of

$$I^\epsilon(t,x) = \sum_{i=0}^{\infty} (\sqrt{\epsilon})^i \, I_i(t,x)$$

with $I_0 := \bar{\sigma}_{4/2}$. By considering Taylor's expansion of $P_{\text{BS}}(t,x;I^\epsilon)$ at I_0 and noting that $P_{\text{BS}}(t,x;I_0) = P_0$, we obtain

$$I_1(t,x) = P_1(t,x)\left(\partial_\sigma P_{\text{BS}}\right)^{-1} = \frac{F}{\bar{\sigma}_{4/2}}\left(\frac{d_1(t,x)}{\bar{\sigma}_{4/2}\sqrt{T-t}} - 1\right), \tag{3.19}$$

which is the same as $P_1 (= -(T-t)F\mathcal{D}_1\mathcal{D}_2P_0)$ times the reciprocal of Vega, where $d_1(t,x)$ is

$$d_1(t,x) \;=\; \frac{\log(x/K) + \left(r + \frac{1}{2}\bar{\sigma}^2_{4/2}\right)(T-t)}{\bar{\sigma}_{4/2}\sqrt{T-t}}. \tag{3.20}$$

For the second equality in (3.19), we have used the Vega-Gamma relationship,

$$\text{Vega} = (T-t)\bar{\sigma}_{4/2}x^2 \text{ Gamma},$$

and the identity

$$\mathcal{D}_1(\text{Vega}) = \left(1 - \frac{d_1(t,x)}{\bar{\sigma}_{4/2}\sqrt{T-t}}\right)\text{Vega}$$

for call options. This leads to the following approximate implied volatility surface formula:

$$\begin{aligned} \tilde{I}^\epsilon(t,x) &:= I_0 + \sqrt{\epsilon} I_1(t,x) \\ &= \bar{\sigma}_{4/2} - \frac{F^\epsilon}{\bar{\sigma}^3_{4/2}}\left(\frac{\log(K/x)}{T-t} - r + \frac{1}{2}\bar{\sigma}^2_{4/2}\right). \end{aligned} \tag{3.21}$$

For European call options, therefore, we present the following corollary of Proposition 3.3.2 about how to estimate the option price and how to estimate explicitly the

relevant pricing parameters $\bar{\sigma}_{4/2}$ and F^{ϵ} from the term structure of implied volatility.

Corollary 3.3.1. *For a European call option with payoff $h(x) = (x-K)^+$, we have an expression*

$$\begin{aligned}\tilde{P}^{\epsilon}(t,x) &= N(d_1)x - N(d_2)Ke^{-r(T-t)} \\ &\quad -F^{\epsilon}\frac{xe^{-d_1^2/2}}{\bar{\sigma}_{4/2}\sqrt{2\pi}}\left(\sqrt{T-t}-\frac{d_1}{\bar{\sigma}_{4/2}}\right),\end{aligned} \tag{3.22}$$

where N denotes the standard normal cumulative distribution function and

$$d_2 = d_1 - \bar{\sigma}_{4/2}\sqrt{T-t}.$$

If the implied volatility $\tilde{I}^{\epsilon}(t,x)$ for a European call option is expressed in the form of

$$\tilde{I}^{\epsilon}(t,x) = \alpha\left(\frac{\log(K/x)}{T-t}\right) + \beta \tag{3.23}$$

for some constants $\alpha \neq 0$ and β satisfying $\alpha r + \beta > 0$ or $\alpha < 0$, then $\bar{\sigma}_{4/2}$ and F^{ϵ} are explicitly given by

$$\begin{aligned}\alpha r+\beta>0: \qquad \bar{\sigma}_{4/2} &= \frac{-1+\sqrt{1+2\alpha(\alpha r+\beta)}}{\alpha}, \\ F^{\epsilon} &= \frac{\left(1-\sqrt{1+2\alpha(\alpha r+\beta)}\right)^3}{\alpha^2}, \\ \alpha<0: \qquad \bar{\sigma}_{4/2} &= \frac{-1-\sqrt{1+2\alpha(\alpha r+\beta)}}{\alpha}, \\ F^{\epsilon} &= \frac{\left(1+\sqrt{1+2\alpha(\alpha r+\beta)}\right)^3}{\alpha^2}\end{aligned} \tag{3.24}$$

in terms of α and β, respectively, under the condition that $\alpha(\alpha r+\beta) \geq -\frac{1}{2}$ holds.

Proof. If we calculate (3.18) directly using the Black-Scholes price $P_{\mathrm{BS}}(\bar{\sigma}_{4/2})$ for the payoff $h(x) = (x-K)^+$, then the formula (3.22) follows immediately. By identifying

Equations (3.21) and (3.23), we obtain the following formulas for α and β:

$$\alpha = -\frac{F^{\epsilon}}{\bar{\sigma}^3_{4/2}}, \qquad \beta = \bar{\sigma}_{4/2} + \frac{F^{\epsilon}}{\bar{\sigma}^3_{4/2}}\left(r - \frac{1}{2}\bar{\sigma}^2_{4/2}\right).$$

Solving these equations for $\bar{\sigma}_{4/2}$ and F^{ϵ} yields (3.24). Note that the condition $\alpha r + \beta > 0$ or $\alpha < 0$ is required. Otherwise, the volatility $\bar{\sigma}_{4/2}$ would become negative. □

In practice, one can estimate the parameters $\bar{\sigma}_{4/2}$ and F^{ϵ} required to price the derivatives by using the algebraic relation in (3.24) once the slope and intercept coefficients α and β of an affine function of the log-moneyness-to-maturity ratio are estimated through fitting the implied volatilities from observed S&P 500 European call option prices. In particular, it is noteworthy to point out that we don't need to calculate directly the long-run historical volatility $\bar{\sigma}_{4/2}$ for the pricing purpose. It can be estimated by the formula (3.24) from the calibrated values of the slope and intercept coefficients of the implied volatilities. This way of estimation is valid as long as the derivative contract is not very close to expiration or deeply out of money. Also, the inequality $\beta > r\alpha$ must be satisfied since the long-run mean volatility $\bar{\sigma}_{4/2}$ has to be positive.

If we define a term $\Psi(a, b)$ as

$$\Psi(a, b) = a\langle \cdot\, \phi'_{ab}(\cdot)\rangle + b\langle \phi'_{ab}(\cdot)\rangle,$$

then from (3.18) we have

$$F^{\epsilon} = -\frac{1}{2}\sqrt{\epsilon}\rho\xi\,\Psi(a, b)$$

and thus the sign of the slope, $F^{\epsilon}/\bar{\sigma}^3_{4/2}$, of the implied volatility function $\tilde{I}^{\epsilon}$ in (3.23) depends on not only the correlation ρ but also the function $\Psi(a, b)$. This suggests how the 4/2 model is more flexible in the implied volatility behavior than the Heston model ($b = 0$) and the 3/2 model ($a = 0$).

In addition to Corollary 3.3.1, by applying the formula for P_2 in Proposition 3.3.1,

we can drive the second order term I_2 of the implied volatility I^ϵ as

$$I_2(t,x,v) = \left(P_2(t,x,v) - \frac{1}{2}\frac{\partial^2 P_{\text{BS}}}{\partial \sigma^2} I_1^2(t,x)\right)\left(\frac{\partial P_{\text{BS}}}{\partial \sigma}\right)^{-1}. \tag{3.25}$$

Since $I_1(t,x)$ is linear in the log-moneyness $\log(K/x)$, this second order term is quadratic in the log-moneyness and thus it is able to account for the convex smile effect which is usually observed in shorter time-to-maturity options.

3.4 Rescaled Double-mean-reverting 4/2 Stochastic Volatility Model

In this section, we consider the derivatives pricing problem under a rescaled double-mean-reverting 4/2 stochastic volatility model. Compared with the model in Section 3.2, double-mean-reverting volatility in this model is incorporated in such a way that variance reverts to its mean level 'fast', and the (intermediate) mean level itself gets back to a constant long-run mean 'slowly'. Given the underlying asset price process X_t at time $t > 0$, the risk-neutral dynamics (3.1) can be extended to

$$\begin{aligned} dX_t &= r\,X_t\,dt + \left(a\sqrt{V_t} + \frac{b}{\sqrt{V_t}}\right) X_t\,dW_t^x, \\ dV_t &= \frac{1}{\epsilon}\,(Z_t - V_t)\,dt + \frac{\xi}{\sqrt{\epsilon}}\sqrt{V_t}\,dW_t^v, \\ dZ_t &= \delta\,(\theta - Z_t)\,dt + \eta\sqrt{\delta}\sqrt{Z_t}\,dW_t^z, \quad Z_0 = \theta, \end{aligned} \tag{3.26}$$

where δ is a small positive parameter such that $0 < \delta,\ \epsilon \ll 1$, θ and η are positive real numbers satisfying $2\theta \geq \eta^2$, $\{W^x : t \geq 0\}$, $\{W^v : t \geq 0\}$ and $\{W^z : t \geq 0\}$ are three standard Brownian motions defined on a filtered probability space $(\Omega, \mathcal{F}, \{\mathcal{F}_t : t \geq 0\}, \mathbb{Q})$

with a correlation structure given by

$$d\langle W^x, W^v\rangle_t = \rho_{xv}dt, \quad d\langle W^x, W^z\rangle_t = \rho_{xz}dt \quad \text{and} \quad d\langle W^v, W^z\rangle_t = \rho_{vz}dt.$$

The other parameters are the same as those in Section 3.2. Given a payoff function $h(\cdot)$, the derivative price $P^{\epsilon,\delta}(t,x,v,z)$, defined by

$$P^{\epsilon,\delta}(t,x,v,z) := \mathbb{E}^{\mathbb{Q}}\left[e^{-r(T-t)}h(X_T)\,|\,X_t = x, V_t = v, Z_t = z\right],$$

satisfies a terminal value problem $\mathcal{L}^{\epsilon,\delta}P^{\epsilon,\delta}(t,x,v,z) = 0$ with$P^{\epsilon,\delta}(T,x,v,z) = h(x)$, where the multiscale operator $\mathcal{L}^{\epsilon,\delta}$ is given by

$$\begin{aligned}
\mathcal{L}^{\epsilon,\delta} &= \frac{1}{\epsilon}\mathcal{L}_0 + \frac{1}{\sqrt{\epsilon}}\mathcal{L}_1 + \mathcal{L}_2 + \sqrt{\delta}\mathcal{M}_1 + \delta\mathcal{M}_2 + \sqrt{\frac{\delta}{\epsilon}}\mathcal{M}_3,\\
\mathcal{L}_0 &:= \frac{1}{2}\xi^2 v\,\partial_{vv} + (z-v)\,\partial_v,\\
\mathcal{L}_1 &:= \rho_{xv}\,\xi\,(av+b)\,\mathcal{D}_1\partial_v,\\
\mathcal{L}_2 &:= \partial_t + \frac{1}{2}\left(a\sqrt{v} + \frac{b}{\sqrt{v}}\right)^2\mathcal{D}_2 + r\,(\mathcal{D}_1 - I),\\
\mathcal{M}_1 &:= \rho_{xz}\,\eta\left(a\sqrt{v} + \frac{b}{\sqrt{v}}\right)\sqrt{z}\,\mathcal{D}_1\partial_z,\\
\mathcal{M}_2 &:= \frac{1}{2}\eta^2\,z\,\partial_{zz} + (\theta - z)\,\partial_z,\\
\mathcal{M}_3 &:= \rho_{vz}\,\xi\,\eta\sqrt{v}\sqrt{z}\,\partial_{vz}.
\end{aligned} \tag{3.27}$$

By the same asymptotic analysis as used in Subsection 2.2.6 and Section 3.3, a few terms of P_{ij} of the expansion

$$P^{\epsilon,\delta}(t,s,v,z) = \sum_{i,j=0}^{\infty}(\sqrt{\delta})^i(\sqrt{\epsilon})^j\,P_{ij}(t,s,v,z)$$

are independent of the variable v and satisfy the following equations:

$$\begin{aligned}
\mathcal{L}_{\text{BS}}(\bar{\sigma}_{4/2}(z))P_{00}(t,x,z) &= 0,\\
\mathcal{L}_{\text{BS}}(\bar{\sigma}_{4/2}(z))P_{01}(t,x,z) &= F(z)\mathcal{D}_1\mathcal{D}_2P_{00}(t,x,z),\\
F(z) &:= \frac{1}{2}\rho_{xv}\xi\left(a\langle\cdot\,\partial_v\phi_{ab}(\cdot,z)\rangle + b\langle\partial_v\phi_{ab}(\cdot,z)\rangle\right),\\
\mathcal{L}_{\text{BS}}(\bar{\sigma}_{4/2}(z))P_{10}(t,x,z) &= -S(z)\mathcal{D}_1\partial_\sigma P_{00}(t,x,z),\\
S(z) &:= \rho_{xz}\eta\left\langle a\sqrt{\cdot} + \frac{b}{\sqrt{\cdot}}\right\rangle\bar{\sigma}'_{4/2}(z)\sqrt{z},
\end{aligned} \tag{3.28}$$

where $\phi_{ab}(v,z)$ is the same as the one defined in Section 3.3, except the slow-scale variable z dependence due to the z-dependence of the invariant distribution $\Phi_{\text{CIR}}(v,z)$ in the double-mean-reverting model. Moreover, the constant volatility $\bar{\sigma}_{4/2}$ is now replaced with the z-dependent volatility $\bar{\sigma}_{4/2}(z)$, and $\mathcal{L}_{\text{BS}}(\bar{\sigma}_{4/2}(z))$ is an intuitive expression of $\langle\mathcal{L}_2\rangle$. Note that $\bar{\sigma}'_{4/2}(z)\partial_\sigma P_{00}$ has been used instead of $\partial_z P_{00}$ so that the Vega-Gamma relationship can be applied to it directly.

Solving equations in (3.28) with the terminal value conditions

$$P_{00}(T,x,z)=h(x),\quad P_{01}(T,x,z)=0\quad\text{and}\quad P_{10}(T,x,z)=0$$

leads to the following proposition, which shows that the approximate derivative price is a superposition of the Black-Scholes derivative price and fast-scale and slow-scale correction terms.

Proposition 3.4.1. *Given the risk-neutral dynamics (3.26) of the underlying asset price, the derivative price $P^{\epsilon,\delta}(t,x,v,z)$ is approximated by*

$$\tilde{P}^{\epsilon,\delta}(t,x,z) := P_{00} + \sqrt{\epsilon}P_{01} + \sqrt{\delta}P_{10}$$

which is

$$\begin{aligned}
\tilde{P}^{\epsilon,\delta}(t,x,z) &= P_{\mathrm{BS}}(\bar{\sigma}_{4/2}(z)) - (T-t)F^{\epsilon}(z)\mathcal{D}_1\mathcal{D}_2 P_{\mathrm{BS}}(\bar{\sigma}_{4/2}(z)) \\
&\quad +(T-t)S^{\delta}(z)\mathcal{D}_1\partial_\sigma P_{\mathrm{BS}}(\bar{\sigma}_{4/2}(z)), \\
F^{\epsilon}(z) &:= \frac{1}{2}\sqrt{\epsilon}\,\rho_{xv}\xi\left(a\langle\cdot\,\partial_v\phi_{ab}(\cdot,z)\rangle + b\langle\partial_v\phi_{ab}(\cdot,z)\rangle\right), \\
S^{\delta}(z) &:= \frac{1}{2}\sqrt{\delta}\,\rho_{xz}\eta\left\langle a\sqrt{\cdot} + \frac{b}{\sqrt{\cdot}}\right\rangle \bar{\sigma}'_{4/2}(z)\sqrt{z}, \qquad (3.29)
\end{aligned}$$

where $P_{\mathrm{BS}}(\bar{\sigma}_{4/2}(z))(t,x,z)$ *is the solution of the first equation for* $P_{00}(t,x,z)$ *in (3.28) with* $P_{00}(T,x,z) = h(x)$.

Proof. The solution of the first PDE in (3.28) with the final condition $P_{00}(T,x,z) = h(x)$ is nothing but the Black-Scholes derivative price with volatility $\bar{\sigma}_{4/2}(z)$. For the fast-scale correction term P_{01}, one can show that $-(T-t)F(z)\mathcal{D}_1\mathcal{D}_2 P_{00}$ satisfies the second equation in (3.28) similarly to the proof of Proposition 3.3.2. Also, it satisfies the terminal condition $P_{01}(T,x,z) = 0$. Hence, $\sqrt{\epsilon}P_{01}$ is given by $-(T-t)F^{\epsilon}(z)\mathcal{D}_1\mathcal{D}_2 P_{00}$. For the slow-scale correction term P_{10}, we prove that $\frac{1}{2}(T-t)S(z)\mathcal{D}_1\partial_\sigma P_{00}$ satisfies the third equation in (3.28) as follows by using the fact that the operators ∂_t, I, $\mathcal{D}_1$ and $\mathcal{D}_2$ commute:

$$\begin{aligned}
\langle\mathcal{L}_2\rangle\left(\frac{1}{2}(T-t)S(z)\mathcal{D}_1\partial_\sigma P_{00}\right) &= \frac{1}{2}\left(\partial_t + \frac{1}{2}(\bar{\sigma}_{4/2})^2\mathcal{D}_2 + r(\mathcal{D}_1 - I)\right) \\
&\quad \times\left((T-t)S(z)\mathcal{D}_1\partial_\sigma P_{00}\right) \\
&= \frac{1}{2}\left[-S(z)\mathcal{D}_1\partial_\sigma P_{00}\right. \\
&\quad +(T-t)S(z)\mathcal{D}_1\partial_\sigma\partial_t P_{00} \\
&\quad +(\bar{\sigma}_{4/2})^2(T-t)S(z)\mathcal{D}_1\partial_\sigma\left(\frac{1}{2}\mathcal{D}_2\right)P_{00} \\
&\quad \left.+(T-t)S(z)\mathcal{D}_1\partial_\sigma\left(r(\mathcal{D}_1 - I)\right)P_{00}\right],
\end{aligned}$$

thus it follows that

$$\begin{aligned}
\langle \mathcal{L}_2 \rangle \left(\frac{1}{2}(T-t)S(z)\mathcal{D}_1 \partial_\sigma P_{00} \right) &= \frac{1}{2}\left[-S(z)\mathcal{D}_1 \partial_\sigma P_{00} \right. \\
&\quad +(T-t)S(z)\mathcal{D}_1 \partial_\sigma \cdot 0 \quad \text{(since } \mathcal{L}_{\text{BS}}(\bar{\sigma}_{4/2})P_{00} = 0\text{)} \\
&\quad +(\bar{\sigma}_{4/2})^2 (T-t)S(z)\mathcal{D}_1 \partial_\sigma \left(\frac{1}{2}\mathcal{D}_2 \right) P_{00} \\
&\quad \left. -(T-t)S(z)\mathcal{D}_1 \partial_\sigma \left(\frac{1}{2}(\bar{\sigma}_{4/2})^2 \mathcal{D}_2 \right) P_{00} \right] \\
&= \frac{1}{2}\left[-S(z)\mathcal{D}_1 \partial_\sigma P_{00} \right. \\
&\quad \left. -(T-t)S(z)\mathcal{D}_1 \left(\bar{\sigma}_{4/2}(z)\bar{\sigma}'_{4/2}(z)\mathcal{D}_2 \right) P_{00} \right] \\
&= -S(z)\mathcal{D}_1 \partial_\sigma P_{00}.
\end{aligned}$$

□

Now, we define the (model) implied volatility $I^{\epsilon,\delta}$ of a call option under the double-mean-reverting 4/2 model as a solution to the following equation

$$P_{\text{BS}}(t, x; I^{\epsilon,\delta}) = \tilde{P}^{\epsilon,\delta}(t, x, z).$$

Then the first-order fast and slow scale correction terms $I^{\epsilon}_{01} := \sqrt{\epsilon} I_{01}$ and $I^{\delta}_{10} := \sqrt{\delta} I_{10}$ of the expansion

$$I^{\epsilon,\delta}(t, x, z) = \sum_{i,j=0}^{\infty} (\sqrt{\delta})^i (\sqrt{\epsilon})^j \, I_{ij}(t, x, z)$$

with $I_{00} := \bar{\sigma}_{4/2}(z)$ are given by

$$\begin{aligned}
I^{\epsilon}_{01}(t, x, z) &= P^{\epsilon}_{01} \left(\partial_\sigma P_{\text{BS}} \right)^{-1} = \frac{1}{\bar{\sigma}_{4/2}(z)} F^{\epsilon}(z) \left(\frac{d_1(t, x, z)}{\bar{\sigma}_{4/2}(z)\sqrt{T-t}} - 1 \right), \\
I^{\delta}_{10}(t, x, z) &= P^{\delta}_{10} \left(\partial_\sigma P_{\text{BS}} \right)^{-1} = (T-t)S^{\delta}(z) \left(1 - \frac{d_1(t, x, z)}{\bar{\sigma}_{4/2}(z)\sqrt{T-t}} \right),
\end{aligned} \tag{3.30}$$

where $d_1(t, x, z)$ is the slow-scale extension of $d_1(t, x)$ defined in (3.20). So, the

implied volatility $\tilde{I}^{\epsilon,\delta} := I_{00} + I^{\epsilon}_{01} + I^{\delta}_{10}$ has a term structure given by

$$\begin{aligned}\tilde{I}^{\epsilon,\delta}(t,x,z) &= \bar{\sigma}_{4/2}(z) + a^{\epsilon}(z)\frac{\log(K/x)}{T-t} + b^{\epsilon}(z) \\ &\quad + c^{\delta}(z)\log(K/x) + d^{\delta}(z)(T-t),\end{aligned} \tag{3.31}$$

where the parameters $\bar{\sigma}_{4/2}$, a^{ϵ}, b^{ϵ}, c^{δ} and d^{δ} satisfy the equations

$$\frac{b^{\epsilon}}{a^{\epsilon}} = \frac{d^{\delta}}{c^{\delta}} = \frac{1}{2}\bar{\sigma}^2_{4/2} - r$$

and they are related to the pricing parameters $\bar{\sigma}_{4/2}$, F^{ϵ} and S^{δ} through

$$F^{\epsilon} = \frac{\bar{\sigma}^3_{4/2}}{2}\left(\frac{b^{\epsilon}}{r - \frac{1}{2}\bar{\sigma}^2_{4/2}} - a^{\epsilon}\right) \quad \text{and} \quad S^{\delta} = \frac{\bar{\sigma}^2_{4/2}}{2}\left(c^{\delta} - \frac{d^{\delta}}{r - \frac{1}{2}\bar{\sigma}^2_{4/2}}\right). \tag{3.32}$$

As observed in Proposition 3.4.1, there are three pricing parameters, that is, the long-run average of volatility $\bar{\sigma}_{4/2}$, the fast-scale parameter F^{ϵ} and the slow-scale parameter S^{δ}, to price the derivatives under the double-mean-reverting 4/2 model. The original nine model parameters have been reduced to the three group parameters through the five intermediate group parameters of the implied volatility surface:

$$a,\, b,\, \epsilon,\, \xi,\, \delta,\, \theta,\, \eta,\, \rho_{xv}, \rho_{xz} \quad \Longrightarrow \quad \bar{\sigma}_{4/2},\, a^{\epsilon},\, b^{\epsilon},\, c^{\delta},\, d^{\delta} \quad \Longrightarrow \quad \bar{\sigma}_{4/2},\, F^{\epsilon},\, S^{\delta}.$$

In practice, the parameter $\bar{\sigma}_{4/2}$ is first estimated from historical SPX data over a period of time in the near past. The slow-scale variable z-dependence of $\bar{\sigma}_{4/2}$ accounts for updating the long-run average term from time to time. The rest parameters a^{ϵ}, b^{ϵ}, c^{δ} and d^{δ} are estimated from calibration to the implied volatility surface of SPX call options. Then we use the relationship (3.32) to estimate the pricing group parameters F^{ϵ} and S^{δ} and calculate the derivative price formula $\tilde{P}^{\epsilon,\delta}(t,x,z)$ obtained in Proposition 3.4.1.

3.5 Numerical Experiments and Sensitivity Analysis

In this section, we present some results on four types of numerical experiments. First of all, we conduct Monte-Carlo simulations of the fast mean-reverting 4/2 stochastic volatility model (3.1) to generate values of European-style call options. Then, we compare these option values with those generated by our approximate analytic formula given in Proposition 3.3.2. For this purpose, the values of the model parameters are chosen according to

$$r = 0.03,\ a = 0.09099,\ b = 0.00111,\ \epsilon = 0.001,\ \theta = 0.04,\ \xi = 0.123,\ \rho = -0.7$$

and results are plotted in Figure 3.1. As we can see from Figure 3.1(A), for short time-to-maturity options, call option values from Monte-Carlo simulations match well with those generated by our approximate analytic formula. For longer time-to-maturity options, the option values from Monte-Carlo simulation are slighter higher than those from the approximate formula. However, in terms of moneyness $\ln(K/x)$, as we can see from Figure 3.1(B), the two types of options values are very close in all cases.

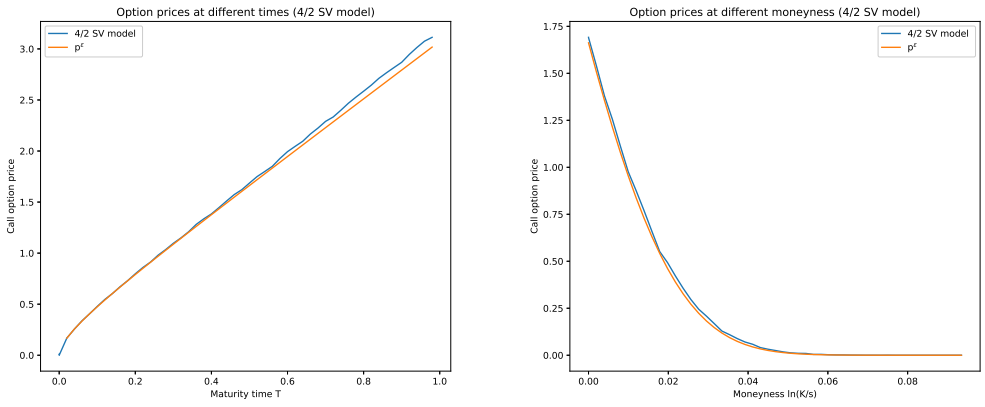

(A) (B)

Figure 3.1: Monte-Carlo versus approximate analytic values, with initial asset price $X_0 = 100$ and strike price $K = 100$

Secondly, we use the market data to test our formula in Proposition 3.3.2. We collect the S&P 500 options data on May 3, 2008. The maturity dates of these options are up to May 3, 2010. According to their maturity times, we split the data into two samples: in-sample (maturity times are from 30 to 270 days) and out-sample (maturity times are 360 and 720 days). The in-sample data are used to estimate the values of α and β in Corollary 3.3.1 via linear regression of implied volatility. Then, the values of $\bar{\sigma}_{4/2}$ and F^{ϵ} are calculated by using equation (3.24). The out-sample data are used for comparison. More precisely, we use market implied volatility to calculate the market option values, which are compared with the option values calculated by the formula in Proposition 3.3.2. The results are presented in Figure 3.2. As we can see from the figure, for in-the-money call options with maturity time 360 days, the values from our appropriate analytic formula match well with the market values. For deep out-of-money call options with the same maturity time, the values from our formula are higher that the market values. For in-the-money call options with maturity time 720 days, the values from our formula are slightly lower than the market values. For out-of-money call options with the same maturity time, the trend is similar to that of call options with maturity time 360 days.

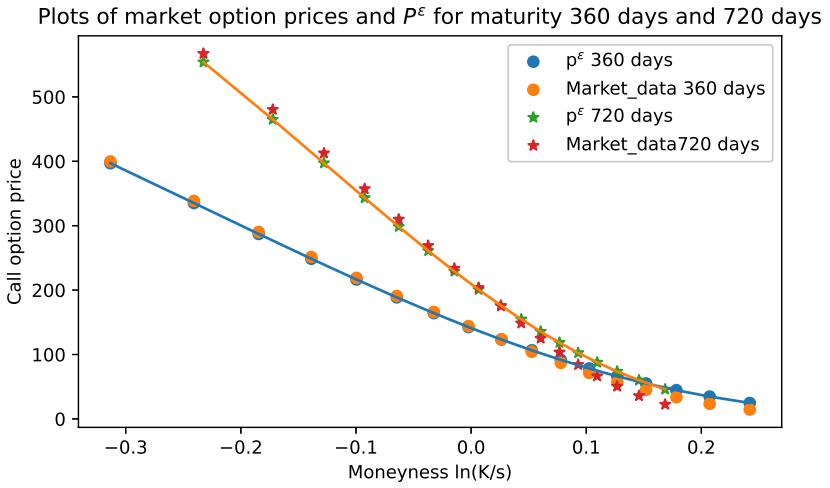

Figure 3.2: S&P 500 market values versus approximate analytic values

In the third type of numerical experiments, we use Monte-Carlo simulations to compare the 4/2 stochastic volatility model with the Heston model and the 3/2 stochastic volatility model, with different combinations of values of parameters a and b. The results are presented in Figures 3.3(A) and 3.3(B), respectively. In Figure 3.3(A), the value of parameter a is fixed at 0.3, 0.6 and 1 respectively, and we let the value of parameter b varies between 0 and 0.05. As we know, when $b = 0$, the $4/2$ model is reduced to the Heston model. For each of the given a values, when the value of b gets larger, the option values from the $4/2$ model are in a general increasing trend and higher than the value from the Heston model. When the value of a gets larger, the option values from both models increase. In Figure 3.3(B), the value of parameter b is fixed at 0.00123, 0.01423 and 0.05423 respectively, and we let the value of parameter a varies between 0 and 1. As we know, when $a = 0$, the $4/2$ model is reduced to the $3/2$ model. For each of the given b values, when the value of a gets larger, the option values from the $4/2$ model are in a general increasing trend and higher than the value from the $3/2$ model. When the value of b gets larger, the option values from both models increase.

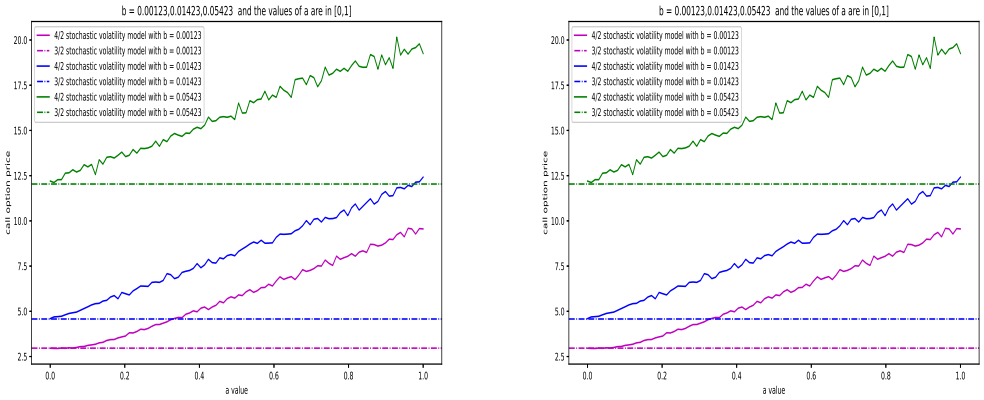

(A) (B)

Figure 3.3: (A) $4/2$ model versus Heston model, (B) $4/2$ model versus $3/2$ model.

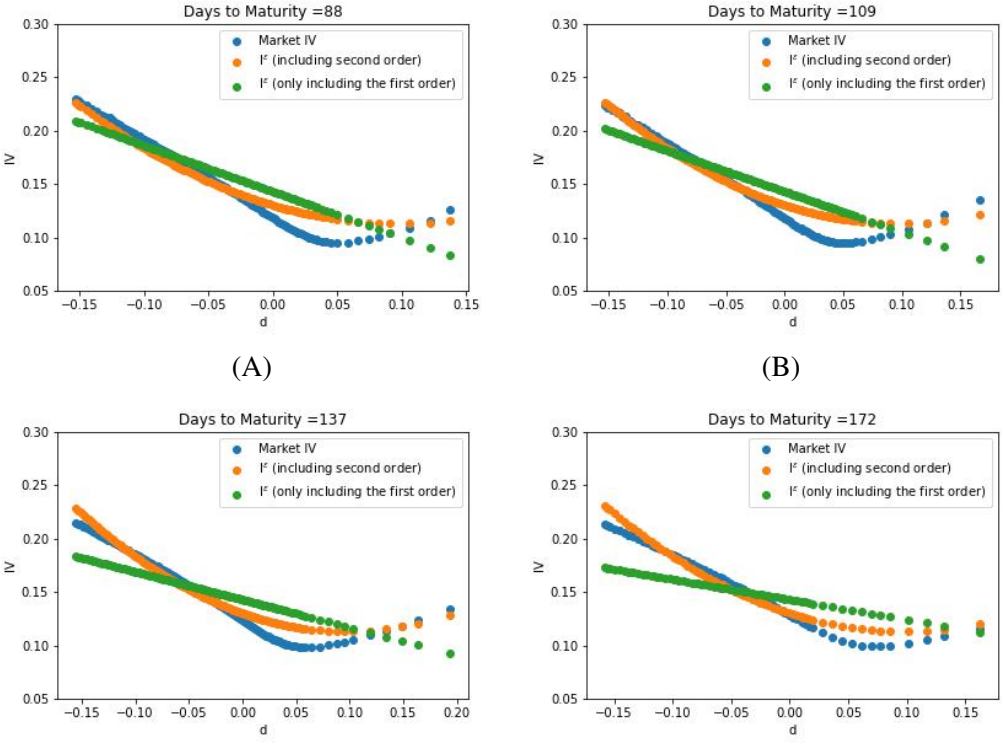

Figure 3.4: S&P500 implied volatilities on 1st April, 2019 for days to maturity 88 through 172.

Lastly, we compare the market implied volatility data with the approximate implied volatility formula given by (3.21) together with (3.25). As shown in Figure 3.4, the first order implied volatility approximation approaches the market implied volatility in terms of slope. The first order implied volatility approximation is shown to be almost linear but the second order implied volatility approximation starts capturing the convexity of the market implied volatility and is closer to the market data than the first order approximation in all time-to-maturities. Inclusion of higher order terms would make the implied volatility move much closer to the market implied volatility.

3.6 Conclusion

In this chapter, we have obtained closed-form approximate formulas for European derivative prices under two rescaled versions of the 4/2 stochastic volatility model. The pricing formulas can be calculated easily starting from the corresponding Black-Scholes derivative price. The first formula is based on a rescaled single mean-reverting (with fast factor only) 4/2 volatility. The corresponding implied volatility formula is a useful tool to approximate the market implied volatility. The market data can be approached by the theoretical formula step by step by adding asymptotic terms. We have shown that the first and second order approximations can capture the slope and the convexity of the market implied volatility, respectively. We have extended the rescaled single mean-reverting 4/2 volatility model to a rescaled double-mean-reverting (with both fast and slow factors) 4/2 volatility model and obtained a pricing formula for European style derivatives. We have conducted four types of numerical experiments to validate our approximate formulas by using Monte Carlo simulation and market data.

After this section, we show some pseudocodes for the main parts of our numerical experiments. These codes explain the key steps we used to calculate and compare prices in different cases. We hope that sharing these pseudocodes helps readers to understand how the calculations were done and to repeat the experiments.

The first group of pseudocodes (numerical experiments 1) explain how to compare option prices calculated by an analytical formula and the Monte Carlo simulation for different maturities and moneyness. They take model parameters, maturity dates, moneyness values, the number of simulations, the strike price, and other parameters as inputs. For each maturity and moneyness, the codes will run the Monte Carlo simulation to generate asset prices and calculate the discounted payoffs, then calculate the European option price. They also compute the option price using a closed-form analytical formula. Both sets of prices are stored separately to allow direct comparison.

Numerical Experiments 1: Evaluating Pricing Accuracy: Analytical Formula vs Monte Carlo under different maturities and moneyness

Input: Model parameters $r, a, b, \epsilon, \theta, \xi, \rho_{sv}$; maturities $\{T_i\}$; moneyness levels $\{m_j\}$; number of simulations N; strike price K

Output: values from the Monte Carlo simulation and pricing formula for different maturities and moneyness

Initialize diffTFormulResults ← empty list;
Initialize diffTMCResults ← empty list;
for *each maturity* $T \in \{T_i\}$ **do**
  Initialize payoff set $P_T \leftarrow \varnothing$;
  for $i \leftarrow 1$ **to** N **do**
    Simulate asset price S_t and volatility processes V_t, Z_t according to the $4/2$ model;
    Calculate terminal asset price S_T at time T;
    Compute payoff $p_i = \max(S_T - K, 0)$;
    Discount payoff: $P_i \leftarrow e^{-rT} p_i$;
    Add P_i to payoff set P_T;
  Compute Monte Carlo price $\hat{C}_{MC,T} \leftarrow \frac{1}{N} \sum P_T$;
  Compute closed-form approximation price $\hat{C}_{approx,T}$ using formula in Proposition 3.3.2 or 3.4.1 ;
  Append pricing result $\hat{C}_{approx,T}$ to diffTFormulResults ;
  Append pricing result $\hat{C}_{MC,T}$ to diffTMCResults;
Initialize diffMFormulResults ← empty list ;
Initialize diffMMCResults ← empty list;
for *each moneyness* $m \in \{m_j\}$ **do**
  Calculate initial asset price $S_0 = m \times K$;
  Initialize payoff set $P_m \leftarrow \varnothing$;
  for $i \leftarrow 1$ **to** N **do**
    Simulate asset price S_t and volatility processes V_t, Z_t according to the $4/2$ model;
    Calculate terminal asset price S_{T^*};
    Compute payoff $p_i = \max(S_{T^*} - K, 0)$;
    Discount payoff: $P_i \leftarrow e^{-rT^*} p_i$;
    Add P_i to payoff set P_m;
  Compute Monte Carlo price $\hat{C}_{MC,m} \leftarrow \frac{1}{N} \sum P_m$;
  Compute closed-form approximation price $\hat{C}_{approx,m}$ using formula in Proposition 3.3.2 or 3.4.1;
  Append pricing result $\hat{C}_{approx,m}$ to diffMFormulResults ;
  Append pricing result $\hat{C}_{MC,m}$ to diffMMCResults;
return Plot the pricing results of the pricing formula and the Monte Carlo simulation under different maturities and moneyness.

Moreover, the pricing results of the pricing formula and the Monte Carlo simulation under different maturities and moneyness are plotted.

The second groups of pseudocodes below (numerical experiments 2) perform a comparison between market implied volatility and implied volatilities calculated from both first- and second-order pricing formulas. The process begins with loading the market data and performing necessary cleaning to ensure data quality. Moreover, some key information should be extracted from the dataset (such as strike prices and maturities). For each data point, the function calculates the moneyness value based on strike price and maturity, then applies the first-order and second-order pricing formulas to compute the implied volatilities. All calculated values, along with the market data, are saved for further analysis. Finally, the function produces visual plots to show the differences and similarities between the calculated implied volatilities and the observed market implied volatility.

Numerical Experiments 2: Comparison between Pricing Formula Implied Volatility and Market Volatility

Input: Market implied volatility data, maturities, initial model parameters (possibly from prior calibration)

Output: Calculated implied volatility results for first- and second-order approximations, along with their plots compared to market data.

Import the market implied volatility dataset and perform data cleaning;

Parse dataset to extract strike prices K_i, maturities T_i, and market implied volatilities $\sigma_{market,i}$;

Set initial parameter values for the pricing formulas;

Create empty lists to hold computed implied volatilities and errors for each data point;

for *each data point* i **do**

Retrieve strike K_i, maturity T_i, and market implied volatility $\sigma_{market,i}$;

Moneyness is calculated based on strike K_i and maturity T_i. Apply first-order pricing formula with current parameters and inputs (K_i, T_i) to get $\sigma_{1st,i}$;

Apply second-order pricing formula with current parameters and inputs (K_i, T_i) to get $\sigma_{2nd,i}$;

Append $(K_i, T_i, \sigma_{market,i}, \text{Moneyness}, \sigma_{1st,i}, \sigma_{2nd,i})$ to results list;

return Plot of the calculated implied volatility results and market implied volatility.;

Numerical Experiments 3: Pricing Formula and S&P 500 Market Data Comparison under different maturities

Input: S&P 500 dataset; calibrated model parameters

Output: Comparison plots and error metrics

Import and clean the the dataset and filter data for valid ranges ;

Select relevant option data ;

for *each option* i **do**

  Normalize maturity: $T_i = T_{days,i}/D$;

Load calibrated parameters θ;

Initialize empty lists: `ModelPrices`, `MarketPrices`, `Moneyness`;

for *each filtered option* i **do**

  Extract K_i, T_i, $P_{market,i}$;

  Compute model price $P_{model,i}$ and moneyness; ;

  Append results to lists;

return Plot market data and formula results against moneyness across various maturities.

The third groups of pseudocodes (numerical experiments 3) show that option prices from the approximated analytic pricing formula can be compared with S&P 500 market data across different maturities by using this function of pseudocodes. The dataset is initially loaded and cleaned, after which invalid options are filtered out. Moreover, relevant data, such as call option prices, need to be selected. After loading the calibrated parameters of the pricing model, the function extracts each option's strike price, maturity, and market price to calculate the model price and moneyness. The results are saved, and plots are generated to show the relationship between market and model prices with respect to moneyness at different maturities.

The pseudocodes of numerical experiment 4 are designed to analyze how two parameters, a and b, affect the $4/2$ model result. The process begins by setting up different

values for the parameters and establishing a baseline result. For each combination of parameters, it calculates the model output. If $a = 0$, it uses the simpler 3/2 model; and if $b = 0$, it becomes the Heston model; otherwise, it applies the full 4/2 model. Once the output is computed, all the results are plotted to clearly show how sensitive the model is to changes in these parameters.

Numerical Experiments 4: Sensitivity Analysis based on Parameters a and b

Input: Parameter sets $A = \{a_1, \ldots, a_m\}$, $B = \{b_1, \ldots, b_n\}$; other fixed parameters of $4/2$ model
Output: Plots showing sensitivity analysis results for all (a, b) combinations
Initialize empty list SensitivityResults;
for *each* $b_j \in B$ **do**
  for *each* $a_i \in A$ **do**
    if $a_i = 0$ **then**
      Compute model output $C_{i,j}$ using 3/2 model with $b = b_j$;
    else if $b_j = 0$ **then**
      Compute model output $C_{i,j}$ using Heston model with $a = a_i$;
    else
      Compute model output $C_{i,j}$ using full 4/2 model with $a = a_i, b = b_j$;
    Compute sensitivity $S_{i,j} = |C_{i,j} - C_{\text{baseline}}|$;
    Append $(a_i, b_j, C_{i,j}, S_{i,j})$ to SensitivityResults;
for *each* $a_k \in A$ **do**
  for *each* $b_l \in B$ **do**
    if $a_k = 0$ **then**
      Compute model output $C_{k,l}$ using 3/2 model with $b = b_l$;
    else if $b_l = 0$ **then**
      Compute model output $C_{k,l}$ using Heston model with $a = a_k$;
    else
      Compute model output $C_{k,l}$ using full 4/2 model with $a = a_k, b = b_l$;
    Compute sensitivity $S_{k,l} = |C_{k,l} - C_{\text{baseline}}|$;
    Append $(a_k, b_l, C_{k,l}, S_{k,l})$ to SensitivityResults;
Plot sensitivity results stored in SensitivityResults;

Chapter 4

Pricing Real Options Under the Rescaled 4/2 Stochastic Volatility Model

4.1 Introduction

As we have discussed in Chapter 2, the right to take certain business initiatives to invest in a given project is called a *real option*. In this chapter, we consider the valuation problem of real options under the double-mean-reverting 4/2 stochastic volatility model introduced by Cao et al. in (Cao et al., 2023a).

Our main contribution is to obtain explicit approximation formulas for the value of an innovative project and the investment threshold in a closed-form expression. Based on these formulas, we understand how the 4/2 stochastic volatility assumption affects the expected value of an innovative project and the investment threshold. The method used in this chapter for deriving the formulas is asymptotic analysis outlined in Section 2.2.6.

The rest of this chapter is organized as follows. In Section 4.2, we present the

double-mean-reverting 4/2 stochastic volatility model for the value of the expected future net cash flows of an innovative project. Section 4.3 solves a partial differential equation (PDE) problem with free boundary. We obtain two approximation formulas: one for the value of a real option and the other for the investment threshold, respectively. In Section 4.4, we undertake numerical experiments on sensitivity analysis of our formulas with respect to the model parameters and the associated variables. Finally, we provide some concluding remarks in Section 4.5. The contents of this chapter are based on (Cao et al., 2024a), (Cao et al., 2024b) and (Cao et al., 2025).

4.2 Model Formulation

Let X_t be the present value of the expected future net cash flows of an innovative project for a given information available up to time t, denoted by $\mathcal{F}_t$. In this chapter, we use the double-mean-reverting 4/2 stochastic volatility model, proposed by Cao et al. (Cao et al., 2023a), for the volatility of the innovative project value. So, the dynamics of X_t is given by the following system of stochastic differential equations (SDEs):

$$\begin{aligned} dX_t &= (r-q)X_t dt + \left(a\sqrt{V_t} + \frac{b}{\sqrt{V_t}}\right) X_t dW_t^x, \\ dV_t &= \frac{1}{\epsilon}(Z_t - V_t)dt + \frac{\xi}{\sqrt{\epsilon}}\sqrt{V_t}dW_t^v, \\ dZ_t &= \delta(\theta - Z_t)dt + \eta\sqrt{\delta}\sqrt{Z_t}dW_t^z, \quad Z_0 = \theta \end{aligned} \tag{4.1}$$

under a risk-neutral probability measure $\mathbb{Q}$. Here, ϵ and δ are two small positive parameters such that $0 < \delta,\ \epsilon \ll 1$, and r, q, ξ, θ and η are positive real numbers and $\{W_t^x : t \geq 0\}$, $\{W_t^v : t \geq 0\}$ and $\{W_t^z : t \geq 0\}$ are three standard Brownian motions defined on a filtered probability space $(\Omega, \mathcal{F}, \{\mathcal{F}_t : t \geq 0\}, \mathbb{Q})$ with their correlation

structure given by

$$d\langle W^x, W^v\rangle_t = \rho_{xv}dt,\ d\langle W^v, W^z\rangle_t = \rho_{vz}dt,\ \text{and}\ d\langle W^z, W^x\rangle_t = \rho_{zx}dt,$$

where the inequalities $\rho_{xv}^2, \rho_{vz}^2, \rho_{zx}^2 < 1$ and $\rho_{xv}^2 + \rho_{vz}^2 + \rho_{zx}^2 - 2\rho_{xv}\rho_{vz}\rho_{zx} - 1 < 0$ are satisfied to guarantee the positive definiteness of the covariance matrix of the Brownian motions. The constant r stands for the riskless rate. The parameter q can be interpreted as the 'rate of return shortfall' in (McDonald & Siegel, 1984) or the 'convenience yield' in (Brennan & Schwartz, 1982), in the real option context. We assume that q is not equal to r. Furthermore, a and b are real numbers. If $b = 0$, Equation (4.1) becomes the double-mean-reverting Heston stochastic volatility model. Note that a generalized version of the double-mean-reverting Heston model has been considered in (Kil & Kim, 2022). If $a = 0$, Equation (4.1) becomes the double-mean-reverting $3/2$ model. Under the assumption on δ and ϵ, the process $\{V_t : t \geq 0\}$ is fast mean-reverting. By substituting $a = \frac{1}{\epsilon}$, $\theta = z$ and $\sigma = \frac{\xi}{\sqrt{\epsilon}}$ into Equation (2.26), we obtain the probability density function of the invariant distribution of $\{V_t : t \geq 0\}$ as

$$\Phi_{\text{CIR}}(v, z) = \frac{(2/\xi^2)^{\frac{2z}{\xi^2}}}{\Gamma(2z/\xi^2)} v^{\frac{2z}{\xi^2}-1} e^{-\frac{2v}{\xi^2}}.$$

If ϵ (and so δ) goes to zero, then V_t goes to the constant mean level θ and thus the model becomes the Black-Scholes model with constant volatility $a\sqrt{\theta} + b/\sqrt{\theta}$. We note that the processes $\{Y_t : t \geq 0\}$ and $\{Z_t : t \geq 0\}$ driving the multiscale volatility in the model described in Equation (4.1) are correlated and coupled while they are correlated but uncoupled in the multiscale stochastic volatility model of Fouque et al. in (Fouque et al., 2011).

4.3 Valuation of Real Options

In this section, we set up a PDE problem with free boundary for the valuation of a real option under our model (4.1). Then, we use an asymptotic analysis approach to derive an approximate solution to the PDE problem.

4.3.1 PDE Problem with Free Boundary

From the fundamental theorem of asset pricing (cf. (Shreve, 2008) for instance), the value of a real option can be expressed by

$$V(x,v,z) = \sup_{\tau\in\mathcal{T}} \mathbb{E}^{\mathbb{Q}}\left[e^{-r\tau}(X_\tau - K)^+ \mathbf{1}_{\tau<\infty} \,|\, X_0 = x, V_0 = v, Z_0 = z\right] \tag{4.2}$$

under a martingale measure $\mathbb{Q}$, where X_t is the value of an investment project at time t, K is a sunk cost paid at an optimal point, and $\mathcal{T}$ is the set of all admissible stopping times for a σ-algebra generated by the joint process $\{(X_t, V_t, Z_t) : t \geq 0\}$.

Let $x_*(y,z)$ denote the critical project value separating the stopping and continuation regions of the real option. Then it is the free boundary of the two regions and it is thought of as the investment threshold in real option problems. Using the dynamic programming principle, refer to (Dixit & Pindyck, 1994, Chapter 5) or (Ting et al., 2013) for example, one can transform the conditional expectation (4.2) into a partial

differential equation (PDE) problem given by

$$\begin{aligned}
\mathcal{A}^{\epsilon,\delta}V(x,v,z) &= 0, \quad 0 < x < x_*, \\
V(x_*,v,z) &= x_* - K, \\
\partial_x V(x_*,v,z) &= 1, \\
\partial_v V(x_*,v,z) &= 0, \\
\partial_z V(x_*,v,z) &= 0, \\
V(x,v,z) &\to 0 \quad \text{as } x \to 0, \\
V(x,v,z) &= x - K, \quad \text{for the region } x \geq x_*,
\end{aligned} \tag{4.3}$$

where the operator $\mathcal{A}^{\epsilon,\delta}$ is given by

$$\mathcal{A}^{\epsilon,\delta} = \frac{1}{\epsilon}\mathcal{A}_0 + \frac{1}{\sqrt{\epsilon}}\mathcal{A}_1 + \mathcal{A}_2 + \sqrt{\delta}\mathcal{M}_1 + \delta\mathcal{M}_2 + \sqrt{\frac{\delta}{\epsilon}}\mathcal{M}_3, \tag{4.4}$$

where the operators $\mathcal{M}_1, \mathcal{M}_2$ and $\mathcal{M}_3$ are the same as those in Equation (3.27). Similarly, $\mathcal{A}_0$ and $\mathcal{A}_1$ correspond to $\mathcal{L}_0$ and $\mathcal{L}_1$ in Equation (3.27), respectively. However, $\mathcal{A}_2$ is different from $\mathcal{L}_2$ in Equation (3.27). Here, $\mathcal{A}_2$ is given by

$$\mathcal{A}_2 := -r\mathcal{D}_0 + (r-q)\mathcal{D}_1 + \frac{1}{2}\left(a\sqrt{v} + \frac{b}{\sqrt{v}}\right)^2 \mathcal{D}_2,$$

and $\mathcal{D}_0$ is nothing but the identity operator. In (4.3), we have used the matching condition between the stopping and continuation regions, the smooth pasting condition with respect to the state variable x and the smooth pasting conditions with respect to v and z based on the intuition that the actual payoff would not depend on the current level of volatility.

4.3.2 Asymptotic PDE Solution

Since the PDE problem (4.3) is a singular perturbation problem, we seek solutions of the forms

$$\begin{aligned} V(x,v,z) &= \sum_{i,j=0}^{\infty} \left(\sqrt{\delta}\right)^i \left(\sqrt{\epsilon}\right)^j V_{ij}(x,v,z), \\ x_*(x,v,z) &= \sum_{i,j=0}^{\infty} \left(\sqrt{\delta}\right)^i \left(\sqrt{\epsilon}\right)^j x_{ij}(x,v,z). \end{aligned} \tag{4.5}$$

Throughout the chapter, we use the operator $\mathcal{A}_{\text{BS}}$ defined by

$$\begin{aligned} \mathcal{A}_{\text{BS}} &:= \langle \mathcal{A}_2 \rangle^{\Phi_{\text{CIR}}(v,z)} = -r\,\mathcal{D}_0 + (r-q)\,\mathcal{D}_1 + \frac{1}{2}\,\bar{\sigma}^2_{4/2}(z)\,\mathcal{D}_2, \\ \bar{\sigma}^2_{4/2}(z) &:= \left\langle \left(a\sqrt{\cdot} + \frac{b}{\sqrt{\cdot}} \right)^2 \right\rangle^{\Phi_{\text{CIR}}(v,z)} = \int_0^\infty \left(a\sqrt{v} + \frac{b}{\sqrt{v}} \right)^2 \Phi_{\text{CIR}}(v,z)\,dv. \end{aligned}$$

We believe that in practice, a real option's sensitivity to changes in volatility level does not increase very fast with volatility, even if the option value itself increases extremely fast with volatility. This implies that a growth condition similar to that described in Lemma 2.1.1 is satisfied. Using Lemma 2.1.1, one can find that V_{00}, V_{01} and V_{10} are independent of variable v under the growth hypothesis similar to that described in Lemma 2.1.1. Furthermore, using Lemma 2.1.2, one can obtain the following ordinary differential equations (ODEs) for them:

$$\mathcal{A}_{\text{BS}}(\bar{\sigma}_{4/2}(z))V_{00}(x,z) = 0, \tag{4.6}$$

$$\mathcal{A}_{\text{BS}}(\bar{\sigma}_{4/2}(z))V_{01}(x,z) = F(z)\mathcal{D}_1\mathcal{D}_2 V_{00}(x,z), \tag{4.7}$$

$$\mathcal{A}_{\text{BS}}(\bar{\sigma}_{4/2}(z))V_{10}(x,z) = -S(z)\mathcal{D}_1\partial_z V_{00}(x,z), \tag{4.8}$$

where $F(z)$ and $S(z)$ are

$$\begin{aligned} F(z) &:= \frac{1}{2}\rho_{xv}\xi\left(a\langle\cdot\partial_v\phi_{\text{ab}}(\cdot,z)\rangle^{\Phi} + b\langle\partial_v\phi_{\text{ab}}(\cdot,z)\rangle^{\Phi}\right), \\ S(z) &:= \rho_{zx}\eta\left\langle a\sqrt{\cdot} + \frac{b}{\sqrt{\cdot}}\right\rangle^{\Phi}\sqrt{z} \end{aligned} \tag{4.9}$$

respectively, and $\phi_{\text{ab}}(v,z)$ is defined as a solution to the ODE

$$\mathcal{A}_0\phi_{\text{ab}} = \left(a\sqrt{v} + \frac{b}{\sqrt{v}}\right)^2 - \bar{\sigma}^2_{4/2}(z). \tag{4.10}$$

For the derivation of (4.6), we follow the asymptotic analysis approach used in Section 2.2.6 and Section 3.3. In order to solve the ODEs (4.6)-(4.8), we need boundary conditions for V_{00}, V_{01} and V_{10}. By substituting the expansions (4.5) into the non-zero boundary conditions (4.3), we have the following boundary conditions for V_{00}:

$$\begin{aligned} V_{00}(x,z) &= x - K, \quad \text{if } x \geq x_{00}, \\ \partial_x V_{00}(x_{00},z) &= 1. \end{aligned} \tag{4.11}$$

For V_{01} and V_{10}, we have

$$\begin{aligned} V_{01}(x,z) &= 0 \text{ if } x \geq x_{00}, \quad x_{01}\,\partial_{xx}V_{00}(x_{00},z) + \partial_x V_{01}(x_{00},z) = 0, \\ V_{10}(x,z) &= 0 \text{ if } x \geq x_{00}, \quad x_{10}\,\partial_{xx}V_{00}(x_{00},z) + \partial_x V_{10}(x_{00},z) = 0 \end{aligned} \tag{4.12}$$

respectively. Since $\mathcal{A}_{\text{BS}} + r\,\mathcal{D}_0$ is the infinitesimal generator of a geometric Brownian motion solving the SDE

$$dX_t = (r-q)\,X_t\,dt + \bar{\sigma}_{4/2}(z)\,X_t\,dW_t^x,$$

the ODE problem $\mathcal{A}_{BS}V_{00}(x,z) = 0$ with boundary conditions (4.11) gives us that V_{00} is the Black-Scholes price with z-dependent volatility. So, we use (more intuitive) notation V_{BS} and x_{BS} instead of V_{00} and x_{00}, respectively. Following (Dixit & Pindyck, 1994), they are given by the formulas

$$\begin{aligned} V_{BS}(x,z) &= \begin{cases} (x_{BS}(z)-K)\left(\frac{x}{x_{BS}(z)}\right)^{\mu_1(z)}, & \text{if } x < x_{BS}(z), \\ x-K, & \text{if } x \geq x_{BS}(z), \end{cases} \\ x_{BS}(z) &= \frac{\mu_1(z)}{\mu_1(z)-1}K, \end{aligned} \tag{4.13}$$

respectively, where

$$\mu_1(z) := \left(\frac{1}{2} - \frac{r-q}{\bar{\sigma}^2_{4/2}(z)}\right) + \sqrt{\left(\frac{1}{2} - \frac{r-q}{\bar{\sigma}^2_{4/2}(z)}\right)^2 + \frac{2r}{\bar{\sigma}^2_{4/2}(z)}}. \tag{4.14}$$

By solving the ODE problem in (4.7) for $V_{01}(x,z)$ and the ODE problem in (4.8) for $V_{10}(x,z)$, we obtain the following price formula.

Proposition 4.3.1. *Under the dynamics (4.1) of the value of an innovative project, the real option price, given in (4.2), is approximated by*

$$\widetilde{V}(x,z) := V_{BS}(x,z) + \sqrt{\epsilon}V_{01}(x,z) + \sqrt{\delta}V_{10}(x,z),$$

where $V_{BS}(x,z)$ is given by (4.13) and $V_{01}(x,z)$ and $V_{10}(x,z)$ are given by

$$
\begin{aligned}
V_{01}(x,z) &= \frac{-2F(z)\mu_1^2(z)(\mu_1(z)-1)}{(\mu_2(z)-\mu_1(z))\bar{\sigma}_{4/2}^2(z)}\left(x_{BS}(z)-K\right)\left(\frac{x}{x_{BS}(z)}\right)^{\mu_1(z)}\log\left(\frac{x}{x_{BS}(z)}\right),\\
V_{10}(x,z) &= \frac{2S(z)x^{\mu_1(z)}}{(\mu_2(z)-\mu_1(z))\bar{\sigma}_{4/2}^2(z)}\left[\left\{\mu_1(z)\frac{x_{BS}^{'}(z)}{x_{BS}^{\mu_1(z)}(z)}\right.\right.\\
&\quad\left.-\frac{x_{BS}(z)-K}{x_{BS}^{\mu_1(z)}(z)}\left(\mu_1(z)\mu_1^{'}(z)\log x_{BS}(z)+\mu_1^2(z)\frac{x_{BS}^{'}(z)}{x_{BS}(z)}-\mu_1^{'}(z)\right)\right\}\\
&\quad\cdot\log\left(\frac{x}{x_{BS}(z)}\right)\\
&\quad+\mu_1(z)\mu_1^{'}(z)\frac{x_{BS}(z)-K}{x_{BS}^{\mu_1(z)}(z)}\left\{\frac{1}{2}\log(x_{BS}(z)x)\log\left(\frac{x}{x_{BS}(z)}\right)\right.\\
&\quad-\frac{1}{\mu_1(z)}\left(\log x-\frac{1}{\mu_1(z)}\right)x^{\mu_2(z)}\\
&\quad\left.\left.+\frac{1}{\mu_1(z)}\left(\log x_{BS}(z)-\frac{1}{\mu_1(z)}\right)x_{BS}^{\mu_2(z)}(z)\right\}\right]
\end{aligned}
\tag{4.15}
$$

respectively, where $F(z)$ and $S(z)$ are given by (4.9), respectively, and $\mu_1(z)$ is given as (4.14) and $\mu_2(z)$ is

$$
\mu_2(z) := \left(\frac{1}{2}-\frac{r-q}{\bar{\sigma}_{4/2}^2(z)}\right)-\sqrt{\left(\frac{1}{2}-\frac{r-q}{\bar{\sigma}_{4/2}^2(z)}\right)^2+\frac{2r}{\bar{\sigma}_{4/2}^2(z)}}. \tag{4.16}
$$

Proof. Calculating $\mathcal{D}_1\mathcal{D}_2V_{BS}$ with V_{BS} given by (4.13), the ODE for V_{01} in (4.6) becomes

$$
\left(-r\,\mathcal{D}_0+(r-q)\,\mathcal{D}_1+\frac{1}{2}\,\bar{\sigma}_{BS}^2(z)\,\mathcal{D}_2\right)V_{01}(x,z) = C_1(z)x^{\mu_1(z)}, \tag{4.17}
$$

where $C_1(z)$ is given by

$$
C_1(z) = F(z)\mu_1^2(z)(\mu_1(z)-1)\frac{x_{BS}(z)-K}{x_{BS}^{\mu_1(z)}(z)}. \tag{4.18}
$$

To solve equation (4.17), we use the variation of parameters method by taking the

substitution $x = e^s$. Then the ODE (4.17) becomes

$$\left(\partial_{ss} - 2\left(\frac{1}{2} - \frac{r-q}{\bar{\sigma}^2_{4/2}(z)}\right)\partial_s - \frac{2r}{\bar{\sigma}^2_{4/2}(z)}\right)V_{01}(s,z) = 2C_1(z)\frac{e^{\mu_1(z)s}}{\bar{\sigma}^2_{4/2}(z)}. \quad (4.19)$$

The two linearly independent solutions to the homogeneous part of (4.19) are

$$u_1(s,z) = e^{\mu_1(z)s}, \qquad \text{and} \qquad u_2(s,z) = e^{\mu_2(z)s},$$

where $\mu_1(z)$ and $\mu_2(z)$ are given by (4.14) and (4.16), respectively. Using the Wronskian

$$W(u_1,u_2) = (\mu_2 - \mu_1)e^{(\mu_1+\mu_2)s}$$

of the two linearly independent solutions, the general solution of (4.19) is given by

$$\begin{aligned} V_{01}(s,z) &= A_{\mu_2}(s,z)u_1(s,z) + A_{\mu_1}(s,z)u_2(s,z), \\ A_{\mu_2}(s,z) &:= \int \frac{-1}{W(s,z)} f(s,z)e^{\mu_2(z)s}\,ds, \\ A_{\mu_1}(s,z) &:= \int \frac{1}{W(s,z)} f(s,z)e^{\mu_1(z)s}\,ds, \end{aligned} \quad (4.20)$$

where f is the source term given by

$$f(s,z) = 2C_1(z)e^{\mu_1(z)s}\bar{\sigma}^{-2}_{4/2}(z).$$

Calculating the integrals in (4.20) and substituting back to the x variable lead to

$$\begin{aligned} V_{01}(x,z) = \frac{2C_1(z)}{(\mu_2(z)-\mu_1(z))\bar{\sigma}^2_{4/2}(z)} &\left(-d_1(z)x^{\mu_1(z)} + d_2(z)x^{\mu_2(z)}\right. \\ &\left. -\left(\frac{1}{\mu_2(z)-\mu_1(z)} + \log x\right)x^{\mu_1(z)}\right) \end{aligned} \quad (4.21)$$

for some functions $d_1(z)$ and $d_2(z)$. Using $\mu_1(z) > 0 > \mu_2(z)$ and applying the

boundary condition that $V_{01}(x,z)$ converges to 0 as x goes to 0, we find that $d_2(z) = 0$. From the boundary condition $V_{01}(x_{\text{BS}},z) = 0$, we have

$$d_1(z) = -(\mu_2(z) - \mu_1(z))^{-1} - \log x_{\text{BS}}(z).$$

Therefore, (4.21) becomes

$$V_{01}(x,z) = \frac{-2C_1(z)}{(\mu_2(z)-\mu_1(z))\bar{\sigma}^2_{4/2}(z)} x^{\mu_1(z)} \log\left(\frac{x}{x_{\text{BS}}(z)}\right). \tag{4.22}$$

Plugging $C_1(z)$ in (4.18) into (4.22), we obtain the result for $V_{01}(x,z)$ in Proposition 4.3.1.

Next, calculating $\mathcal{D}_1\partial_z V_{\text{BS}}$ with V_{BS} given by (4.13), the ODE for V_{10} in (4.6) becomes

$$\begin{aligned}\left(-r\,\mathcal{D}_0 + (r-q)\,\mathcal{D}_1 + \frac{1}{2}\,\bar{\sigma}^2_{\text{BS}}(z)\,\mathcal{D}_2\right) V_{10}(x,z) &= C_2^a(z)x^{\mu_1(z)} \\ &\quad + C_2^b(z)x^{\mu_1(z)}\log x, \end{aligned}\tag{4.23}$$

where $C_2^a(z)$ and $C_2^b(z)$ are given by

$$\begin{aligned} C_2^a(z) &= -S(z)\left(\mu_1(z)\frac{x'_{\text{BS}}(z)}{x^{\mu_1(z)}_{\text{BS}}(z)}\right. \\ &\quad \left. -\frac{x_{\text{BS}}(z)-K}{x^{\mu_1(z)}_{\text{BS}}(z)}\left(\mu_1(z)\mu_1'(z)\log x_{\text{BS}}(z) + \mu_1^2(z)\frac{x'_{\text{BS}}(z)}{x_{\text{BS}}(z)} - \mu_1'(z)\right)\right), \\ C_2^b(z) &= -S(z)\left(\mu_1(z)\mu_1'(z)\frac{x_{\text{BS}}(z)-K}{x^{\mu_1(z)}_{\text{BS}}(z)}\right). \end{aligned}\tag{4.24}$$

By the change of variables $x = e^s$, the ODE (4.23) becomes

$$\begin{aligned}\left(\partial_{ss} - 2\left(\frac{1}{2} - \frac{r-q}{\bar{\sigma}^2_{4/2}(z)}\right)\partial_s - \frac{2r}{\bar{\sigma}^2_{4/2}(z)}\right) V_{10}(s,z) \\ = \frac{2}{\bar{\sigma}^2_{\text{BS}}(z)}\left(C_2^a(z)e^{\mu_1(z)s} + C_2^b(z)se^{\mu_1(z)s}\right). \end{aligned}\tag{4.25}$$

Using the same method as above for $V_{01}(s,z)$ and substituting back to the x variable, we can obtain

$$\begin{aligned} V_{10}(x,z) &= \frac{2}{(\mu_2(z)-\mu_1(z))\bar{\sigma}_{4/2}^2(z)}\Bigg[-\left(C_2^a(z)\log x+\frac{1}{2}C_2^b(z)(\log x)^2+d_2(z)\right)x^{\mu_1(z)} \\ &\quad+\left(C_2^a(z)\frac{x^{\mu_1(z)-\mu_2(z)}}{\mu_1(z)-\mu_2(z)}\right. \\ &\quad\left.+C_2^b(z)\frac{1}{\mu_1(z)}\left(\log x-\frac{1}{\mu_1(z)}\right)x^{\mu_1(z)}+d_1(z)\right)x^{\mu_2(z)}\Bigg] \end{aligned} \tag{4.26}$$

for some functions $d_1(z)$ and $d_2(z)$. From the boundary condition that $V_{10}(x,z)$ converges to 0 as x goes to 0, $d_1(z) = 0$. The boundary condition

$$V_{10}(x_{\text{BS}},z) = 0$$

leads to

$$\begin{aligned} d_2(z) &= \frac{C_2^a(z)}{\mu_1(z)-\mu_2(z)}+\frac{C_2^b(z)}{\mu_1(z)}\left(\log x_{\text{BS}}(z)-\frac{1}{\mu_1(z)}\right)x_{\text{BS}}^{\mu_2(z)}(z) \\ &\quad-\left(C_2^a(z)\log x_{\text{BS}}(z)+\frac{1}{2}C_2^b(z)(\log x_{\text{BS}}(z))^2\right). \end{aligned} \tag{4.27}$$

Therefore, substituting $C_2^a(z)$ and $C_2^a(z)$ in (4.24) into (4.26), we obtain the result for $V_{10}(x,z)$ in Proposition 4.3.1.

As a corollary of Proposition 4.3.1, we obtain an approximation formula for the free boundary $x_*(z)$. □

Corollary 4.3.1. *Under the dynamics (4.1) of the value of an innovative project, the free boundary x_* is approximated by*

$$x_*(z) := x_{\text{BS}}(z)+\sqrt{\epsilon}x_{01}(z)+\sqrt{\delta}x_{10}(z),$$

where

$$
\begin{aligned}
x_{01}(z) &= 2F(z)\frac{\mu_1(z)}{(\mu_2(z)-\mu_1(z))\bar{\sigma}_{4/2}^2(z)}x_{\text{BS}}(z), \\
x_{10}(z) &= \frac{-2S(z)x_{\text{BS}}^2(z)}{\mu_1(z)(\mu_1(z)-1)(\mu_2(z)-\mu_1(z))\bar{\sigma}_{4/2}^2(z)(x_{\text{BS}}(z)-K)}\left[\mu_1(z)\frac{x_{\text{BS}}^{'}(z)}{x_{\text{BS}}(z)}\right. \\
&\quad \left.-\frac{x_{\text{BS}}(z)-K}{x_{\text{BS}}(z)}\left(\mu_1^2(z)\frac{x_{\text{BS}}^{'}(z)}{x_{\text{BS}}(z)}-\mu_1^{'}(z)\right)\right] \\
&\quad -\mu_1^{'}(z)\frac{x_{\text{BS}}(z)-K}{x_{\text{BS}}(z)}\left\{1-\left(\log x_{\text{BS}}(z)-\frac{1}{\mu_1(z)}\right)\mu_2(z)\right\}, \qquad (4.28)
\end{aligned}
$$

where $F(z)$ and $S(z)$ are given by (4.9), respectively, and $\mu_1(z)$ and $\mu_2(z)$ are given by (4.14) and (4.16), respectively.

Proof. Taking the second partial derivative of $V_{\text{BS}}(x,z)$ in (4.13) with respect to x, we have

$$
\partial_{xx}V_{\text{BS}}(x_{\text{BS}},z) = \mu_1(z)(\mu_1(z)-1)\frac{x_{\text{BS}}(z)-K}{x_{\text{BS}}^2(z)}. \qquad (4.29)
$$

The first partial derivative of $V_{01}(x,z)$ in (4.15) with respect to x leads to

$$
\partial_x V_{01}(x_{\text{BS}},z) = \frac{-2F(z)\mu_1^2(z)(\mu_1(z)-1)}{(\mu_2(z)-\mu_1(z))\bar{\sigma}_{4/2}^2(z)}\frac{x_{\text{BS}}(z)-K}{x_{\text{BS}}(z)}. \qquad (4.30)
$$

From (4.12), we have

$$
x_{01}(z) = -\left.\frac{\partial_x V_{01}(x,z)}{\partial_{xx}V_{\text{BS}}(x,z)}\right|_{x=x_{\text{BS}}(z)}.
$$

Thus $x_{01}(z)$ becomes the result in Corollary 4.3.1 from (4.29) and (4.30). On the other

hand, the first partial derivative of $V_{10}(x,z)$ in (4.15) with respect to x yields

$$\begin{aligned}
\partial_x V_{10}(x_{\text{BS}},z) &= \frac{2S(z)x^{\mu_1(z)}}{(\mu_2(z)-\mu_1(z))\bar{\sigma}^2_{4/2}(z)} \\
&\quad\times\left[\mu_1(z)\frac{x'_{\text{BS}}(z)}{x^{\mu_1(z)}_{\text{BS}}(z)}-\frac{x_{\text{BS}}(z)-K}{x^{\mu_1(z)}_{\text{BS}}(z)}\right. \\
&\quad\times\left(\mu_1(z)\mu_1'(z)\log x_{\text{BS}}(z)+\mu_1^2(z)\frac{x'_{\text{BS}}(z)}{x_{\text{BS}}(z)}-\mu_1'(z)\right)\frac{1}{x} \\
&\quad+\mu_1(z)\mu_1'(z)\frac{x_{\text{BS}}(z)-K}{x^{\mu_1(z)}_{\text{BS}}(z)} \\
&\quad\left.\times\left(\frac{1}{x}\log x-\frac{x^{\mu_2(z)-1}}{\mu_1(z)}\left(1-\left(\log x-\frac{1}{\mu_1(z)}\right)\mu_2(z)\right)\right)\right]_{x=x_{\text{BS}}(z)} \\
&= \frac{2S(z)}{(\mu_2(z)-\mu_1(z))\bar{\sigma}^2_{4/2}(z)} \\
&\quad\times\left[\mu_1(z)\frac{x'_{\text{BS}}(z)}{x_{\text{BS}}(z)}-\frac{x_{\text{BS}}(z)-K}{x_{\text{BS}}(z)}\right. \\
&\quad\times\left(\mu_1^2(z)\frac{x'_{\text{BS}}(z)}{x_{\text{BS}}(z)}-\mu_1'(z)\right) \\
&\quad\left.-\mu_1'(z)\frac{x_{\text{BS}}(z)-K}{x_{\text{BS}}(z)}\left(1-\left(\log x_{\text{BS}}(z)-\frac{1}{\mu_1(z)}\right)\mu_2(z)\right)\right]. \qquad (4.31)
\end{aligned}$$

Since from (4.12), we have

$$x_{10}(z) = -\left.\frac{\partial_x V_{10}(x,z)}{\partial_{xx}V_{\text{BS}}(x,z)}\right|_{x=x_{\text{BS}}(z)}, \qquad (4.32)$$

the result for $x_{10}(z)$ in Corollary 4.3.1 follows by plugging (4.29) and (4.31) into (4.32). □

4.4 Numerical Results

In this section, we present some results on five types of numerical experiments. In each type of these experiments, when the model parameters need to be fixed, their values are

designated as

$r = 0.06$, $q = 0.04$, $\epsilon = 0.001$, $\delta = 0.000099$, $\theta = 0.04$, $\xi = 0.123$, $\eta = 0.001$, $\rho_{sv} = -0.7$.

Regarding the real option considered, we define $X_0 = 100$, $T = 1$ and $K = 100$.

a	b	V_{BS}	V_{01}	V_{10}	$\widetilde{V}$	V_{LSM}	Relative error (%)
0	0.000	14.815	61.276	0.000	36.305	36.222	0.2286
	0.010	17.274	39.931	-3.105	30.911	30.850	0.1973
	0.020	22.271	20.851	-5.526	28.930	28.927	0.0104
	0.031	27.805	12.139	-7.797	31.140	31.235	0.3051
	0.041	33.292	7.808	-10.030	34.844	34.925	0.2325
	0.051	38.531	5.377	-12.195	38.973	38.937	0.0924
	0.061	43.433	3.881	-14.242	43.109	43.030	0.1833
	0.071	47.966	2.897	-16.132	47.073	47.173	0.2124
	0.082	52.120	2.218	-17.837	50.788	50.712	0.1496
	0.092	55.906	1.731	-19.345	54.224	54.200	0.0443
0.09099	0.000	15.107	57.898	-1.103	35.283	35.206	0.2182
	0.010	18.628	32.731	-3.941	29.641	29.665	0.0810
	0.020	23.879	17.572	-6.279	29.298	29.322	0.0819
	0.031	29.426	10.577	-8.535	32.125	32.125	0.0000
	0.041	34.850	6.962	-10.751	36.020	35.921	0.2748
	0.051	39.994	4.870	-12.885	40.178	40.179	0.0025
	0.061	44.790	3.554	-14.888	44.275	44.294	0.0460
	0.071	49.212	2.675	-16.723	48.171	48.237	0.1370
	0.082	53.257	2.060	-18.369	51.806	51.807	0.0019
	0.092	56.938	1.616	-19.817	55.160	55.251	0.1650
0.3	0.000	17.530	38.396	-3.280	30.608	30.578	0.0980
	0.010	22.310	20.762	-5.706	28.916	28.880	0.1245
	0.020	27.746	12.202	-7.976	31.081	31.148	0.2156
	0.031	33.186	7.870	-10.206	34.739	34.673	0.1900
	0.041	38.403	5.424	-12.369	38.842	38.826	0.0412
	0.051	43.298	3.916	-14.416	42.966	42.917	0.1140
	0.061	47.830	2.922	-16.305	46.926	46.934	0.0170
	0.071	51.989	2.237	-18.009	50.642	50.561	0.1599
	0.082	55.781	1.746	-19.517	54.084	54.128	0.0814
	0.092	59.225	1.384	-20.827	57.246	57.332	0.1502
0.6	0.000	22.914	19.440	-5.838	29.041	29.002	0.1343
	0.010	28.081	11.851	-8.130	31.275	31.337	0.1982
	0.020	33.369	7.763	-10.366	34.865	34.883	0.0516
	0.031	38.495	5.390	-12.530	38.902	38.879	0.0591
	0.041	43.332	3.907	-14.575	42.978	43.021	0.1001
	0.051	47.828	2.923	-16.463	46.906	46.882	0.0512
	0.061	51.964	2.240	-18.166	50.600	50.513	0.1719
	0.071	55.742	1.750	-19.672	54.028	54.096	0.1259
	0.082	59.178	1.389	-20.980	57.183	57.159	0.0420
	0.092	62.293	1.117	-22.098	60.070	60.023	0.0782
0.9	0.000	28.788	11.157	-8.260	31.723	31.797	0.2333
	0.010	33.833	7.500	-10.509	35.219	35.243	0.0681
	0.020	38.801	5.279	-12.676	39.153	39.065	0.2248
	0.031	43.535	3.856	-14.720	43.145	43.072	0.1692
	0.041	47.960	2.898	-16.604	47.011	47.005	0.0128
	0.051	52.046	2.228	-18.305	50.662	50.621	0.0809
	0.061	55.790	1.745	-19.809	54.058	53.989	0.1276
	0.071	59.202	1.386	-21.115	57.190	57.276	0.1504
	0.082	62.300	1.116	-22.231	60.061	60.074	0.0216
	0.092	65.108	0.908	-23.169	62.685	62.602	0.1324

Table 4.1: Real option values for a fixed and b varying

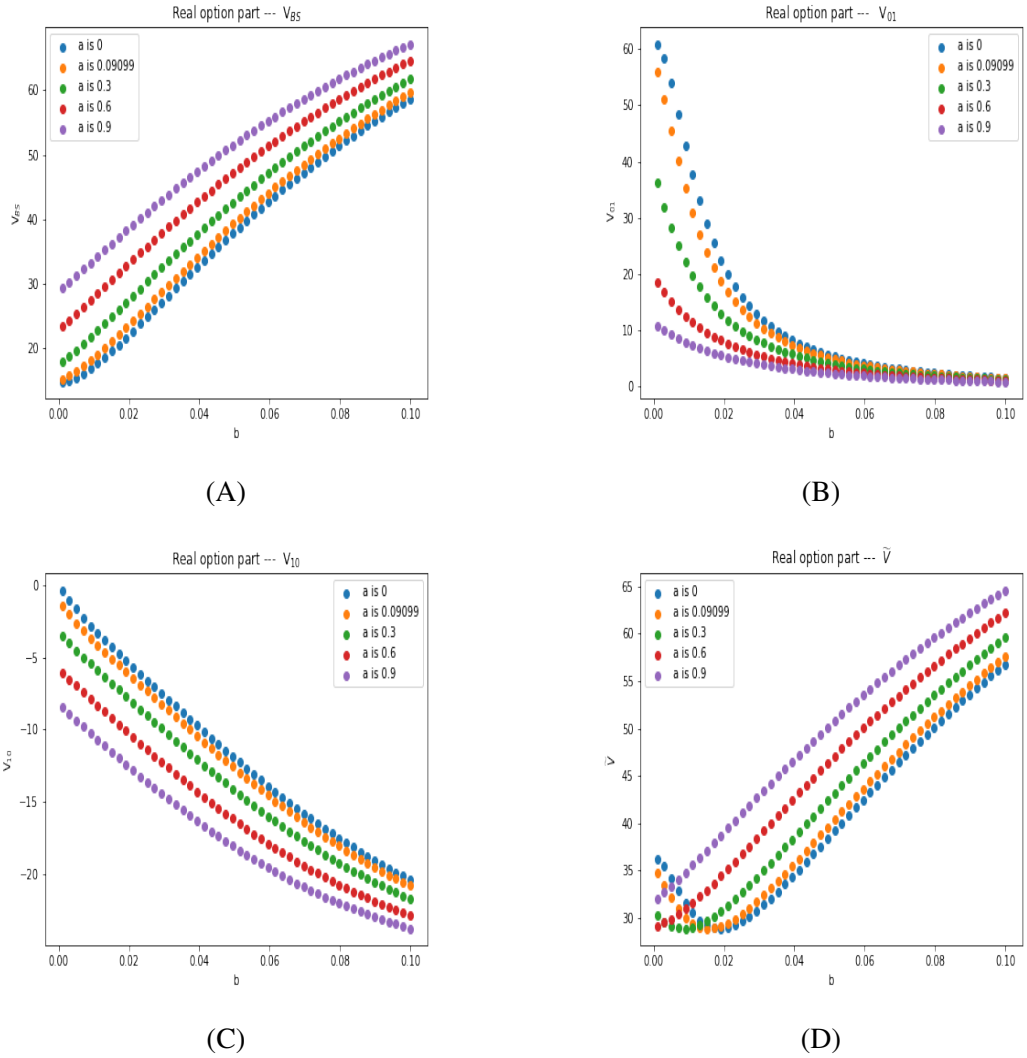

Figure 4.1: Trends of the real option values with variable b

The first type of experiments, shown in Tables 4.1 and 4.2 as well as Figures 4.1 (A)–(D) and Figures 4.2 (A)–(D), are conducted to examine how the values of the real option and the free boundary (investment thresholds) change with varying parameter b (the 3/2 factor), while keeping parameter a (the Heston model factor) fixed at 0, 0.09099, 0.3, 0.6, or 0.9, respectively. In table 1, the V_{LSM} is the simulation results from the least square Monte Carlo approach, and the last column is relative errors $\left(= \left|\widetilde{V} - V_{\text{LSM}}\right| / \widetilde{V}\right)$ between $\widetilde{V}$ (the formula in Proposition 4.3.1) and V_{LSM}. As shown in Table 4.1, apart from the case where $a = 0$ and $b = 0.031$, the relative errors remain below 0.3% in all

other cases. This means that the approximation formula has high accuracy compared with the real option values obtained from simulations of our model.

Figure 4.1(A) shows the changing trend of the leading order term V_{BS}. For all chosen values of a, the V_{BS} rises as b increases. At any fixed b value, V_{BS} grows with an increase in a. In Figures 4.1(B) and 4.1(C), the first-order correction terms V_{01} and V_{10} are described. For a given value of a , the functional curve of V_{01} is convex and decreases as b increases, while V_{10} decreases approximately linearly with respect to b increase. Moreover, Figures 4.1(B)-(C) also describe the V_{01} and V_{10} decrease as a increases, when b is held fixed. In Figure 4.1(D), for a smaller value of a (such as 0, 0.09099, or 0.3), $\widetilde{V}$ decreases as b increases, reflecting the stronger $3/2$ factor in the model. The $\widetilde{V}$ reaches a minimum between 0 and 0.02 before starting to increase again. As a increases with small values of b, the Heston model factor exerts a stronger influence on the model, causing the trend to become less evident. In general, for $b > 0.02$, $\widetilde{V}$ tends to increase with a increase. Additionally, Figures 4.1(A), 4.1(B), and 4.1(D) show that the correction term associated with the fast-varying factor has a greater impact on the real option value than that of the slowly-varying factor, when both a and b are small.

a	b	x_{BS}	x_{01}	x_{10}	x_*
0	0.000	150.000	255.023	0.000	239.440
	0.010	160.633	179.306	0.524	223.580
	0.020	184.948	109.875	0.761	223.573
	0.031	216.988	77.129	0.927	244.148
	0.041	255.496	60.449	1.068	276.823
	0.051	300.383	50.946	1.190	318.392
	0.061	351.824	45.047	1.291	367.776
	0.071	410.043	41.146	1.373	424.635
	0.082	475.252	38.440	1.436	488.903
	0.092	547.639	36.491	1.482	560.613
0.09099	0.000	151.223	243.132	-0.175	236.472
	0.010	166.845	153.369	0.338	220.673
	0.020	193.649	97.656	0.612	227.970
	0.031	227.584	71.151	0.804	252.633
	0.041	267.916	57.155	0.961	288.075
	0.051	314.671	48.951	1.092	331.968
	0.061	368.044	43.752	1.200	383.531
	0.071	428.261	40.261	1.287	442.533
	0.082	495.527	37.810	1.354	508.947
	0.092	570.019	36.028	1.404	582.821
0.3	0.000	161.785	173.797	-0.446	222.685
	0.010	185.153	109.543	0.015	223.573
	0.020	216.610	77.371	0.325	243.783
	0.031	254.678	60.691	0.552	276.028
	0.041	299.181	51.131	0.733	317.200
	0.051	350.260	45.183	0.881	366.210
	0.061	408.124	41.247	1.000	422.708
	0.071	472.982	38.516	1.097	486.620
	0.082	545.017	36.549	1.172	557.974
	0.092	624.384	35.090	1.230	636.836
0.6	0.000	188.372	104.630	-0.639	224.991
	0.010	218.749	76.032	-0.275	245.382
	0.020	256.093	60.275	0.021	277.235
	0.031	300.042	50.998	0.258	317.959
	0.041	350.653	45.149	0.452	366.541
	0.051	408.095	41.248	0.611	422.633
	0.061	472.554	38.530	0.742	486.155
	0.071	544.204	36.567	0.848	557.129
	0.082	623.194	35.108	0.934	635.617
	0.092	709.648	33.996	1.001	721.689
0.9	0.000	223.340	73.375	-0.777	248.982
	0.010	259.720	59.253	-0.474	280.445
	0.020	302.961	50.560	-0.205	320.669
	0.031	353.002	44.946	0.025	368.769
	0.041	409.954	41.151	0.219	424.412
	0.051	473.969	38.483	0.383	487.511
	0.061	545.202	36.545	0.519	558.081
	0.071	623.793	35.099	0.631	636.177
	0.082	709.857	33.994	0.723	721.865
	0.092	803.494	33.134	0.798	815.209

Table 4.2: Free boundary values for a fixed and b varying

The values of x_{BS}, x_{01}, x_{10} and x_* from Table 4.2 are displayed in Figures 4.2(A)–4.2(D), plotted for each fixed a across varying b.

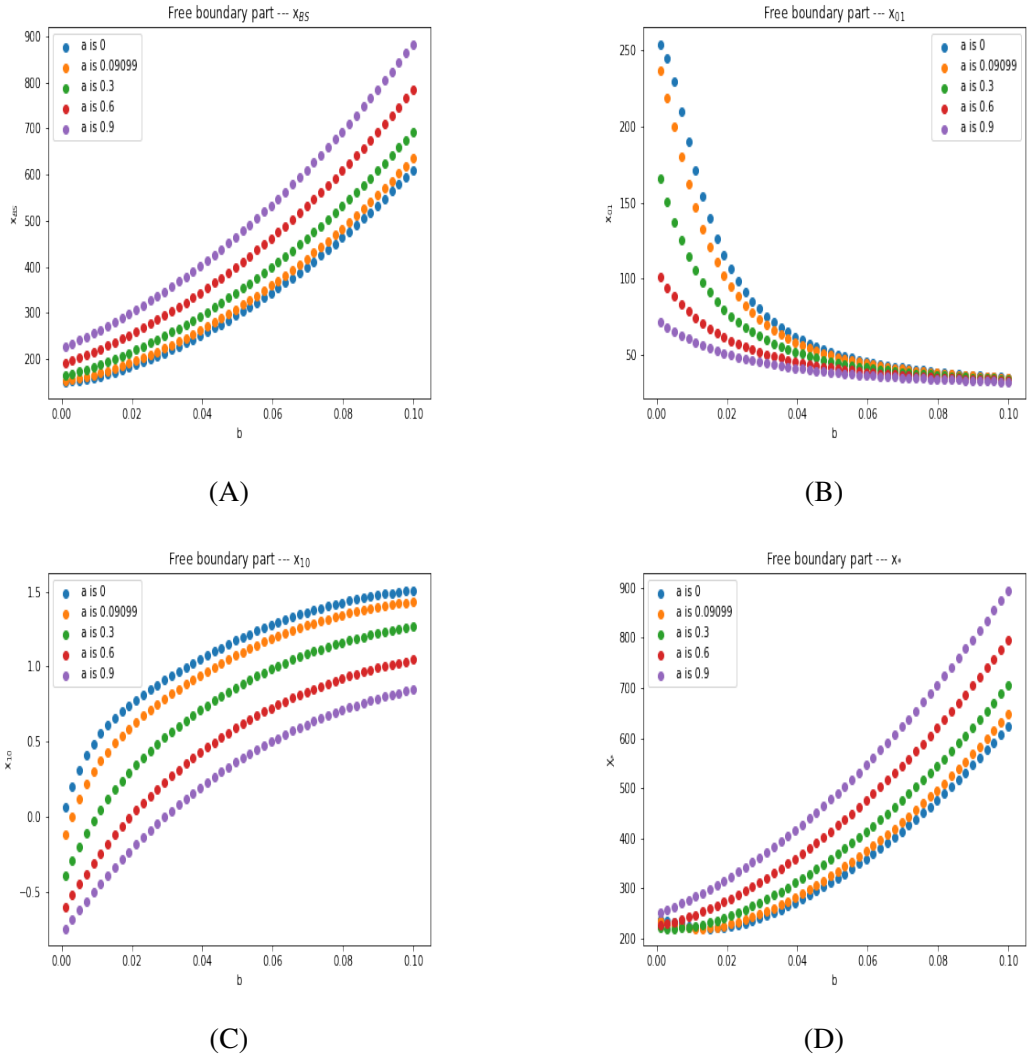

(A) (B)

(C) (D)

Figure 4.2: Trends of free boundary values with variable b

In Figures 4.2(A)-(D), the changing trends of the free boundary values as the parameter b changes are presented. The variation of free boundary values concerning changing b under different values of a is represented by each curve. As b increases, both the leading-order term x_{BS} and the first correction term x_{10}, which are tied to slow mean reversion, become larger. Moreover, the first correction term x_{01}, associated with fast-varying mean-reverting, tends to decrease as b increases. Just like that in Figure 4.1(D), when $a = 0$, as b ($3/2$ factor) increases, the approximate value x_* decreases initially and reaches a minimum around $b = 0.02$, and then starts to increase. As the parameter

a (the Heston model factor) increases, the trend becomes less obvious. For a fixed b greater than 0.02, the value of x_* tends to increase as a increases. The leading order term x_{BS} increases as a increases, for a given value of b, but the free boundary values show an upward trend with respect to a, only when $b > 0.02$. The curves in Figures 4.2(A), 4.2(B), and 4.2(D) are convex, whereas those in Figure 4.2(C) are concave. Moreover, the correction term from the fast-varying factor has a strong influence on the free boundary values when both a and b are small. In all cases, the correction term from the slowly varying factor has a relatively minor impact on the free boundary value.

As detailed in Tables 4.3 and 4.4, the second type of experiments investigate how the real option and free boundary values respond to changes in parameter a (the Heston model factor), while parameter b ($3/2$ factor) is held constant at 0, 0.000111, 0.01, 0.05, and 0.09999, respectively. Table 4.3 reports the results of V_{LSM} from the least square Monte Carlo approach and the results of relative errors between $\widetilde{V}$ (the formula in Proposition 4.3.1) and V_{LSM}. As shown in Table 4.3, the relative errors are less than 0.3% in all cases. This result further substantiates the elevated precision of our approximation formula for the value of the real option within our model.

b	a	V_{BS}	V_{01}	V_{10}	$\widetilde{V}$	V_{LSM}	Relative error (%)
0	0.000	14.815	61.276	0.000	36.305	36.224	0.2231
	0.102	15.181	57.098	-1.232	35.060	35.129	0.1968
	0.204	16.183	47.689	-2.348	32.630	32.649	0.0582
	0.306	17.625	37.848	-3.336	30.504	30.422	0.2688
	0.408	19.336	29.733	-4.241	29.262	29.336	0.2529
	0.510	21.201	23.562	-5.100	28.861	28.851	0.0346
	0.612	23.150	18.957	-5.938	29.096	29.183	0.2990
	0.714	25.141	15.500	-6.766	29.776	29.834	0.1948
	0.816	27.146	12.867	-7.588	30.760	30.809	0.1593
	0.918	29.146	10.826	-8.407	31.948	32.003	0.1722
0.00111	0.000	14.849	60.866	-0.377	36.151	36.218	0.1853
	0.102	15.404	54.764	-1.583	34.423	34.506	0.2411
	0.204	16.545	44.874	-2.660	31.968	32.047	0.2471
	0.306	18.074	35.417	-3.619	30.067	30.149	0.2727
	0.408	19.835	27.861	-4.507	29.073	29.048	0.0860
	0.510	21.728	22.165	-5.357	28.867	28.870	0.0104
	0.612	23.691	17.913	-6.191	29.241	29.252	0.0376
	0.714	25.688	14.710	-7.016	30.017	29.932	0.2832
	0.816	27.693	12.258	-7.837	31.065	31.044	0.0676
	0.918	29.690	10.349	-8.654	32.296	32.299	0.0093
0.01	0.000	17.189	40.464	-3.052	31.019	31.053	0.1096
	0.102	18.710	32.363	-3.989	29.588	29.600	0.0406
	0.204	20.450	25.790	-4.865	28.919	28.854	0.2248
	0.306	22.318	20.742	-5.710	28.917	28.893	0.0830
	0.408	24.257	16.910	-6.540	29.414	29.458	0.1496
	0.510	26.230	13.983	-7.363	30.263	30.178	0.2809
	0.612	28.212	11.718	-8.182	31.354	31.446	0.1977
	0.714	30.188	9.937	-8.997	32.609	32.531	0.2392
	0.816	32.146	8.517	-9.807	33.972	34.069	0.2855
	0.918	34.076	7.366	-10.609	35.405	35.332	0.2062
0.05	0.000	38.021	5.568	-11.983	38.556	38.610	0.1401
	0.102	39.673	4.976	-12.760	39.909	39.889	0.0501
	0.204	41.308	4.462	-13.520	41.274	41.179	0.2302
	0.306	42.920	4.013	-14.262	42.641	42.654	0.0305
	0.408	44.505	3.620	-14.983	44.001	44.071	0.1591
	0.510	46.057	3.275	-15.684	45.350	45.364	0.0309
	0.612	47.575	2.971	-16.362	46.681	46.772	0.1949
	0.714	49.056	2.701	-17.016	47.990	47.924	0.1375
	0.816	50.499	2.462	-17.646	49.275	49.277	0.0041
	0.918	51.903	2.249	-18.250	50.532	50.505	0.0534
0.0999	0.000	58.649	1.440	-20.397	56.741	56.820	0.1392
	0.102	59.718	1.338	-20.872	57.718	57.814	0.1663
	0.204	60.761	1.245	-21.324	58.674	58.722	0.0818
	0.306	61.776	1.159	-21.752	59.608	59.592	0.0268
	0.408	62.7634	1.079	-22.156	60.520	60.573	0.0876
	0.510	63.723	1.007	-22.538	61.409	61.400	0.0147
	0.612	64.655	0.940	-22.897	62.275	62.217	0.0931
	0.714	65.560	0.878	-23.234	63.119	63.180	0.0966
	0.816	66.438	0.821	-23.551	63.940	63.883	0.0891
	0.918	67.290	0.768	-23.847	64.738	64.696	0.0649

Table 4.3: Real option values for b fixed and a varying

In Figures 4.3(A)-(D), the values of V_{BS}, V_{01}, V_{10} and $\widetilde{V}$ corresponding to each fixed b and varying a from Table 4.3 are shown, respectively.

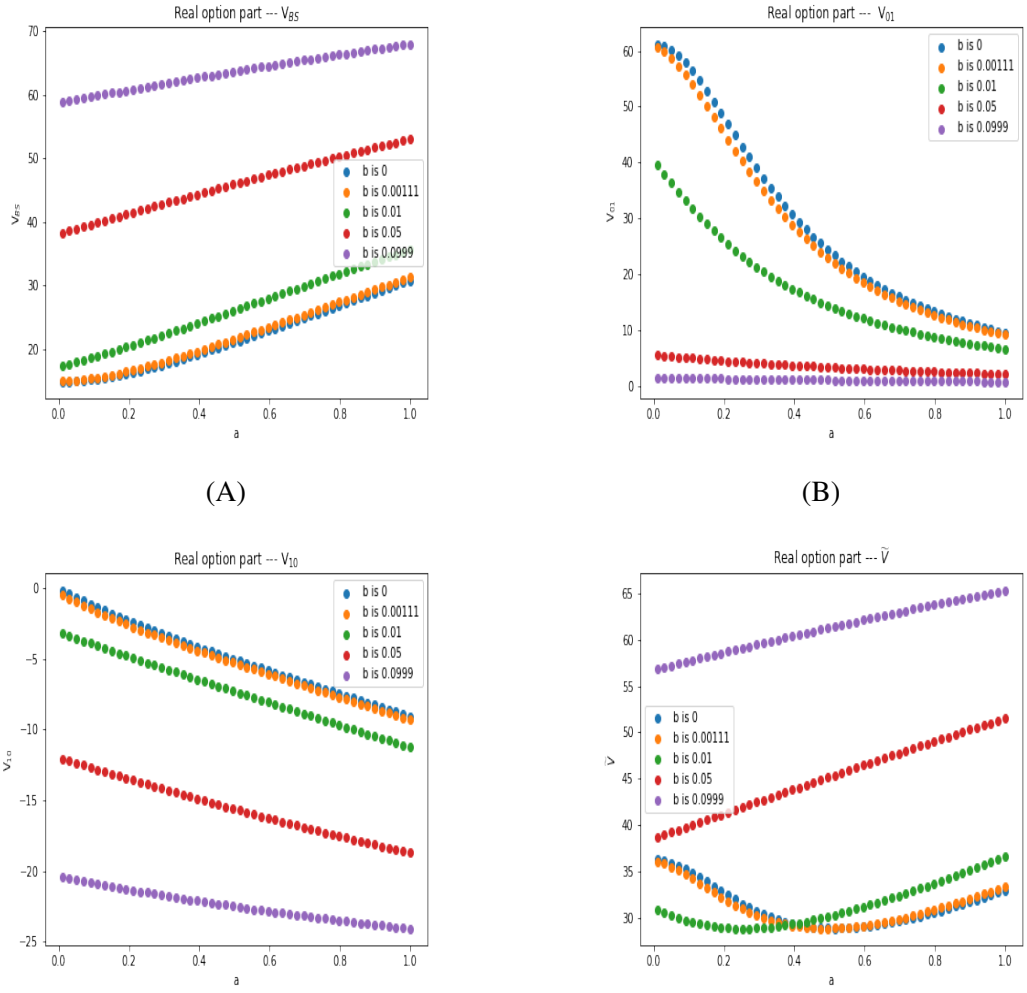

(A) (B)

(C) (D)

Figure 4.3: Trends of real option values with variable a

In Figures 4.3(A)–(D), the trend of the real option value with respect to the parameter a is described. Each curve illustrates how the real option value changes as a increases under different fixed values of b. As shown in Figure 4.3(A), the leading-order term increases a when b is fixed. Figures 4.3(B) and 4.3(C) illustrate that the first-order correction term declines with increasing a when b is fixed. We see from Figure 4.3(D) that for small value of b (e.g., 0, 0.00111 or 0.01), as a increases, the approximate value $\widetilde{V}$ of the real option exhibits a trend of initially decreasing and then increasing as a increases. However, for large values of b (e.g., 0.05 or 0.0999), $\widetilde{V}$ grows as a

increases. These figures indicate that the correction term from the fast-varying factor has a significant impact on the real option value when a and b are small. However, the impact of the fast-varying factor decreases as b increases.

b	a	x_{BS}	x_{01}	x_{10}	x_*
0	0.000	150.000	255.023	-0.000	239.440
	0.102	151.531	240.310	-0.194	235.788
	0.204	155.814	206.997	-0.345	228.369
	0.306	162.217	171.827	-0.451	222.425
	0.408	170.196	142.487	-0.529	220.106
	0.510	179.406	119.896	-0.591	221.385
	0.612	189.648	102.829	-0.645	225.636
	0.714	200.814	89.872	-0.695	232.252
	0.816	212.846	79.902	-0.741	240.781
	0.918	225.714	72.105	-0.784	250.910
0.00111	0.000	150.142	253.581	0.074	239.085
	0.102	152.474	232.072	-0.134	233.848
	0.204	157.394	196.975	-0.287	226.442
	0.306	164.269	163.077	-0.397	221.415
	0.408	172.608	135.664	-0.479	220.130
	0.510	182.112	114.741	-0.546	222.288
	0.612	192.612	98.933	-0.604	227.237
	0.714	204.016	86.892	-0.657	234.413
	0.816	216.277	77.585	-0.705	243.403
	0.918	229.369	70.276	-0.751	253.927
0.01	0.000	160.250	181.217	0.517	223.867
	0.102	167.227	152.035	0.310	220.584
	0.204	175.633	128.085	0.137	220.570
	0.306	185.198	109.471	-0.000	223.591
	0.408	195.765	95.177	-0.113	229.132
	0.510	207.247	84.142	-0.208	236.732
	0.612	219.594	75.521	-0.291	246.046
	0.714	232.784	68.690	-0.364	256.831
	0.816	246.805	63.201	-0.430	268.919
	0.918	261.656	58.732	-0.490	282.196
0.05	0.000	295.601	51.697	1.178	313.871
	0.102	311.461	49.370	1.068	328.902
	0.204	328.239	47.342	0.962	344.957
	0.306	345.935	45.569	0.861	362.019
	0.408	364.549	44.015	0.765	380.076
	0.510	384.082	42.647	0.673	399.118
	0.612	404.539	41.439	0.587	419.141
	0.714	425.923	40.368	0.505	440.141
	0.816	448.241	39.415	0.428	462.115
	0.918	471.497	38.566	0.355	485.065
0.0999	0.000	610.021	35.315	1.509	622.585
	0.102	637.070	34.902	1.423	649.479
	0.204	665.109	34.521	1.340	677.374
	0.306	694.140	34.169	1.260	706.273
	0.408	724.165	33.844	1.182	736.174
	0.510	755.186	33.543	1.107	767.081
	0.612	787.205	33.264	1.035	798.994
	0.714	820.225	33.006	0.965	831.915
	0.816	854.248	32.766	0.899	865.845
	0.918	889.274	32.543	0.835	900.787

Table 4.4: Free boundary values for b fixed and a varying

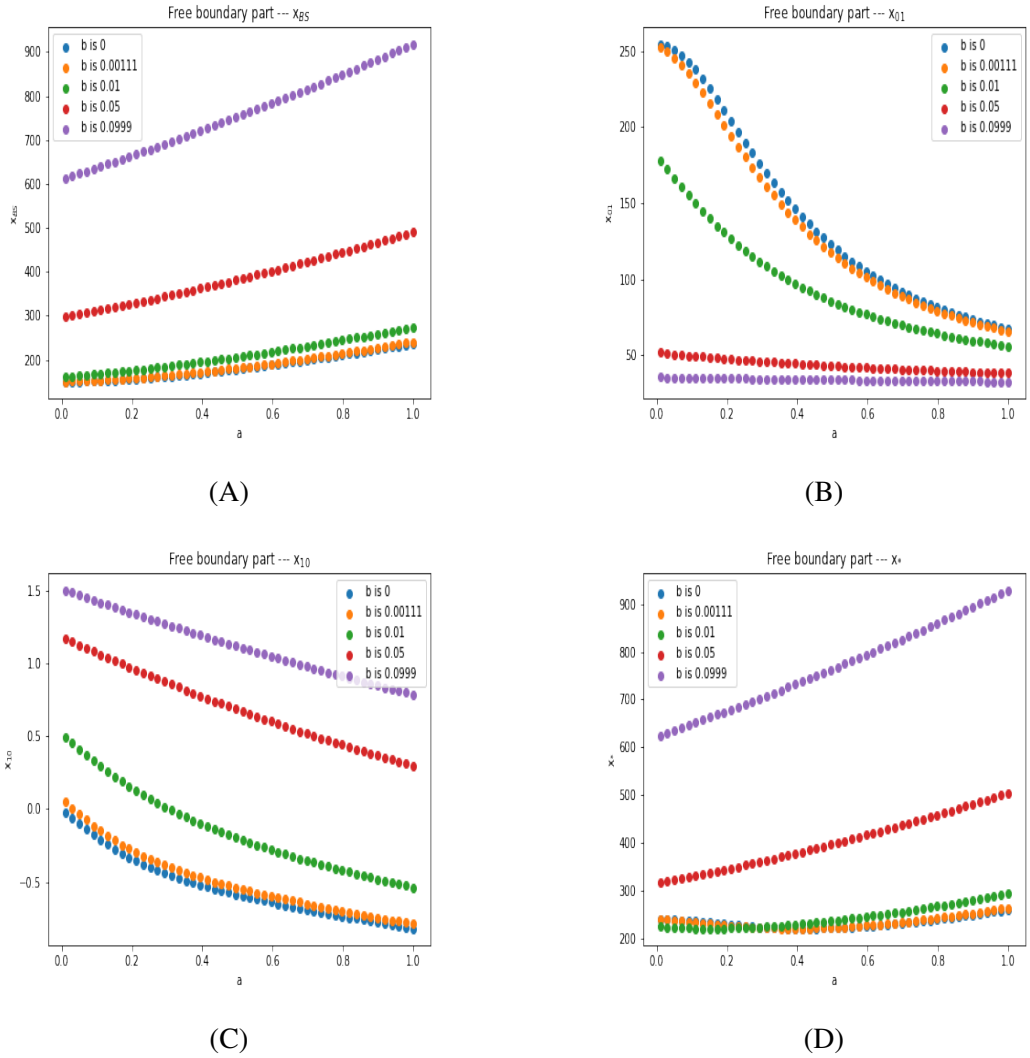

Figure 4.4: Free boundary value trends with variable a

Figures 4.4(A)-(D) display the relationships between b and the values of x_{BS}, x_{01}, x_{10} and x_*, for each fixed value of a, as shown in Table 4.4. Figures 4.4(A)-(D) show the trends of variation in the free boundary value relative to changes in parameter a, while highlighting the differences in free boundary values across various values of b (sensitivity). Each curve illustrates the trend of the free boundary value in relation to variations a at a certain value of b. As we can see from Figures 4.4(A)-(C), for a fixed value of b, as a increases, the leading order term x_{BS} increases slightly, but the first order correction terms decrease. When the value b is little (e.g., 0, 0.00111, or 0.01), the

estimated value x_* shows a small variation, as a increases. However, when $b = 0.05$ or $b = 0.0999$, a clear upward trend in the free boundary value emerges as a increases. Moreover, as b increases, for a fixed a, x_{BS} or x_* is higher compared to their values at smaller b.

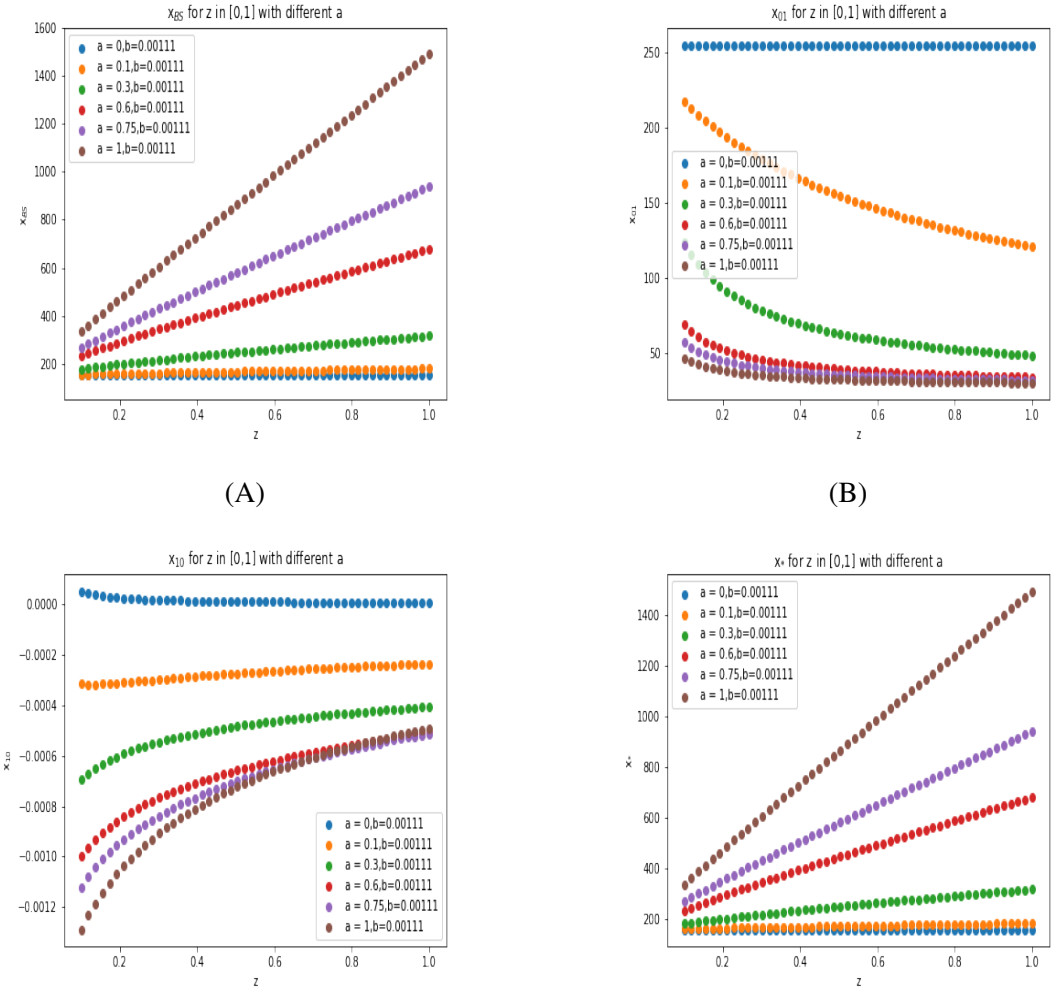

(A) (B)

(C) (D)

Figure 4.5: Effect of z on free boundary values with variable a and fixed b

From Figures 4.1-4.4, we observe that both real option and free boundary values vary more drastically with respect to the 3/2-factor than the Heston factor. This means the 3/2-factor of the 4/2 model can play a role in capturing extreme behaviors of the project value.

The third type of experiment is to examine the variation of the free border in relation to the volatility variable z, when a and b assume a predetermined set of values. In Figures 4.5(A)–(D), the variation trends of the free boundary value with respect to variable z (ranging from 0 to 1) are shown, with b = 0.0011 and a set to 0.1, 0.3, 0.6, 0.75, and 1, respectively. Figures 4.5(A) and 4.5(D) show that the leading order term and the approximate value of the free boundary increase as z increases. Overall, when z is fixed, both values increase as a increases. In Figure 4.5(B), all curves except for the case $a = 0$ are convex, and the first-order correction term corresponding to the fast-varying factor decreases as z increases.

In contrast, Figure 4.5(C) shows an opposite trend for the first-order correction term associated with the slowly-varying factor. Moreover, for a fixed value of z, both values decrease as a increases. Overall, the first-order correction term contributes little to the free boundary value. In contrast, Figure 4.5(C) shows that the first-order correction term related to the slowly-varying factor exhibits an opposite trend. Moreover, when z is fixed, these two values decline as a increases. In general, the first-order correction term has minimal impact on the free boundary value.

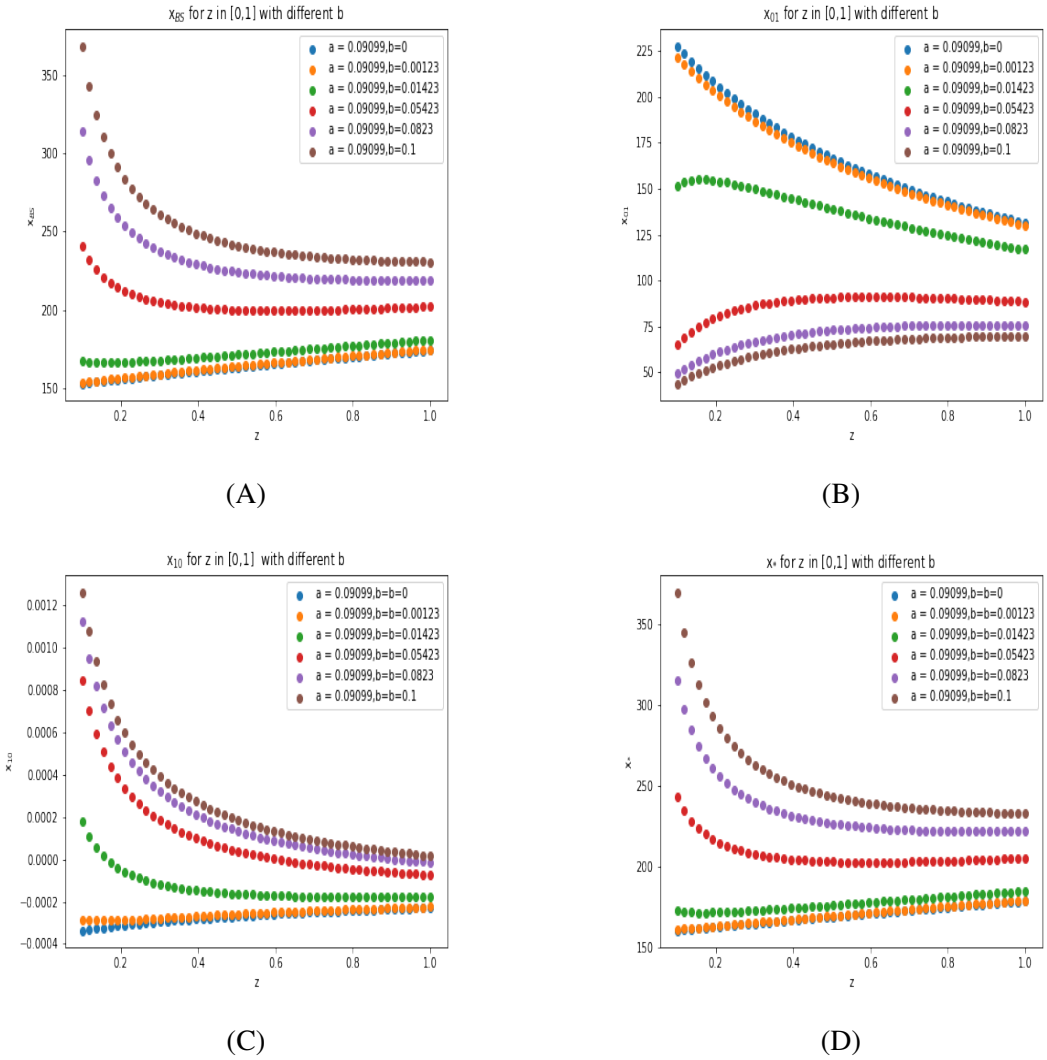

(A) (B)

(C) (D)

Figure 4.6: Effect of z on free boundary values with variable b and fixed value of a

In Figures 4.6(A)–(D), the variation trends of the free boundary value concerning the volatility variable z (ranging from 0 to 1) are presented, where $a = 0.0909911$ and b is set to 0.00123, 0.01423, 0.05423, 0.0823, and 0.1, respectively.

The similar patterns are shown in Figures 4.6(A), 4.6(C) and 4.6(D). When b takes relatively large values (such as 0.05423, 0.0823, or 0.1), the corresponding curves are convex, and x_{BS}, x_{10}, and x_* show a decreasing trend as z increases. But, when b takes relatively small values (e.g., $b = 0$ or 0.00123), x_{BS}, x_{10} and x_* increase as straight lines in z. In these figures, for a fixed value of z, both x_{BS} and x_* increase as b increases.

For a fixed value z, as b increases, x_{01} decreases but x_{10} increases. Due to the strong similarity in the patterns of the curves in Figures 4.6(A) and 4.6(D), it can be concluded that the correction term's effect on the free boundary value is minimal.

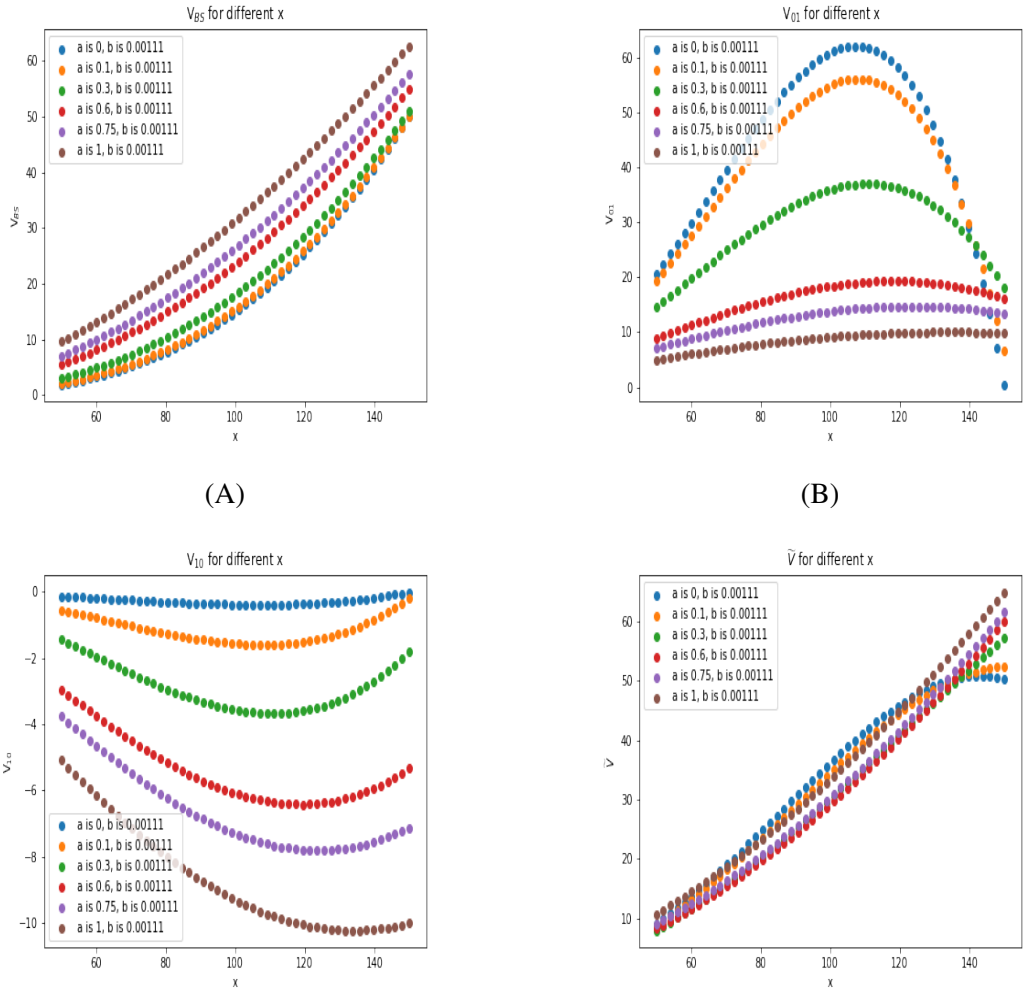

Figure 4.7: Real option value trends with respect to project value, fixed b and variable a

In the fourth type of experiments, the change of the real option value relative to the initial real project value x is investigated for selected paired values of parameters a and b. Figures 4.7(A)-(D) show the changing trends of real option values concerning changes in x when the parameter b is fixed and the parameter a varies. As shown in

Figure 4.7(A), the leading order term V_{BS} exhibits an increasing trend as the project value rises. This finding corresponds to the results under the Black–Scholes model framework. Moreover, with other parameters held constant, an increase in the parameter a leads to a higher value of V_{BS}. Figures 4.7(B) and 4.7(C) exhibit distinctly different qualitative characteristics of the two correction components. The curves in Figure 4.7(B) are convex. As the project value increases, the first-order correction term V_{01} initially rises and then declines. For $a = 0, 0.1$, or 0.3, V_{01} attains a maximum around a project value of 115. Thereafter, V_{01} decreases sharply when $x > 115$. The curves in Figure 4.7(C) are concave, and when the project value increases, the first-order corrective term V_{01} initially decreases before subsequently growing. Figures 4.7(B) and 4.7(C) show that when x is held constant, the correction term declines as the parameter a grows. In Figure 4.7(D), it is shown that when volatility has stochastic characteristics, the real option value does not always increase as the initial project value rises. This differs from the results within the Black–Scholes model framework. In particular, for relatively small values of parameters a and b, the real option value initially rises to a peak and then declines as the project value increases. This behavior arises from the impact of the correction term V_{01}, linked to the rapidly fluctuating component. For relatively large values of a (e.g., $a \geq 0.3$), the curves depicted in Figures 4.7(A) and 4.7(D) show similar qualitative behavior.

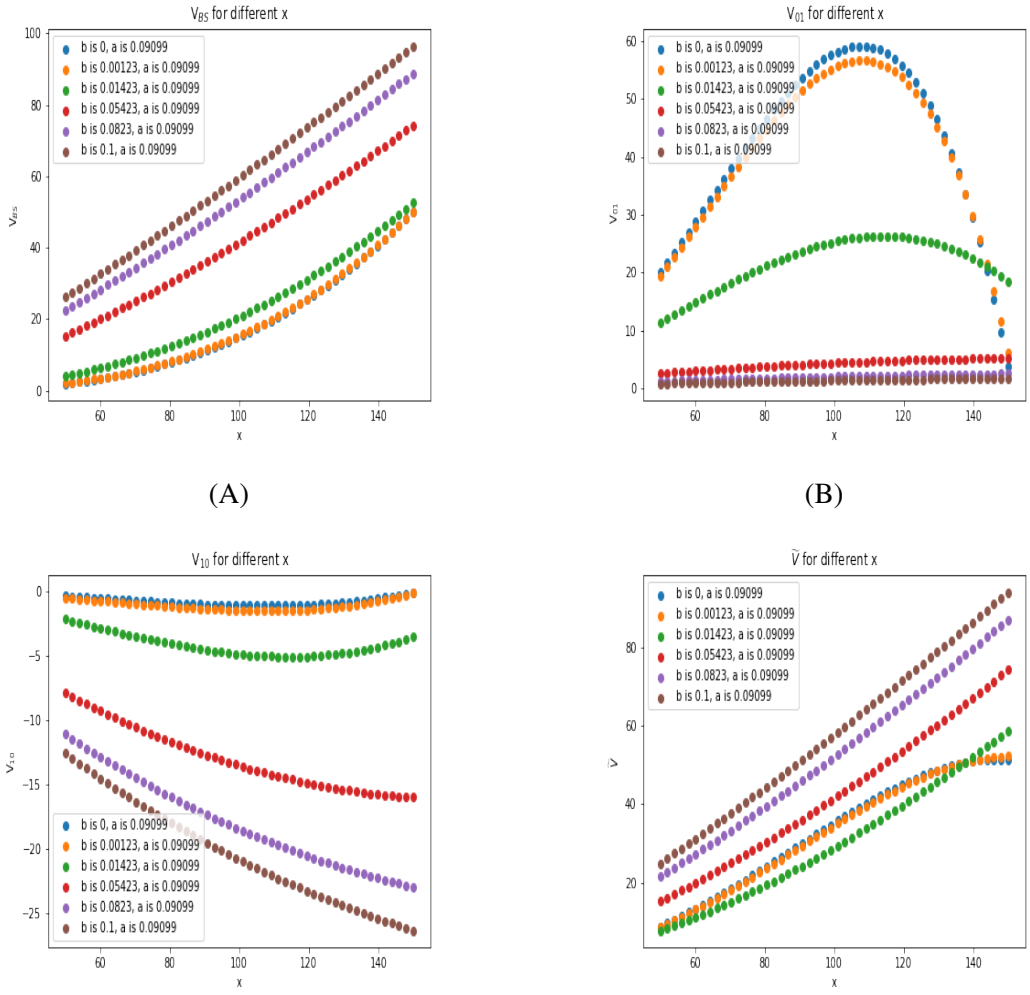

(A) (B)

(C) (D)

Figure 4.8: Real option value trends with project value, fixed a and variable b

Figures 4.8(A)-(D) present how the real option value changes with the initial project value, given a fixed parameter $a = 0.09099$ and varying parameter b. Figures 4.8(A)-(D) show qualitative behaviors similar to their counterparts in Figures 4.7(A)-(D), differing only in quantitative scales.

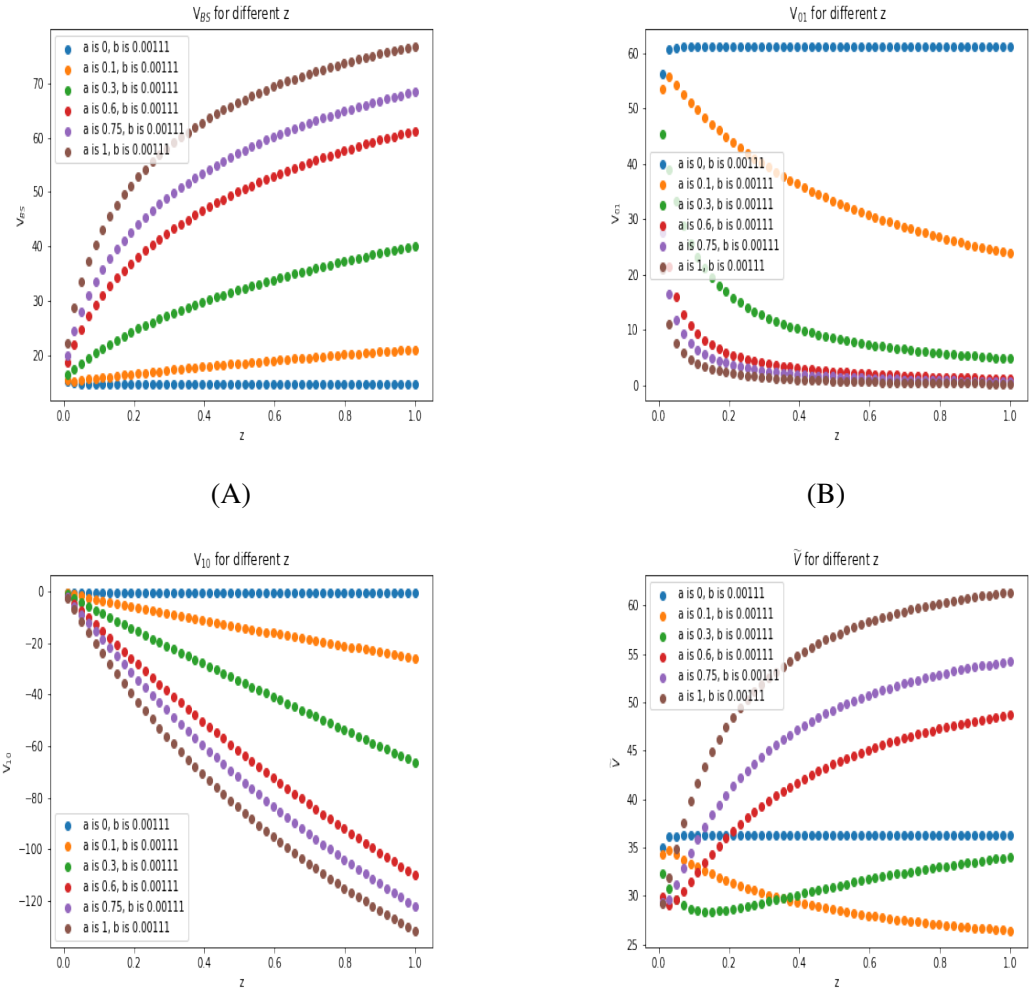

(A) (B)

(C) (D)

Figure 4.9: Effect of z on real option values with variable a and fixed b

The variation of the real option value with respect to the volatility variable z is investigated in the fifth type of experiments, where parameters a and b are assigned a selected set of paired values. Figures 4.9(A)-(D) display the trends in real option value relative to changes in z, with parameter b fixed at 0.00111 and parameter a varying. Figure 4.9(A) shows that the leading order term V_{BS} rises with increasing z. Additionally, the curves are concave, with concavity becoming more obvious as a increases. When a is large, the upward trend becomes more pronounced. Moreover, for a fixed z, increasing a leads to higher values of V_{BS}. In Figures 4.9(B) and 4.9(C), the

correction terms V_{01} and V_{10} generally decrease as z increases. The curves in Figure 4.9(B) are convex, while those in Figure 4.9(C) appear more linear. Moreover, with z held constant, increasing a leads to a reduction in V_{01} and V_{10}. Figure 4.9(D) reveals several noteworthy features. Specifically, when a is relatively small (e.g., $a = 0.1$), $\widetilde{V}$ decreases as z increases. Conversely, for larger values of a (e.g., $a \geq 0.6$), $\widetilde{V}$ exhibits an increasing trend with respect to z. The reason is that, for relatively small values of a (excluding $a = 0$), the correction terms decline more rapidly than the leading term increases. In contrast, for larger values of a, the leading term grows at a faster rate. The case $a = 0.3$ is unique, with $\widetilde{V}$ first decreasing to a minimum before increasing as z rises. Overall, when $a = 0$, the values of V_{BS}, V_{01}, V_{10}, and $\widetilde{V}$ remain unchanged as z increases.

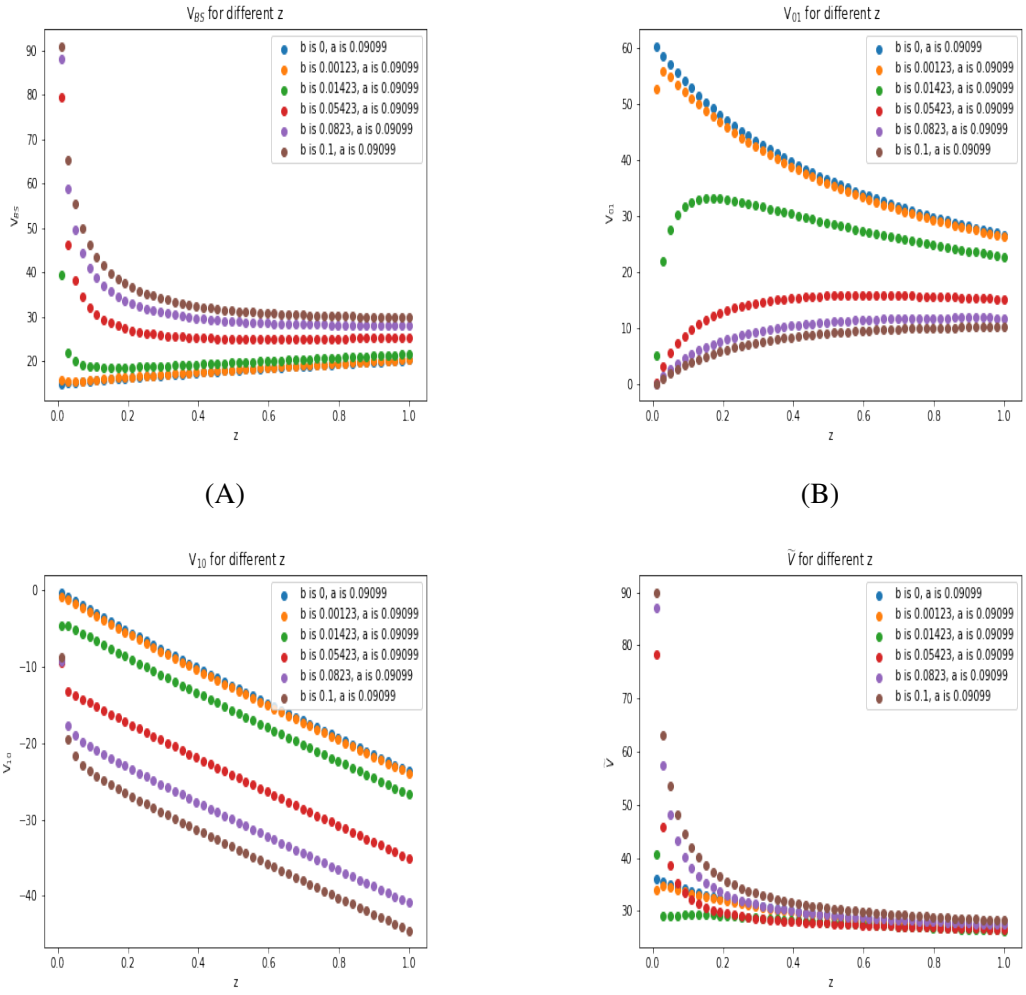

(A) (B)

(C) (D)

Figure 4.10: Effect of z on real option values with variable b and fixed a

Figures 4.10(A)-(D) illustrate how the real option value varies with the volatility variable z, given a fixed parameter $a = 0.09099$ and varying parameter b. Figure 4.10(A) illustrates that the curves are generally convex. For larger values of b (e.g., $b = 0.05423$), the leading order term V_{BS} decreases as z increases. However, for smaller values of b (e.g., $b = 0, 0.00123,$ or 0.01423), V_{BS} initially declines before rising with increasing z. Moreover, when other parameters are fixed, a larger value of b results in a larger value of V_{BS}. In Figure 4.10(B), when parameter b takes on smaller values such as 0 or 0.00123, the correction term V_{01} tends to decrease as z increases, with the associated curves

displaying convexity. On the contrary, at larger b values such as b = $0.05423,\ 0.0823$ or 1, V_{01} rises with increasing z, and the curves have a concave form. An interesting case happens at b = 0.01423, where the correction term V_{01} first increases to a maximum and then decreases. In Figure 4.10(C), the first correction term V_{10} generally decreases as z increases. Moreover, in Figures 4.10(B) and 4.10(C), the correction term decreases with increasing b for a fixed value of z. In Figure 4.10(D), the real option value $\widetilde{V}$ generally decreases as z increases. This trend is caused by the effect of the correction term linked to the slowly-varying factor.

4.5 Conclusion

In this chapter, the real option pricing problem is investigated under a stochastic environment, with the assumption that the dynamics of the present value of the expected future net cash flows from an innovative project follow the double-mean-reverting 4/2 stochastic volatility model introduced by Cao et al. in (Cao et al., 2023a).

Following the introduction of the model in Section 4.2, closed-form approximation formulas for the real option value and the free boundary value were derived by using an asymptotic method in Section 4.3. Each formula comprises two parts: the leading order term, corresponding to the Black–Scholes value as established in (Dixit & Pindyck, 1994), and a first-order correction term coming from the volatility components, specifically, the fast-varying and slowly-varying components. The findings presented here extend the work of Ting et al., which focused on the Heston model (Ting et al., 2013).

Section 4.4 presents five types of numerical experiments. Sensitivity analyses on model parameters a (the "Heston" factor) and b (the "3/2" factor) reveal that when either a or b assumes relatively small values, the real option value and the free boundary value exhibit behavior distinct from that within the Black–Scholes framework as functions of a or b. Conversely, at larger values of a or b, the contributions of the correction

terms arising from the 4/2 volatility factors to the qualitative features of the real option value become negligible. Under these circumstances, the qualitative behavior of the real option value is primarily dictated by its leading term, i.e., the Black–Scholes price. Additionally, sensitivity analyses concerning the free boundary with respect to parameters a, b, and the volatility variable z indicate that its qualitative nature is predominantly governed by its leading term.

Numerical experiments investigating the variation of the real option value with respect to the initial project value indicate that, unlike the Black–Scholes framework, the real option value does not necessarily increase monotonically when volatility exhibits stochastic behavior. Specifically, for relatively small values of parameters a and b, the real option value initially rises to a peak before declining as the project value increases. In contrast, when parameter a assumes relatively large values, the qualitative behavior aligns closely with that predicted by the Black–Scholes model.

The final observation derived from sensitivity analyses of parameters a, b, and the initial project value is that, generally, the fast-varying mean-reverting factor contributes more significantly to the qualitative characteristics of both the real option value and the free boundary value than the slowly-varying mean-reverting factor. Nonetheless, with respect to sensitivity to the volatility variable z, there are instances where the slowly-varying mean-reverting factor plays a more prominent role in shaping these qualitative features.

In this chapter, pseudocodes (the numerical experiment 5) will also be provided for the numerical experiments of this chapter. Since this chapter mainly focuses on the sensitivity analysis of various parameters, the overall structure of the codes remains highly similar for different parameter sets. To avoid redundancy and improve clarity, only one representative example will be selected to show the pseudocodes, and their detailed process will be presented. The pseudocodes corresponding to this example are shown as follows

Numerical Experiments 5: Real Option Valuation Using Approximate Formula and LSM

Input: Model parameters $r, q, \varepsilon, \delta, \eta, \xi, \theta, \rho_{sv}$; factors a, b; starting value X_0, cost K;

LSM settings: number of paths N, number of steps M, time length T.

Output: Option value by formula V_{formula}, by LSM V_{LSM}, relative error $\%$.

$V_{\text{formula}} \leftarrow$ `CalculateFormula`$(X_0, K, a, b, \ldots)$

$V_{\text{LSM}} \leftarrow$ `RunLSM`$(X_0, K, a, b, \ldots, N, M, T)$

error% $\leftarrow \left|\frac{V_{\text{formula}} - V_{\text{LSM}}}{V_{\text{formula}}}\right| \times 100\%$

`CalculateFormula`$(X_0, K, a, b, \ldots)$ Find $V_{\text{BSM}}, x_{\text{BSM}}$;

Find correction terms V_{01}, V_{10};

return $V_{\text{BSM}} + \sqrt{\varepsilon}V_{01} + \sqrt{\delta}V_{10}$, which is proosition 4.3.1.;

`RunLSM`$(X_0, K, a, b, \ldots, N, M, T)$ $\Delta t \leftarrow T/M$;

Create arrays $X[N][M+1]$, $V[N][M+1]$, set $X[i][0] = X_0$;

for $j \leftarrow 1$ **to** M **do**

  for $i \leftarrow 1$ **to** N **do**

    Simulate $X[i][j]$ using the 4/2 model;

for $i \leftarrow 1$ **to** N **do**

  $V[i][M] \leftarrow \max(X[i][M] - K, 0)$;

for $j \leftarrow M - 1$ **to** 1 **do**

  Find in-the-money paths: $\mathcal{I} \leftarrow \{i | X[i][j] > K\}$;

  Fit regression $C(\cdot)$ using $\{(X[i][j], V[i][j+1]e^{-r\Delta t}) | i \in \mathcal{I}\}$;

  for $i \leftarrow 1$ **to** N **do**

    if $i \in \mathcal{I}$ **then**

      $V[i][j] \leftarrow \max(X[i][j] - K, C(X[i][j]))$;

    else

      $V[i][j] \leftarrow V[i][j+1]e^{-r\Delta t}$;

return average of $V[i][1]$ over all paths i;

return $V_{\text{formula}}, V_{\text{LSM}}$, error%

The aim of the above pseudocodes is to find the value of a real option by using our approximated analytical pricing formula and LSM. The pseudocodes list the required parameters and relative pricing formulas (such as $V_{\text{formula}}, V_{\text{LSM}}$, error). Then, the V_{formula} will be calculated by proposition 4.3.1. For the V_{LSM} part, it will be obtained by using the LSM. For the LSM part, it simulates a lot of pathways (indexed by i) of asset prices over time and calculates the payoff for each path at the end (T). Then, the LSM works backward to identify paths where exercising the real option is possible. It applies regression to estimate the value of continuing to hold the option. For each path, it chooses the higher value between immediate exercise and continuation. And then, it calculates the option price by averaging the values at the initial time across all paths. Once we get the $(V_{\text{formula}}, V_{\text{LSM}}$, the value of the relative error between them can also be obtained.

Chapter 5

Conclusion and Future Directions

This chapter provides a summary of the main contributions of this thesis and outlines several promising directions for future research. The core objectives of this thesis were to derive fair valuation formulas for both European options and real options under some rescaled $4/2$ stochastic volatility models, and to determine optimal investment thresholds for real options within this framework. These objectives have been addressed through a combination of analytical derivation and numerical analysis. Additionally, new research ideas have emerged during the course of the study, which are also discussed as potential avenues for future investigation.

5.1 Conclusion

This thesis explores the valuation of European and real options under rescaled $4/2$ stochastic volatility models, with the aim of enhancing the accuracy and tractability of pricing methods in stochastic volatility environments. Specifically, approximate closed-form pricing formulas have been derived for both types of options. These analytical results address Research Questions 1 and 2, which focus on obtaining tractable pricing models under the $4/2$ volatility structure. Furthermore, a pricing methodology

for determining the optimal investment threshold for real options has been developed, addressing Research Question 3. To validate the analytical results, a series of numerical experiments were conducted. These include comparisons with Monte Carlo simulations and empirical market data. The outcomes demonstrate that the proposed pricing formulas perform comparably to benchmark stochastic volatility models, notably the Heston and $3/2$ models, thereby addressing Research Question 4. In addressing Research Question 5, the sensitivity of the $4/2$ model to various parameters was analyzed. This sensitivity analysis provides insights into the dynamic behavior of the model, in comparison to traditional models.

Chapter 1 outlines the motivation, background, and existing literature on option pricing, providing the context and significance of the problem. Chapter 2 presents the theoretical foundations necessary to develop the models and understand the methodological approaches.

In Chapter 3, two re-formulations of the $4/2$ model are proposed: the rescaled mean-reverting model and the rescaled double-mean reverting model. Using asymptotic expansion techniques, approximate closed-form pricing formulas for European options are derived for both versions. The first model focuses solely on fast mean reversion and leads to a pricing formula that extends the classic Black-Scholes framework. This approach allows for calibration via implied volatility and captures market behaviors such as skew and convexity through first- and second-order approximations. The second model incorporates both fast and slow mean-reverting components. The resulting formula is validated through simulations and empirical comparison, confirming its practical applicability.

Chapter 4 shifts focus to the pricing of real options. Under the rescaled double-mean reverting $4/2$ model, closed-form approximations are obtained for both the option value and its associated free boundary. These formulas combine the leading order term from the Black-Scholes model with correction terms that account for the model's stochastic

volatility structure. Sensitivity analysis reveals that the correction terms play a more pronounced role when the a (Heston-factor) or b ($3/2$-factor) parameters are small. As these parameters increase, the pricing results converge towards those of the Black-Scholes model. Notably, the influence of the fast mean-reverting component proves to be the dominant factor among the model's dynamics. Additional analysis of free boundary behavior with respect to key parameters further supports the robustness of the leading-order approximation in characterizing the qualitative features of optimal investment thresholds.

5.2 Future Directions

While this thesis has achieved its primary goals, several promising directions for future research remain open. The flexible structure of the rescaled double-mean reverting $4/2$ stochastic volatility model allows it to capture both short- and long-term dynamics of volatility. As such, it holds potential for broader application beyond European and real options pricing. Two interesting extensions involve the valuation of American-style derivatives and variance swaps.

5.2.1 Pricing American Put Options

One natural extension of the current work is to develop a pricing framework for American options under the $4/2$ stochastic volatility model. Unlike European options, American options can be exercised at any time before expiration, introducing an optimal stopping problem that complicates their valuation. Traditional methods often rely on free boundary formulations or simulation-based approaches such as the LSM method.

The literature on American option pricing is extensive. Parkinson (1977) provided early results under the Black-Scholes model and highlighted the equivalence in value between European and American call options. Subsequent work, such as Zhu & Chen

(2011), used perturbation methods to derive semi-analytic pricing formulas under fast mean-reverting stochastic volatility models. These results showed that mean reversion plays a key role in American put pricing, especially in declining markets. More recently, Fallah & Mehrdoust (2019) applied the LSM approach under the double Heston model, achieving high accuracy and computational efficiency.

Given the richer volatility dynamics of the $4/2$ volatility model, we propose investigating the valuation of American put options under the rescaled double-mean reverting version of this model. The LSM method provides a practical and flexible tool for this purpose. Comparative studies between the $4/2$, Heston, and $3/2$ models would also be valuable in evaluating the relative performance of these frameworks.

5.2.2 Pricing Variance Swaps

Another promising area for future work is the pricing of variance swaps. Variance swaps are forward contracts on future realized variance and are widely used for hedging and speculative purposes in volatility markets. A variance swap allows the buyer to receive a payoff based on the difference between the realized variance and a pre-agreed strike, making its valuation highly sensitive to the modeling of volatility dynamics.

Prior studies have addressed the pricing of variance swaps under various models. Zhu & Lian (2011) derived closed-form solutions under the Heston model using Fourier transform. Yuen et al. (2015) developed quasi-closed-form solutions for discrete variance swaps under the $3/2$ stochastic volatility model with jumps using partial integro-differential equations. These works demonstrate that analytical methods can outperform simulation-based approaches in terms of both efficiency and accuracy, particularly as the sampling frequency increases.

To date, no known research has explored the pricing of variance swaps under the $4/2$ stochastic volatility model. Given its ability to capture both Heston-like and $3/2$-like

behavior, the $4/2$ volatility model is a strong candidate for accurately modeling the dynamics relevant to variance swaps. Future research could focus on deriving analytical or semi-analytical pricing formulas for discrete variance swaps using the $4/2$ volatility framework. These results could then be validated against Monte Carlo simulations and compared with those from the Heston and $3/2$ models.

References

Bakshi, G., Ju, N. & Ou-Yang, H. (2006). Estimation of continuous-time models with an application to equity volatility dynamics. *Journal of Financial Economics*, *82*(1), 227–249.

Bates, D. S. (2000). Post-'87 crash fears in the S&P 500 futures option market. *Journal of Econometrics*, *94*(1-2), 181–238.

Black, F. (1975). Fact and fantasy in the use of options. *Financial Analysts Journal*, *31*(4), 36–41.

Black, F. & Scholes, M. (1973). The pricing of options and corporate liabilities. *Journal of Political Economy*, *81*(3), 637–654.

Borison, A. (2005). Real options analysis: Where are the emperor's clothes? *Journal of Applied Corporate Finance*, *17*(2), 17–31.

Boyle, P. P. (1977). Options: A Monte Carlo approach. *Journal of Financial Economics*, *4*(3), 323–338.

Brennan, M. J. & Schwartz, E. S. (1982). An equilibrium model of bond pricing and a test of market efficiency. *Journal of Financial and Quantitative Analysis*, *17*(3), 301–329.

Brenner, M. & Subrahmanyam, M. G. (1994). A simple approach to option valuation and hedging in the Black-Scholes model. *Financial Analysts Journal*, *50*(2), 25–28.

Broadie, M. & Detemple, J. B. (2004). Option pricing: Valuation models and applications. *Management Science*, *50*(9), 1145–1177.

Brockhaus, O. & Long, D. (2000). Volatility swaps made simple. *Risk*, *19*(1), 92–95.

Cao, J., Kim, J.-H., Liu, W. & Zhang, W. (2023a). Rescaling the double-mean-reverting 4/2 stochastic volatility model for derivative pricing. *Finance Research Letters*, *58*, 104374.

Cao, J., Kim, J.-H., Liu, W. & Zhang, W. (2023b, September). *Rescaling the double-mean-reverting 4/2 stochastic volatility model for derivative pricing.* Auckland, New Zealand. (Oral presentation at the 2023 Derivative Markets Conference)

Cao, J., Kim, J.-H., Liu, W. & Zhang, W. (2024a, December). *Investment opportunity strategy in a double-mean-reverting 4/2 stochastic volatility environment.* Auckland, New Zealand. (Oral presentation at AUT Mathematical Modelling and Analytics Symposium)

Cao, J., Kim, J.-H., Liu, W. & Zhang, W. (2024b, December). *Investment opportunity strategy in a double-mean-reverting 4/2 stochastic volatility environment.* Sydney, Australia. (Oral presentation at Quantitative Methods in Finance 2024 Conference)

Cao, J., Kim, J.-H., Liu, W. & Zhang, W. (2025). Investment opportunity strategy in a double-mean-reverting 4/2 stochastic volatility environment. *The North American Journal of Economics and Finance*, *76*, 102358.

Carr, P. & Sun, J. (2007). A new approach for option pricing under stochastic volatility. *Review of Derivatives Research*, *10*(2), 87–150.

Chen, N. & Hong, L. J. (2007). Monte Carlo simulation in financial engineering. In *2007 Winter Simulation Conference* (pp. 919–931).

Cheng, Y. & Escobar-Anel, M. (2021). Optimal investment strategy in the family of 4/2 stochastic volatility models. *Quantitative Finance*, *21*(10), 1723–1751.

Choi, S.-Y., Fouque, J.-P. & Kim, J.-H. (2013). Option pricing under hybrid stochastic and local volatility. *Quantitative Finance*, *13*(8), 1157–1165.

Christoffersen, P., Heston, S. L. & Jacobs, K. (2009). The shape and term structure of the index option smirk: Why multifactor stochastic volatility models work so well. *Management Science*, *55*(12), 1914–1932.

Chuma, R. N. & Fadugba, S. E. (2015). On stochastic volatility in the valuation of European options. *British Journal of Mathematics & Computer Science*, *5*(1), 104.

Cont, R. & Tankov, P. (2003). *Financial Modelling with Jump Processes*. Chapman and Hall/CRC.

Cox, J. C. (1975). *Notes on option pricing I: Constant elasticity of variance diffusions* (Working paper). Stanford University.

Cox, J. C., Ingersoll, J. E. & Ross, S. A. (1985). A theory of the term structure of interest rates. *Econometrica*, *53*(2), 385–407.

Cox, J. C., Ross, S. A. & Rubinstein, M. (1979). Option pricing: A simplified approach. *Journal of Financial Economics*, *7*(3), 229–263.

Cox, J. C., Ross, S. A. & Rubinstein, M. (2014). Pricing contingent claims: Option pricing theory and evidence. In T. E. Copeland, J. F. Weston & K. Shastri (Eds.), *Financial Theory and Corporate Policy* (4th ed., pp. 197–210). Boston: Pearson.

Derman, E. & Miller, M. B. (2016). *The volatility smile*. John Wiley & Sons.

Dias, J. C. & Nunes, J. P. (2011). Pricing real options under the constant elasticity of variance diffusion. *Journal of Futures Markets*, *31*(3), 230–250.

Dias, J. C., Nunes, J. P. V. & da Silva, F. C. (2024). Finite maturity caps and floors on continuous flows under the constant elasticity of variance process. *European Journal of Operational Research*, *316*(1), 361–385.

Dixit, A. K. & Pindyck, R. S. (1994). *Investment under Uncertainty*. Princeton University Press.

Drimus, G. (2012). Options on realized variance by transform methods: a non-affine stochastic volatility model. *Quantitative Finance*, *12*(11), 1679–1694.

Duan, J.-C. & Yeh, C.-Y. (2010). Jump and volatility risk premiums implied by VIX. *Journal of Economic Dynamics and Control*, *34*(11), 2232–2244.

Dupire, B. et al. (1994). Pricing with a smile. *Risk*, *7*(1), 18–20.

Escobar, M. & Gong, Z. (2020). The mean-reverting 4/2 stochastic volatility model: Properties and financial applications. *Quantitative Finance*, *20*(4), 555–573.

Ewald, C.-O., Ouyang, R. & Siu, T. K. (2017). On the market-consistent valuation of fish farms: Using the real option approach and salmon futures. *American Journal of Agricultural Economics*, *99*(1), 207–224.

Fallah, S. & Mehrdoust, F. (2019). American option pricing under double Heston stochastic volatility model: Simulation and strong convergence analysis. *Journal of Statistical Computation and Simulation*, *89*(7), 1322–1339.

Fama, E. F. (1965). The behavior of stock-market prices. *The Journal of Business*, *38*(1), 34–105.

Feller, W. (1951). Two singular diffusion problems. *Annals of Mathematics*, *54*(1), 173–182.

Fouque, J.-P., Lorig, M. & Sircar, R. (2016). Second order multiscale stochastic volatility asymptotics: Stochastic terminal layer analysis and calibration. *Finance and Stochastics*, *20*(3), 543–588.

Fouque, J.-P., Papanicolaou, G. & Sircar, K. R. (2000). *Derivatives in Financial Markets with Stochastic Volatility*. Cambridge University Press.

Fouque, J.-P., Papanicolaou, G., Sircar, R. & Sølna, K. (2011). *Multiscale Stochastic Volatility for Equity, Interest Rate, and Credit Derivatives*. Cambridge University Press.

Gatheral, J. (2008, July). Consistent modeling of SPX and VIX options. In *Fifth World Congress of the Bachelier Finance Society, London.*

Grasselli, M. (2017). The 4/2 stochastic volatility model: A unified approach for the Heston and the 3/2 model. *Mathematical Finance*, *27*, 1013–1034.

Hagan, P. S., Kumar, D., Lesniewski, A. S. & Woodward, D. E. (2002). Managing smile risk. *Wilmott*, *1*, 84–108.

Heston, S. L. (1993). A closed-form solution for options with stochastic volatility with applications to bond and currency options. *The Review of Financial Studies*, *6*(2), 327–343.

Heston, S. L. (1997). *A simple new formula for options with stochastic volatility* (Technical report). Washington University of St. Louis.

Hildebrand, F. B. (1987). *Introduction to Numerical Analysis*. Courier Corporation.

Hillman, T., Zhang, N. & Jin, Z. (2018). Real-option valuation in a finite-time, incomplete market with jump diffusion and investor-utility inflation. *Risks*, *6*(2), 51.

Huang, B., Cao, J. & Chung, H. (2014). Strategic real options with stochastic volatility in a duopoly model. *Chaos, Solitons & Fractals*, *58*, 40–51.

Huang, S.-D. & He, X.-J. (2022). Analytical approximation of European option prices under a new two-factor non-affine stochastic volatility model. *AIMS Mathematics*, *8*(2), 4875–4891.

Huh, J., Jeon, J., Kim, J.-H. & Park, H. (2019). A reduced PDE method for European option pricing under multi-scale, multi-factor stochastic volatility. *Quantitative Finance*, *19*(1), 155–175.

Hull, J. & White, A. (1987). The pricing of options on assets with stochastic volatilities. *The Journal of Finance*, *42*(2), 281–300.

Hull, J. & White, A. (1990). Pricing interest-rate-derivative securities. *The Review of Financial Studies*, *3*(4), 573–592.

Jäckel, P. (2002). *Monte carlo methods in finance*. John Wiley & Sons.

Jackwerth, J. C. & Rubinstein, M. (1996). Recovering probability distributions from option prices. *The Journal of Finance*, *51*(5), 1611–1631.

Johnson, H. & Shanno, D. (1987). Option pricing when the variance is changing. *Journal of Financial and Quantitative Analysis*, *22*(2), 143–151.

Jones, C. S. (2003). The dynamics of stochastic volatility: Evidence from underlying and options markets. *Journal of Econometrics*, *116*(1-2), 181–224.

Kariya, T. & Liu, R. Y. (2003). Options, futures and other derivatives. In *Asset Pricing: Discrete Time Approach* (pp. 9–26). New York: Springer.

Kil, H.-M. & Kim, J.-H. (2022). A closed-form approximation formula for pricing European options under a three-factor model. *Probability in the Engineering and Informational Sciences*, *36*(4), 1214–1240.

Kim, J.-H., Lee, J., Zhu, S.-P. & Yu, S.-H. (2014). A multiscale correction to the Black–Scholes formula. *Applied Stochastic Models in Business and Industry*, *30*(6), 753–765.

Kim, J.-H., Lee, M.-K. & Sohn, S.-Y. (2014). Investment timing under hybrid stochastic and local volatility. *Chaos, Solitons & Fractals*, *67*, 58–72.

Kim, J.-H., Yoon, J.-H., Lee, J. & Choi, S.-Y. (2015). On the stochastic elasticity of variance diffusions. *Economic Modelling*, *51*, 263–268.

Klebaner, F. C. (2005). *Introduction to Stochastic Calculus with Applications* (2nd ed.). London, UK: Imperial College Press.

Klein, P. (1996). Pricing Black-Scholes options with correlated credit risk. *Journal of Banking & Finance*, *20*(7), 1211–1229.

Lewis, A. L. (2009). Option valuation under Stochastic Volatility II. *Finance Press*.

Li, X. & Wu, Z. (2008). On an approximation method for pricing a high-dimensional basket option on assets with mean-reverting prices. *Computers & Operations Research*, *35*(1), 76–89.

Lin, W., Li, S., Luo, X. & Chern, S. (2017). Consistent pricing of VIX and equity derivatives with the 4/2 stochastic volatility plus jumps model. *Journal of Mathematical Analysis and Applications*, *447*(2), 778–797.

Longstaff, F. A. & Schwartz, E. S. (2001). Valuing American options by simulation: A simple least-squares approach. *The Review of Financial Studies*, *14*(1), 113–147.

Mandelbrot, B. B. & Mandelbrot, B. B. (1997). *The Variation of Certain Speculative Prices*. Springer.

Martin, I. (2011). *Simple variance swaps* (Tech. Rep.). National Bureau of Economic Research.

McDonald, R. & Siegel, D. (1984). Option pricing when the underlying asset earns a below-equilibrium rate of return: A note. *The Journal of Finance*, *39*(1), 261–266.

McDonald, R. & Siegel, D. (1986). The value of waiting to invest. *The Quarterly Journal of Economics*, *101*(4), 707–727.

Mencia, J. & Sentana, E. (2013). Valuation of VIX derivatives. *Journal of Financial Economics*, *108*(2), 367–391.

Merton, R. C. (1973). Theory of rational option pricing. *The Bell Journal of Economics and Management Science*, *4*(1), 141–183.

Myers, S. C. (1977). Determinants of corporate borrowing. *Journal of Financial Economics*, *5*(2), 147–175.

Oksendal, B. (2013). *Stochastic Differential Equations: An Introduction with Applications*. Springer, Berlin.

Papanicolaou, A. & Sircar, R. (2014). A regime-switching Heston model for VIX and S&P 500 implied volatilities. *Quantitative Finance*, *14*(10), 1811–1827.

Parkinson, M. (1977). Option pricing: The American put. *The Journal of Business*, *50*(1), 21–36.

Pham, H. (2009). *Continuous-time Stochastic Control and Optimization with Financial Applications*. Springer.

Platen, E. (1997). *A non-linear stochastic volatility model* (Financial Mathematics Research Report No. FMRR 005-97). Canberra: Center for Financial Mathematics, Australian National University.

Ramm, A. G. (2001). A simple proof of the fredholm alternative and a characterization of the fredholm operators. *American Mathematical Monthly*, *108*(9), 855–860.

Ross, S. M. (2014). *Introduction to Probability Models* (11th ed.). Elsevier.

Sabanis, S. (2002). Stochastic volatility. *International Journal of Theoretical and Applied Finance*, *5*(05), 515–530.

Schwartz, E. S. (2004). Patents and R&D as real options. *Economic Notes*, *33*(1), 23–54.

Scott, L. O. (1987). Option pricing when the variance changes randomly: Theory, estimation, and an application. *Journal of Financial and Quantitative Analysis*, *22*(4), 419–438.

Shreve, S. (2008). *Stochastic Calculus for Finance II: Continuous-Time Models* (8th ed.). New York, USA: Springer.

Ting, S. H. M., Ewald, C.-O. & Wang, W.-K. (2013). On the investment-uncertainty relationship in a real option model with stochastic volatility. *Mathematical Social Sciences*, *66*(1), 22–32.

Veng, S., Yoon, H., Ji & Choi, S.-Y. (2019). Multifactor Heston's stochastic volatility model for European option pricing. *Applied Stochastic Models in Business and Industry*, *35*(5), 1202–1227.

Wiggins, J. B. (1987). Option values under stochastic volatility: Theory and empirical estimates. *Journal of Financial Economics*, *19*(2), 351–372.

Yuen, C. H., Zheng, W. & Kwok, Y. K. (2015). Pricing exotic discrete variance swaps under the 3/2-stochastic volatility models. *Applied Mathematical Finance*, *22*(5), 421–449.

Zhu, S.-P. & Chen, W.-T. (2011). Pricing perpetual American options under a stochastic-volatility model with fast mean reversion. *Applied Mathematics Letters*, *24*(10), 1663–1669.

Zhu, S.-P. & Lian, G.-H. (2011). A closed-form exact solution for pricing variance swaps with stochastic volatility. *Mathematical Finance*, *21*(2), 233–256.